VAPOR SEPARATION BY MIXED MATRIX POLYMERIC MEMBRANES

A THESIS SUBMITTED TO
THE GRADUATE SCHOOL OF NATURAL AND APPLIED SCIENCES
OF
MIDDLE EAST TECHNICAL UNIVERSITY

BY

FATMA ŞAHİN

IN PARTIAL FULFILLMENT OF THE REQUIREMENTS
FOR
THE DEGREE OF DOCTOR OF PHILOSOPHY
IN
CHEMICAL ENGINEERING

SEPTEMBER 2018

Approval of the thesis:

VAPOR SEPARATION BY MIXED MATRIX POLYMERIC MEMBRANES

submitted by **FATMA ŞAHİN** in partial fulfillment of the requirements for the degree of **Doctor of Philosophy in Chemical Engineering Department, Middle East Technical University** by,

Prof. Dr. Halil Kalıpçılar
Dean, Graduate School of **Natural and Applied Sciences** ____________________

Prof. Dr. Pınar Çalık
Head of Department, **Chemical Engineering** ____________________

Prof. Dr. Halil Kalıpçılar
Supervisor, **Chemical Engineering Dept., METU** ____________________

Assist. Prof. Dr. Berna Topuz
Co-Supervisor, **Chemical Engineering Dept., Ankara University** ____________________

Examining Committee Members:

Prof. Dr. Levent Yılmaz
Chemical Engineering Dept., METU ____________________

Prof. Dr. Halil Kalıpçılar
Chemical Engineering Dept., METU ____________________

Prof. Dr. Fatma Çiğdem Güldür
Chemical Engineering Dept., Gazi University ____________________

Prof. Dr. Nihal Aydoğan
Chemical Engineering Dept., Hacettepe University ____________________

Assist. Prof. Dr. Emre Büküşoğlu
Chemical Engineering Dept., METU ____________________

Date: ____________________

I hereby declare that all information in this document has been obtained and presented in accordance with academic rules and ethical conduct. I also declare that, as required by these rules and conduct, I have fully cited and referenced all material and results that are not original to this work.

Name, Last name : Fatma Şahin

Signature :

ABSTRACT

VAPOR SEPARATION BY MIXED MATRIX POLYMERIC MEMBRANES

Şahin, Fatma
Ph.D., Department of Chemical Engineering
Supervisor : Prof. Dr. Halil Kalıpçılar
Co-Supervisor: Asst. Prof. Dr. Berna Topuz

September 2018, 137 pages

ZIF-8, ZIF-L, ZIF-7 and ZIF-67 were synthesized from fresh and recycled synthesis solutions. The crystal morphology, N_2 adsorption capacity and thermal behavior of ZIFs from recycled solutions were similar to those obtained from the fresh solution. The recycling procedures improved the efficiency of crystallization such that 0.36 g ZIF-7/g organic linker was obtained after two recycling steps, although only 0.16 g ZIF-7/ g organic linker can be obtained after single step synthesis using fresh solution. From an environmental perspective, the developed procedures allowed to consume a great extent of organic linker used for synthesis, therefore the amount of waste organic linker was reduced.

A PDMS-based membrane is potentially appropriate for separation of organic solvents from N_2. Six different membrane - pure PDMS membrane, ZIF-8/PDMS MMMs, ZIF-L/PDMS MMMs, ZIF-67/PDMS MMMs, ZIF-7/PDMS MMMs and ZIF-71/PDMS MMMs were prepared. Incorporation of ZIF-L enhanced the VOCs permeability and VOC/N_2 selectivity by 60 % and 33 % with respect to pure PDMS membrane. Single VOCs/N_2 mixtures and multicomponent VOCs/N_2 mixtures were tested at different temperatures. It was found that VOCs and N_2 showed inverse response with temperature change. Effect of VOCs concentration in the feed stream was determined via decreasing VOCs concentration by 1 % in the feed stream. It was observed that VOCs permeability and α_{VOCs/N_2} decreased % 27 and 40 %, respectively.

Keywords: Zeolitic imidazole framework, PDMS, mixed matrix membrane, solvent recovery

ÖZ

KARIŞIK MATRİSLİ POLİMERİK MEMBRANLAR İLE BUHAR AYIRMA

Şahin, Fatma
Doktora, Kimya Mühendisliği Bölümü
Tez Yöneticisi : Prof. Dr. Halil Kalıpçılar
Ortak Tez Yöneticisi: Dr. Öğr. Üyesi Berna Topuz

Eylül 2018, 137 sayfa

ZIF-8, ZIF-L, ZIF-7 ve ZIF-67 kristalleri orijinal ve geri dönüştürülmüş çözeltilerden sentezlenmiştir. İki farklı çözelti kullanılarak sentezlenen bu kristallerin morfolojisi, N_2 adsopsiyon kapasitesi ve ısıl kararlılıkları benzer bulunmuştur. Geri dönüşüm yönteminin uygulanmasıyla kristalleşme tepkimesinin verimi artırılmıştır. Örneğin sadece orijinal çözeltiden elde edilen ZIF-7 miktarı 0.16 gr ZIF-7 /gr organik bağlayıcı iken, bu miktar iki kere geri dönüşüm prosedürü uygulanması sonucunda 0.36 gr ZIF-7/ gr organik bağlayıcıya çıkarılmıştır. Geri dönüşüm prosedürü uygunlanan ZIF-8, ZIF-L ve ZIF-67'de de benzer sonuçlar elde edilmiştir. Geliştirilen yöntem ile reaksiyonda kullanılan organik bağlayıcının büyük kısmı tüketilecek böylece atığa giden organik bağlayıcı miktarı azalacatır.

PDMS bazlı membranlar, çözücülerin azottan ayrılmasında kullanılabilir. Bu amaçla altı farklı membran sentezlenmiştir: saf PDMS membran, ZIF-8/PDMS karışık matrisli membran (KMM), ZIF-L/PDMS KKM, ZIF-67/PDMS KKM, ZIF-7/PDMS KKM ve ZIF-71/PDMS KMM. Karışık matriksli membranlar arasından sadece ZIF-L/PDMS KMM'ın, saf PDMS membrana göre uçucu organik bileşik (UOB) geçirimlilik ve UOB/N_2 seçilik değerinin sırasıyla % 60 ve % 33 arttırtığı gözlenmiştir. Besleme içinde sadece bir UOB içeren ve birden fazla UOB içeren N_2 karışımları farklı sıcaklıklarda test edilmiştir. Sıcaklık degişimine UOB'ler ve N_2

birbirine göre zıt tepki vermişlerdir. UOB’lerin besleme içindeki derişimi %1 azaltıldığında, UOB geçirimlilik ve UOB/N_2 seçicilik değeri sırasıyla % 27 ve % 40 azalmıştır.

Anahtar Kelimeler: Zeolitik İmizidazolat Kafes, PDMS, karışık matrisli membrane, çözücü geri kazanımı

To my beloved family

ACKNOWLEDGMENTS

I wish to express my sincere gratitude to my supervisor Prof. Dr. Halil Kalıpçılar for his guidance, advice, criticism, encouragements, and insight throughout this study. I have learned so much about research and life under his tutelage. I would also thank my co-supervisor Assist. Dr. Berna Topuz for her suggestion and helps.

I'm deeply grateful to my thesis committee members Prof. Dr. Levent Yılmaz and Prof. Dr. F. Çiğdem Güldür for reading my thesis and sharing their invaluable consideration. I would like to thank Assoc. Prof. Dr. Zeynep Çulfaz-Emecen and Assist. Dr. Emre Büküşoğlu for their suggestions and sharing their precious experiences.

I would like to thank The Scientific and Technological Council of Turkey (TUBITAK) through the grant number 116M438 and Middle East Technical University coordinatorship of scientific research projects (BAP-07-02-2014-007-463 and BAP-03-04-2015-007) for financial support.

I would like to thank Süleyman Kuşhan, İsa Çağlar, Gazi Saranay and Cemil Araçlı for their technical help. I also would like to thank all staff of the Department of Chemical Engineering for their help throughout the study.

I would like to thank my colleague Merve Özkutlu, Seda Sivri, Ezgi Yavuzyılmaz, Elif İrem Şenyurt , and Merve Sarıyer for their endless support, patience and understanding. I also thank to Zeynep Karakaş, Aslı Karausta, Atalay Çalışan, İlker Şener, Berrak Erkmen, Özge Batır, Veysi Helvacı, Soner Yaşar, Berkan Atman, Nisa Erişen, Almira Çaldıklıoğlu, Nur Ber Emerce, Yağmur Çulhacıoğlu, Burak Akdeniz and Selin Şahin for their friendship and help during my study.

I would like to thank Banu Atabey, Işıl Kabacaoğlu and Bengü Yıldırım for their endless support, love and patience since we met. Finally, I thank my parent for their unceasing love, encouragements, understanding, and support throughout my whole life. It would not be possible to carry out this study without them.

TABLE OF CONTENTS

ABSTRACT v

ÖZ vii

ACKNOWLEDGMENTS x

TABLE OF CONTENTS xi

LIST OF TABLES xiv

LIST OF FIGURES xvi

CHAPTERS

1. INTRODUCTION 1
    - 1.1 Zeolitic Imidazole Frameworks (ZIFs) 1
    - 1.2 Volatile Organic Compounds (VOCs) 2
        - 1.2.1 Control of VOCs Emission 3
    - 1.3 Polymeric Membranes 6
        - 1.3.1 Basic Principles of Separation in Polymeric Membranes 8
        - 1.3.2 Mixed Matrix Membranes (MMMs) 11
    - 1.4 Objective and Thesis Outline 13
    - 1.4.1 Statement of the Problem and Significance of Synthesis of ZIFs crystals from Recycled Mother Liquors 14
    - 1.4.2 Statement of the Problem and Significance of Vapor/Gas Separation 15

2. LITERATURE REVIEW 19
    - 2.1 Synthesis of ZIFs 19
    - 2.2 Application of PDMS Based MMMs for Vapor/Gas Separation 22
    - 2.3 Hansen Solubility Parameter 28

3. SYNTHESIS ZEOLITIC IMIDAZILE FRAMEWORKS 31
    - 3.1 Introduction 31
    - 3.2 Experimental Study 33
        - 3.2.1 Materials 33

3.2.2 Synthesis of ZIFs Crystals from Fresh Solution 33
3.2.3 Synthesis of ZIFs Crystals from Recycled of Mother Liquors 34
3.2.4 Characterization of ZIFs 35
3.3 Results and Discussion 37
3.3.1 Synthesis of ZIFs from Fresh Crystallization Solution 37
3.3.2 Synthesis of ZIFs from Recycled Mother Liquor 40
3.3.3 Assessment of the Recycling Procedures 59
3.4 Conclusion 63
4. ZIF -X /PDMS MMMs FOR SEPARATION OF SOLVENTS FROM NITROGEN 65
4.1 Introduction 65
4.2 Experimental 67
4.2.1 Materials 67
4.2.2 Synthesizes of ZIFs 67
4.2.3 Membrane Preparation 68
4.2.4 Characterization 69
4.2.5 Membrane Permeation Test 69
4.3 Results and Discussion 71
4.3.1 ZIFs characterization 71
4.3.2 Morphology of ZIF-X/PDMS MMMs 77
4.3.3 Nitrogen permeation through pure PDMS membrane 85
4.3.4 Single gas permeation through ZIF-X/PDMS MMMs 88
4.3.5 VOCs/N_2 Separation performance of 20 wt % ZIF loaded MMMs 90
4.3.6 Separation of single VOC from N_2 through 20 % ZIF-L PDMS MMMs 94
4.3.7 Effect of VOCs concentration on 20 % ZIF-L/PDMS MMMs performance 99
4.3.8 Separation of multicomponent VOCs mixture from N_2 through 20 % ZIF-L/PDMS MMMs 100
4.4 Conclusion 104
REFERENCES 105
APPENDICES 117
A. Reproducibility of ZIFs 117

B. Relative Crystallinity of ZIFs 121
C. Yield of Crystallization Reactions 125
D. Mass Flow Controller (Mfc) Calibration Curve 127
E. Gas Chromatography Calibration Curve 129
CURRICULUM VITAE 135

LIST OF TABLES

TABLES

Table 1. Commercial polymeric membranes (Basu et al. 2010).................................7

Table 2. Predicted market of membrane in the future (Sridhar et al. 2014) 7

Table 3. Classification of vapor permeation (S.A.Stern 1995).................................10

Table 4. Terminology for defining membrane performance 11

Table 5. Metal sources, organic linker sources, molar composition of metal ion: organic ligand and unit cell formula 20

Table 6. Yield of the ZIF-8, ZIF-L, ZIF-67 and ZIF-7 with respect to literature......21

Table 7. Zeolite topology, density of metal atoms per unit volume (T/V^f), diameter the largest pore through which a sphere can pass (dag) , the diameter of the largest sphere which can fit into the framework (dph) (Banerjee et al. 2008; Park et al. 2006).....22

Table 8. Literature for PDMS based membrane for separation of vapor from gas ...25

Table 9. Amount of components used for the synthesis of ZIFs. Superscripts indicate the type of metal ion, organic linker and solvent used for the synthesis of a particular ZIF. Aging was carried out at room temperature overnight. 35

Table 10. Crystallization time and temperature of the ZIFs synthesized from fresh and recycled solution, and centrifugation period (at 2655 RCF) to recover ZIF crystals; molar compositions of synthesis solution, remaining mother liquor by mass balance and modified mother liquors. The solution composition is given in the order of metal ion: organic ligand: solvent...36

Table 11. The yield and crystallinity ZIFs obtained from fresh and recycled mother liquors 44

Table 12. The average particle size based on SEM images and BET-equivalent surface area of ZIFs obtained from fresh and recycled mother liquors.................................46

Table 13. The efficiency of single step synthesis from fresh solution and three step synthesis using two mother liquors. The efficiency is defined as total amount of ZIF produced per total amount of organic linker used throughout the process. 63

Table 14. Pore size, topology and unit cell formula of ZIFs 68

Table 15. Average particle size, N_2 adsorption amount and BET surface area of ZIFs 76

Table 16. Thickness of the membrane 81
Table 17. Residual weight percentages after TGA 84
Table 18. Pure PDMS N_2 permeability comparison with literature 86
Table 19. Molecular weight, vapor pressure and HSP of solvents 96
Table 20. Effect of VOCs concentration on membrane performance of 20 % ZIF-L/PDMS MMMs (P_{feed} = 2.92 bar and 35 °C) 100
Table B. 1. Relative crystallinity of ZIF-8 crystals 121
Table B. 2. Relative crystallinity calculation results of ZIF-L crystals 122
Table B. 3. Relative crystallinity calculation results of ZIF-67 crystals 123
Table B. 4. Relative crystallinity calculation results of ZIF-7 crystals 123
Table C. 1. Product yields of ZIF-8 crystals 125
Table C. 2. Product yields of ZIF-L crystals 126
Table C. 3. Product yields of ZIF-67 crystals 126
Table C. 4. Product yields of ZIF-7 crystals 126

LIST OF FIGURES

FIGURES

Figure 1. The bridging angles in ZIFs (a) and zeolites (b) (Phan et al. 2010) 1

Figure 2. Classification of VOCs emission control techniques (Khan & Kr. Ghoshal 2000) 4

Figure 3. The application range of VOCs recovery processes (Scott 1998) 5

Figure 4. Basic principle of gas permeation (Hunger et al. 2012) 8

Figure 5. Solution-diffusion model 9

Figure 6. Schematic presentation of Robeson upper bounds (Hunger et al. 2012) ... 12

Figure 7. Schematic representation of a mixed matrix membrane 13

Figure 8. Schematic expression of recycle mother liquor 15

Figure 9. Schematic representation of VOCs recovery system in food-packing printing industry 16

Figure 10. A representative method of membrane-based separation process 17

Figure 11. ZIF structure (a) ZIF-8 (Park et al. 2006) (b) ZIF-L (Zhong et al. 2015) (c) ZIF-67 (Daojun et al. 2013) (d) ZIF-7 (Yunpan et al. 2013) 22

Figure 12. Scheme of PDMS 23

Figure 13. Selectivities of varioous VOCs over nitrogen by 1 μm PDMS composite membranes (Peinemann 2006) 24

Figure 14. PDMS swelling ratio with solvent vapors (Dam 2006) 29

Figure 15. XRD patterns of ZIFs produced from fresh synthesis solution; (a) ZIF-8.0 (b) ZIF-L.0 (c) ZIF-67.0 (d) ZIF-7.0 (e) ZIF-71.0. The red line shows the reference patterns. 40

Figure 16. XRD patterns of ZIFs synthesized from fresh solutions and mother liquors (a) ZIF-8 (b) ZIF-L (c) ZIF-67 (d) ZIF-7. ZIF-X.0 synthesis from fresh solution, ZIF-X.1 synthesis from first mother liquor, and ZIF-X.2 synthesis from second mother liquor. 42

Figure 17. SEM images of ZIF-8.0, ZIF-8.1 and ZIF-8.2, which are synthesized from fresh solutions and mother liquors. 47

Figure 18. SEM images of ZIF-L.0, ZIF-L.1 and ZIF-L.2, which are synthesized from fresh solutions and mother liquors. 48

Figure 19. SEM images of ZIF-67.0, ZIF-67.1 and ZIF-67.2, which are synthesized from fresh solutions and mother liquors. 49
Figure 20. SEM images of ZIF-7. ZIF-7.0, ZIF-7.1 and ZIF-7.2, which are synthesized from fresh solutions and mother liquors. 50
Figure 21. SEM images of ZIF-71.0 51
Figure 22. N_2 adsorption/desorption isotherms of (a) ZIF-8 (b) ZIF-L (c) ZIF-67 (d) ZIF-7 (e) ZIF-71synthesized from fresh solutions and mother liquors......54
Figure 23. CO_2 adsorption/desorption isotherms of ZIF-7.0, ZIF-7.1 and ZIF-7.2, which are synthesized from fresh solutions and mother liquors. 55
Figure 24. TGA curves (a) ZIF-8 (b) ZIF-L (c) ZIF-67 (d) ZIF-7 (e) ZIF-71 synthesized from fresh solutions and mother liquors......58
Figure 25. pH change of fresh solution during the course of crystallization of ZIFs in fresh and recycled solutions (a) ZIF-8 (b) ZIF-L (c) ZIF-67. 61
Figure 26. Schematic representation of VOCs permeation system......70
Figure 27. XRD patterns of ZIFs (The bar graph bellowed each pattern represent the references pattern). 72
Figure 28. Sem image of as-synthesized ZIF a) ZIF-8 b) ZIF-L c) ZIF-67 d) ZIF-7 e) ZIF-71 73
Figure 29. N_2 adsorption isotherms of ZIFs crystals 75
Figure 30. SEM image of pure PDMS membrane 78
Figure 31. SEM image (a) 20 % ZIF-8 PDMS MMMs (b) 20 % ZIF-L PDMS MMMs (c) 20 % ZIF-67 PDMS MMMs (d) 20 % ZIF-7 PDMS MMMs (d) 20 % ZIF-71 PDMS MMMs......80
Figure 32. EDX Analyzed of 20 % ZIF-L/PDMS MMMs (blue dots: Si and yellow dots: Zn^{+2}) 81
Figure 33. Schematic representation of parts that analyzed by TG 82
Figure 34. TGA curves of (a) ZIFs (b) Pure PDMS and PES support membrane......83
Figure 35. TGA curves of 20 % ZIF-L PDMS MMMs' pieces......85
Figure 36. N_2 permeability of pure PDMS membrane (a) at different temperature (P_{feed} = 2.92 bar) (b) at different feed pressure (T = 35 ^oC) 87
Figure 37. $N_{2,}$ CO_2 permeability and CO_2/N_2 selectivity of the synthesized membranes 89

Figure 38. Gas flow direction through the 20 % ZIF-L/PDMS MMMs...................90
Figure 39. 20 % ZIF-X/PDMS MMMs performance (a) N_2 permeability, VOCs permeability and VOCs/N_2 selectivity (b) EtOH/IPA selectivity.............................93
Figure 40. 20 % ZIF L/PDMS MMMs membrane performance (a) N_2 permeability value (b) VOCs permeability value (c) VOCs/N_2 selectivity 99
Figure 41. Performance of 20 % ZIF L/PDMS MMMs at different mass fraction and temperature (a) Permeability (b) VOCs/N_2 selectivity (c) Dew point relationship between feed and permeate...103
Figure A. 1. XRD Patterns of ZIF-8 crystals with different batches.......................117
Figure A. 2. XRD Patterns of ZIF-L crystals with different batches.......................118
Figure A. 3. XRD Patterns of ZIF-67 crystals with different batches..................119
Figure A. 4. XRD Patterns of ZIF-7 crystals with different batches....................120
Figure D. 1. MFC-1 calibration curve 127
Figure D. 2. MFC-2 calibration curve 127
Figure E. 1. GC calibration curve of ethanol..129
Figure E. 2. GC calibration curve of IPA 129
Figure E. 3. GC calibration curve of ethyl acetate..130
Figure E. 4. GC calibration curve of propanol..130
Figure E. 5. GC calibration curve of methanol...131
Figure E. 6. GC calibration curve of butanol..131
Figure E. 7. GC calibration curve of water...132
Figure E. 8. GC calibration curve of nitrogen 132
Figure F. 1. TGA curves of 20 % ZIF-8 PDMS MMMs.......................................133
Figure F. 2. TGA curves of 20 % ZIF-67 PDMS MMMs.....................................133
Figure F. 3. TGA curves of 20 % ZIF-7 PDMS MMMs.......................................134
Figure F. 4. TGA curves of 20 % ZIF-71 PDMS MMMs.....................................134

CHAPTER 1

INTRODUCTION

1.1 Zeolitic Imidazole Frameworks (ZIFs)

ZIFs, crystalline microporous materials with the topology of zeolites, is a subclass of metal-organic frameworks (MOFs). ZIFs comprise the valuable properties of both zeolite and MOFs such as diversity of framework structure and pore systems, modifiable organic and bridging ligand. The angle between Si-O-Si and M-IM-M are equal, 145 ^{o} (Figure 1). They have high thermal and chemical stability, large specific surface area and higher adsorption amount toward VOCs over nitrogen or oxygen. Due to these properties, they have been used in many areas such as catalytic application in petroleum refining and selective separation for gas or/and vapor mixture.

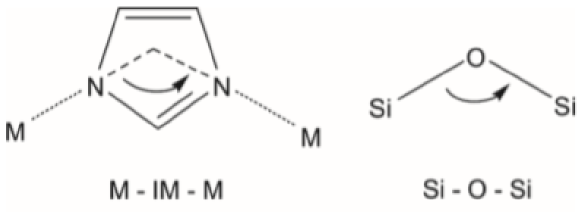

(a) (b)

Figure 1. The bridging angles in ZIFs (a) and zeolites (b) (Phan et al. 2010)

There are different methods to synthesize ZIFs. These are solvothermal method, dry-gel conversion method, microwave method, microfluidic method, mechanochemical method, electrochemical method and sonochemical method. Among those methods, mostly solvothermal method is preferred to synthesize ZIFs (Bhattacharjee et al. 2014). In this method, metal ions (e.g. Zn $^{+2}$, Co $^{+2}$) and organic linker (e.g. Hmim, Bim) are mixed at an isothermal temperature (Banerjee et al. 2008). At the end of the reaction, ZIF crystals are separated from the mother liquor by applying centrifugation. Finally, the solid crystals are washed several times with a solvent (e.g. methanol, ethanol, DMF, water) to get rid of unreacted chemical thus ZIFs are obtain with a high purity.

1.2 Volatile Organic Compounds (VOCs)

Volatile organic compounds (VOCs) highly reactive hydrocarbons. Their boiling points are in the range of 50 and 260°C and they have vapor pressures greater than 0.01 kPa at room temperature (Berenjian et al. 2012). VOCs are. They react to produce ozone (O_3) and other chemical compounds in the presence of sunlight and nitrogen oxides, (NOx), as represented in Eqn. 1 (Nevers 2000). Those chemicals are toxic and carcinogenic so that they cause a negative effect on human health and harmful effects on the environment.

$$NO_x \ + VOCs \xrightarrow[sunlight]{} O_3 + other\ products \quad (1)$$

Solvents are one of the main sources of VOCs. They compose approximately 35 % of all VOCs in the atmosphere. They are used in a wide variety of manufacturing processes: petroleum refining, painting, printing, metal cleaning, gluing and coating, electronic, press-packaging, textile (Lue, Chen, et al. 2008; Smallwood 2002). All scale of industrial manufacturing process often releases off-gases including VOCs. Hence, recovery and reuse of those solvents are essential due to economic losses and environmental concern.

1.2.1 Control of VOCs Emission

The recovery VOCs is significant to reduce the operating cost of a chemical process. Different techniques are available to control VOCs emission in the industry (Figure 2). These techniques are classified as (i) process and equipment modification (ii) add-on control techniques.

In the first technique, VOC emission is controlled by modifying the process equipment, raw material, and/or change of the process. For instance: replacing standard solvent-based printing with fluidized-bed powder coating can be regarded as equipment modification or substitution (Nevers 2000). Although, this method is seen as effective and efficient; its application area is limited because of economical issues.

The add-on control technique is classified into two sub-groups: destruction and recovery. VOCs are decomposed by either oxidation or bio-filtration in destruction method. Oxidation can be either catalytic or thermal. In *thermal oxidation method*, VOCs are burned out at a temperature range 1300-1800 ^{o}F. This system is not practicable for treating waste stream with low VOCs concentration. A low concentration VOC stream requires high amount of heat input and retention time (Brown 2002). Furthermore, nitrogen in the air may turn into nitrogen oxide at high temperatures, which is a secondary pollutant (Louglin 2011).

Catalytic oxidation method is similar to thermal one. The main difference is the operating temperature (700-900 ^{o} F). The drawback of this technique is to produce toxic by-products unless catalyst materials are recyclable. Beside, catalyst materials can be sensitive to poisoning by non-VOCs materials such as sulphur, chlorides ,and silicon (Khan & Kr. Ghoshal 2000).

In the *bio-filtration method*, the waste stream flows throughout a porous packed pipe in which microorganisms thrive. The waste stream cleans itself by an adaptation of biodegradation. Microorganisms convert sorbed VOCs into CO_2 and water. This method is valid for low VOCs concentrations (between 1000 to 1500 ppm as methane) (Brown 2002). The main drawback of this method is that chemicals may cause microorganisms to become more resistant. Those microorganisms may even produce by-products more toxic than the VOCs. Thus, destruction of VOCs may cause more harmless and objectionable form of compound.

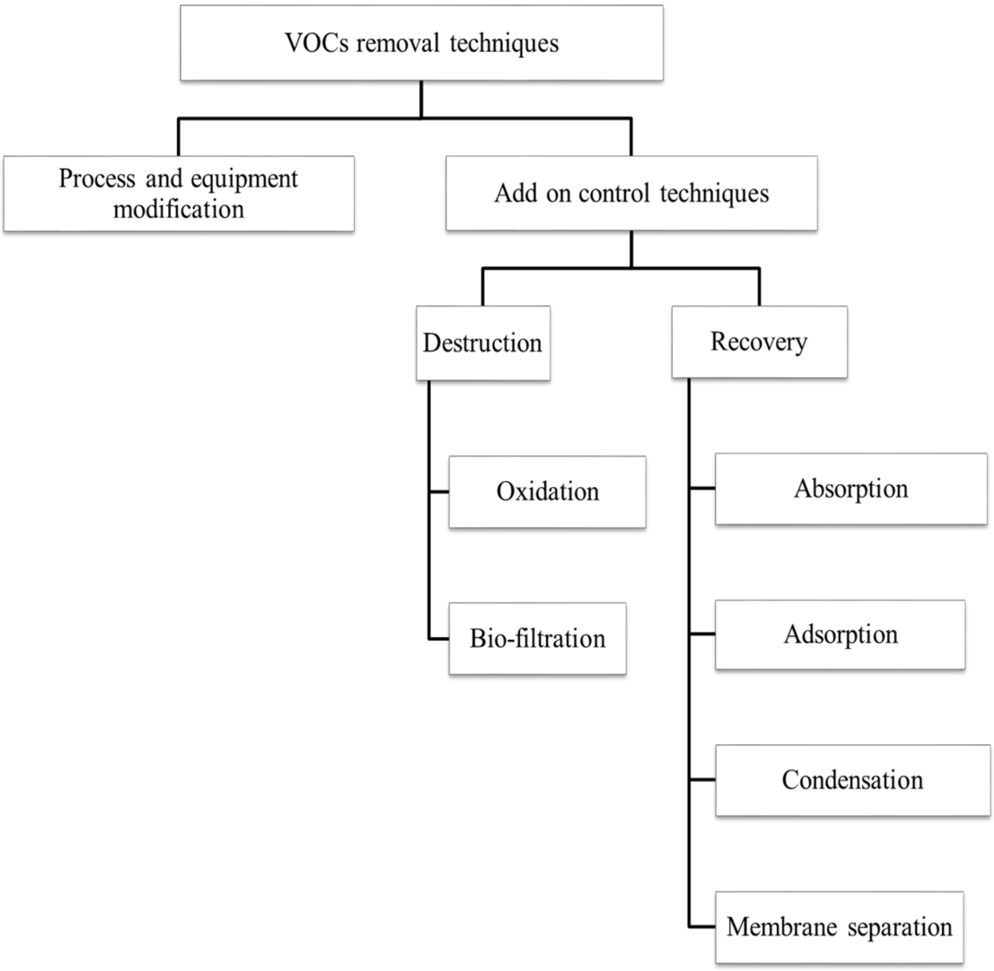

Figure 2. Classification of VOCs emission control techniques (Khan & Kr. Ghoshal 2000)

Recovery of VOCs is feasible with different processes such as absorption, condensation and membrane separation. *Absorption* is a diffusional mass-transfer operation used to remove VOCs by contacting the waste air with a liquid solvent, so that any soluble VOCs will transfer to the liquid phase. This method valid for solvents that have a low volatility. There is an important restriction for this process; a high humidity air stream (50% RH). In addition to this, this process is not suitable for a cyclic operation because of start-up time constraints (Tsai 2002).

Adsorption is a method based on the attachment of VOCs on to the adsorbent. Activated carbon is one of the most common adsorbents that prefers to remove VOCs from the air. VOCs diffuse from the waste stream and cohere on the surface of adsorbent by the weak Vander Waals force. At least two carbon adsorption column is required for continues adsorption process. The main advantage of adsorption is to be effective for very low VOCs concentration up to ~0.002 (vol %) (Figure 3).

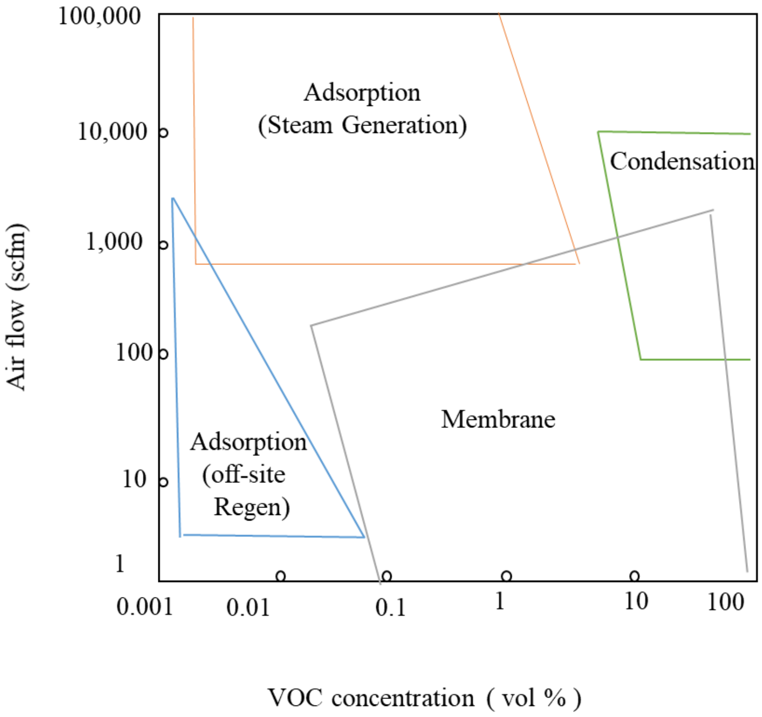

Figure 3. The application range of VOCs recovery processes (Scott 1998)

Condensation is achieved by cooling VOCs-laden air to a sufficiently low temperature that vapor pressure decrease. VOCs condense and then the liquid is separated from the gas by gravity. Condensation is most effective when the concentration of VOC is higher than 5000 ppm (Brown 2002). Air flows up to 1000 scfm can be handled in condensers (Figure 3). VOCs with the low-boiling point increase cooling process operating cost.

Membrane separation is an effective and modern separation technology for recovery of organic solvents from waste gas streams. A treated stream is separated into a permeate that consist of concentrated VOCs and a retentate that contains depleted of VOCs. The substances do not expose to high temperatures during the recovery process thus, VOCs chemical structure do not change. Furthermore, it can simultaneously remove and recover VOCs from gaseous streams. Membrane separation method is most effective for VOC stream that consists of more than VOCs concentration 0.1 (vol %) (Figure 3). Air flow rates can be moderated up to 1000 scfm.

1.3 Polymeric Membranes

The history of polymeric membranes dates back to 1830. In the first publication, they reported that hydrogen diffuse from the surface of a natural rubber balloon (Norman N Li et al. 2008). Despite a long history, the polymeric membrane could not be utilized for a long time because of their high thicknesses. In 1963, ultrathin asymmetric membranes were introduced for a reverse osmosis process (Baker 2006). Since that time, membrane-based separation technology is very significant to solve some problems in the industry.

Currently, many commercial polymers are available such as polydimethylsiloxane, polysulfone, polycarbonate, polyimide and, cellulose acetates. For over years, polymeric membranes have served as key elements in the several application areas such as hydrocarbon-vapor separation, air enrichment (O_2 enrichment or N_2 generation), syngas ratio adjustment (H_2/CO_2), refinery H_2 recovery, acid gas treatment (CO_2/CH_4), and natural gas treatment (Table 1)

Membrane-based separation technology is preferred due to reducing process cost via saving energy. The market size and number of application area has grown up over the years. The market has annually become larger and sales of membrane separation system have reached approximately $ 500 million/year (Norman N Li et al. 2008). Table 2 represented the future of industrial membrane separation technology. As it seen, membrane based separation system undergo a wide usage in the industry area.

Table 1. Commercial polymeric membranes (Basu et al. 2010)

Membrane	Application Area
Polydimethlysiloxane (PDMS)	Hydrocarbon- vapor separation
Polysulfone (PSF)	H_2 and air separation
Polycarbonate (PC)	Air separation
Polyimide (PI)	CO_2 - CH_4, H_2- CH_4 and air separation
Polyaramide (PA)	H_2 separation
Celluslose Acetate (CA)	CO_2 - CH_4 separation
Celluslose tri-Acetate (CTA)	CO_2 - CH_4 separation

Table 2. Predicted market of membrane in the future (Sridhar et al. 2014)

Type of separation	Membrane Markets (US $ Million)	
	2010	2020
Vapor/N_2 separation	30	60
Vapor/Vapor Separation	20	100
CO_2 removal from natural gas	60	100
Isolation of inert N_2 from air	100	125
O_2 enrichment from air	10	30
H_2 recovery	60	150
Removal of moisture from air and others	30	100

Polymer- based membranes are utilized with respect to their ability to separate the chemical compound. However, all membranes should have following requirements: separation efficiency, high flux, mechanical strength over wide range of operating conditions, durability, and productivity (Freeman 2010). If there is no defect, separation efficiency directly depend on operating conditions. Productivity shows inverse ratio with membrane thickness, the lower thickness means the higher flux. The higher flux means the smaller membrane area and thus, the lower operating cost of the membrane-based separation process (Koros & Mahajan 2001).

1.3.1 Basic Principles of Separation in Polymeric Membranes

The polymeric membranes consist of a thin selective layer that performs the separation. The principle of either gas or vapor permeation through the membrane is illustrated in Figure 4. Feed flows throughout the membrane. Some of the components diffuse easily and enriched to the permeate side. While the others cannot cross through the membrane and pass over it due to the semi-permeable property of the membrane. The penetration of molecules through the membrane depends on the polymer properties, the relative size of penetrant, alignment of voids in the membrane, and driving forces such as pressure, temperature and concentration gradient (Louglin 2011).

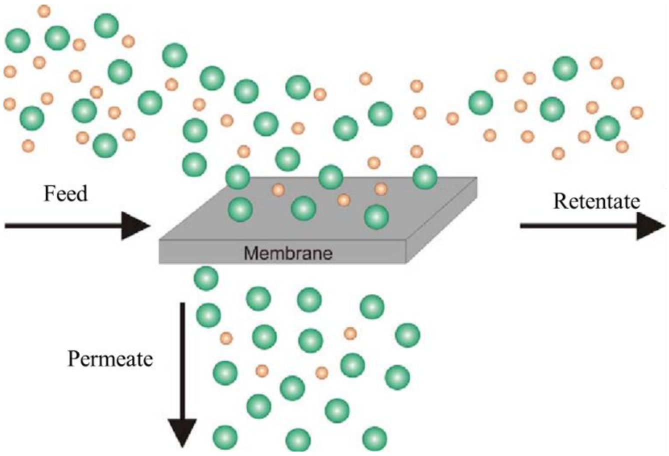

Figure 4. Basic principle of gas permeation (Hunger et al. 2012)

The driving force for the transport of permeant through a membrane is the difference of its chemical potential between feed and permeate side (S.A.Stern 1995). The mechanism of permeation through the transmembrane material is widely described by a solution-diffusion model (Figure 5). The permeant transport phenomenon is taking place in three steps: (1) diffusion through the boundary layer and sorption at the upstream surface; (2) diffusion of components inside the membrane; (3) desorption of permeants from membrane into the vapor phase at the permeate side and diffusion out the boundary layer of the downstream side . The last step usually negligible mass transfer resistance compared with the others. On account of this, the sorption and diffusivity properties will be utilized to determine permeability (Lue, Wang, et al. 2008).

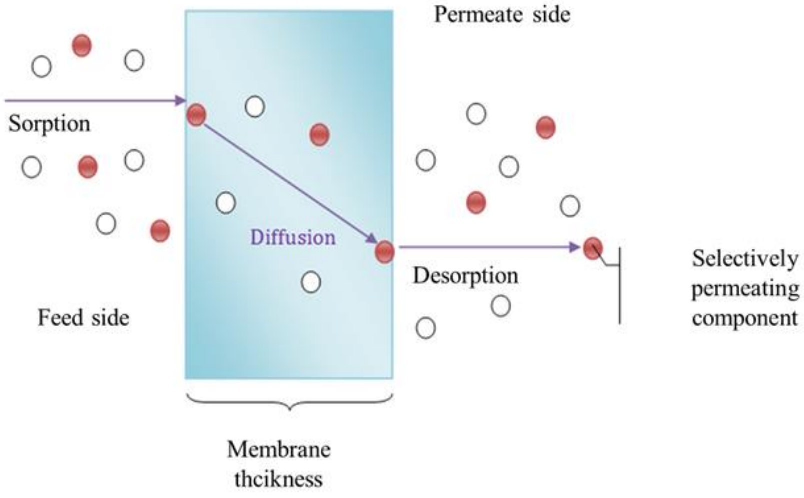

Figure 5. Solution-diffusion model

Vapor permeation through polymeric membrane is classified into two categories (Table 3). In category 1, there is no gas in the feed stream, only vapor exits, e.g., a mixture of alcohol vapors. In category 2, both vapor and gas present in the feed stream e.g., VOCs and N_2. Either vacuum or purge gas applied from the permeate side to sweep permeate from the downstream side of the membrane for each category. A porous or non-porous membrane can be chosen with respect to necessity.

Table 3. Classification of vapor permeation (S.A.Stern 1995)

<table>
<tr><td colspan="2">Category 1</td><td colspan="4">Category 2</td></tr>
<tr><td colspan="2">no gases in the feed</td><td colspan="4">with gases in the feed</td></tr>
<tr><td>vacuum on</td><td>purge gas on</td><td colspan="2">vacuum on</td><td colspan="2">purge gas on</td></tr>
<tr><td>permeate side</td><td>permeate side</td><td colspan="2">permeate side</td><td colspan="2">permeate side</td></tr>
<tr><td>porous</td><td>nonporous</td><td>porous</td><td>nonporous</td><td>porous</td><td>nonporous</td></tr>
</table>

The principles of gas permeation through polymeric membrane alike vapor permeation. There is only gas exist in the feed. Gas permeation strongly depends on feed pressure. Gas permeation has advantages compared to the vapor permeation: no phase may occur during the permeation through the membrane. To conclude that, gas permeation and vapor permeation are feasible separation processes for application in the industry although they have some disadvantages too.

Membrane performance is defined with permeability (P), ideal selectivity (α), and permeance (R) (Table 4). Permeability represents the ability of a component that transport through a membrane. Ideal selectivity is obtained by dividing two components' permeability value, for instance i and j. It represents the separation efficiency of a membrane. Permeance is equal to dividing permeability by the thickness of the membrane (ℓ). Permeability and permeance have the units of " Barrer" and "GPU" that are given in Eq 2 and 3 , respectively.

Table 4. Terminology for defining membrane performance

	Abbreviation	Formulas	Unit
Permeance	J	$J = \frac{P}{\ell}$	$\frac{cm^3\ (STP)}{cm^2 \times s\ \times cmHg}$
Permeability	P	$P_i = \frac{J \times \ell}{\Delta P}$	$\frac{cm^3\ (STP)\ \times cm}{cm^2 \times s\ \times cmHg}$
Ideal Selectivity	α_{ij}	$\alpha_{ij} = \frac{P_i}{P_j}$	

$$1\ Barrer = 1 \times 10^{-10}\ \frac{cm^3(STP)\ \times cm}{cm^2\ \times s\ \times cmHg}\quad (Eq\ 2)$$

$$1\ GPU = 1 \times 10^{-6}\ \frac{cm^3(STP)}{cm^2\ \times s\ \times cmHg}\quad (Eq\ 3)$$

1.3.2 Mixed Matrix Membranes (MMMs)

The main features of membrane-based separation process are high energy yield, low capital investment, simple operation system, easy installation, scalability, high mechanical and thermal durability over the wide range of operating conditions (Basu et al. 2010). Nevertheless, there is a trade-off between permeability and selectivity for polymeric membranes. If permeability increases, selectivity decreases that is shown by “Robeson upper bound” in the literature (Figure 6). Inorganic membranes have higher selectivity and permeability values than the organic polymers as it seen from Figure 6. In addition to this, they have high thermal and chemical stability. However, the manufacture of large-scale is expensive and difficult.

MMMs bring valuable properties of polymers - low cost, commercial-scale manufacture- and desirable properties of inorganic fillers – high selectivity. Inorganic materials - zeolites, metal organic frameworks (MOFs), zeolitic imidazole frameworks (ZIFs), carbon nanotubes (CNT) etc. - are introduced into polymeric membranes to enhance performance. First MMMs was discovered for CO_2/CH_4 separation by addition of 5A to polydimethylsiloxane (PDMS) matrix in 1970. It was reported that, diffusion time lag delayed for CO_2 and CH_4 , on the other hand there was a small effect on permeation (Chung et al. 2007). MMMs have been studied since 1970, their permeability versus selectivity values reaches above the Robeson upper bond .

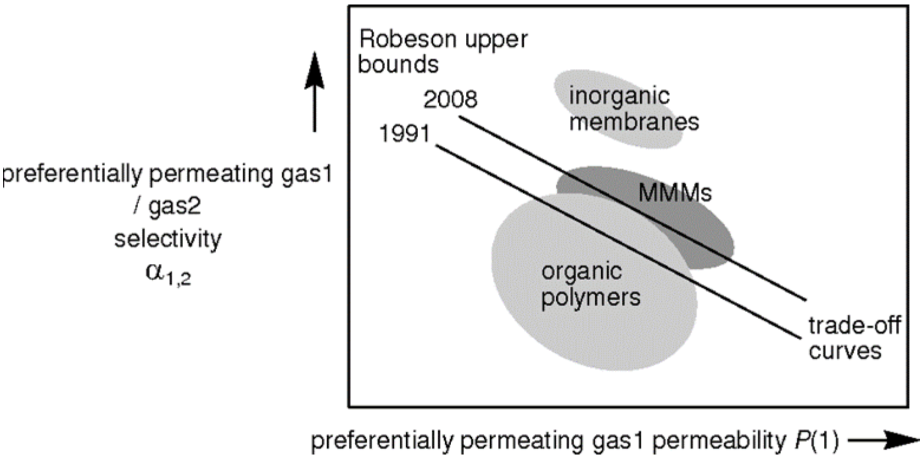

Figure 6. Schematic presentation of Robeson upper bounds (Hunger et al. 2012)

MMMs includes two phase: polymeric bulk phase and inorganic particle phase (Figure 7). As represented in this figure, it is possible to synthesize MMMs with various types of filler with different sizes and shapes. The important situation is homogeneously dispersing fillers in polymer matrix due to getting same performance throughout the membrane.

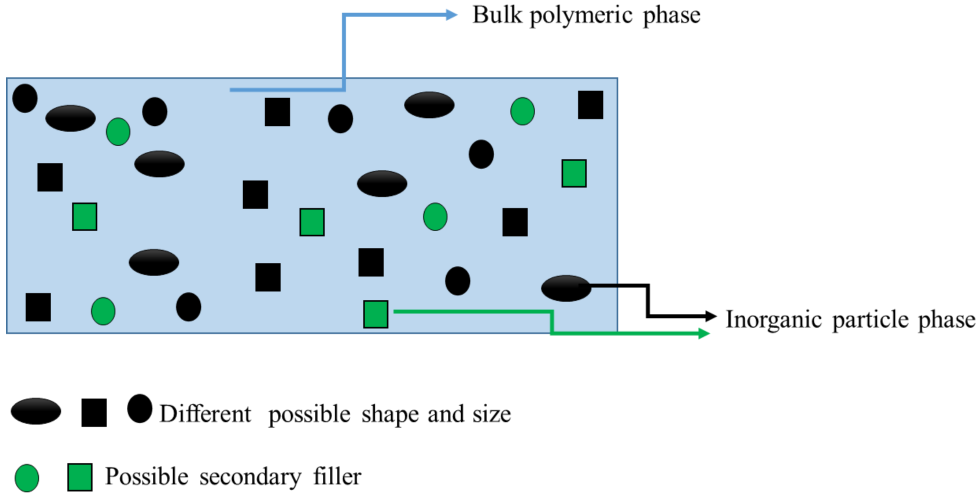

Figure 7. Schematic representation of a mixed matrix membrane

1.4 Objective and Thesis Outline

This Ph.D. study has two objectives:

i. Synthesis of ZIF crystals from recycled mother liquors to increase the yield of crystallization reaction and reduce the amount of waste organic linker

ii. Vapor/gas separation by PDMS based mixed matrix membranes to recover solvents from waste gases

This Ph.D. thesis includes 4 chapter.

Chapter 2 comprises a detailed literature survey of Chapter 3 and Chapter 4. Here is given a background information of ZIFs, VOCs and vapor/gas separation.

Chapter 3 consists of the synthesis of ZIF-7, ZIF-8, ZIF-67 and, ZIF-L crystals by applying the recycling procedure. It mentions about the crystals morphology, thermal behavior, N_2 adsorption capacity of crystals. This chapter has been published in Microporous and Mesoporous Materials.

Chapter 4 focuses on the vapor/ gas separation performance of ZIF/PDMS MMMs. ZIF-8, ZIF-L, ZIF-67, ZIF-7, and ZIF-71 were used as filler. All the ZIFs were synthesized and characterized before using in mixed matrix membranes. Effect of operating temperature, pressure and, feed composition on membrane performance was determined.

1.4.1 Statement of the Problem and Significance of Synthesis of ZIFs crystals from Recycled Mother Liquors

Zeolitic imidazole frameworks (ZIFs) are one of the most valuable synthetic products in the global economy (350 $ billion) (Phan et al. 2010). In recent years, ZIFs have charmed notable interest due to their potential in applications such as adsorption/separation process, drug delivery, chemical sensors, and catalysis.

105 different types of ZIF have been declared by 2010 (Bhattacharjee et al. 2014). Different ZIFs were synthesized by the combination of transition metals and organic imidazole linkers. Generally, ZIFs can be synthesized in the presence of excess amount of imidazole in the reaction medium. For instance, the molar composition of solution that yields ZIF-67 has a molar Hmim/Co^{+2} ratio of 58 whie the ZIF-67 crystal has Hmim/Co ratio of only 2. Besides the yield of crystallization reaction is 66 %, indicating that the reaction medium contains a considerable amount of unreacted imidazole, Hmim. If the mother liquor is recycled to use again in the crystallization, the yield of crystallization reaction increases. It is essential to recycle unreacted chemicals for economical and environmental issue.

The concept of recycling procedure had been shown by synthesizing new generation of ZIF-8 crystals from mother liquor in our research group (Keser Demir et al. 2014). In the present study, I aimed to show that this recycle procedure is also applicable for other ZIFs crystals. The recycling procedure is summarized in Figure 8. After synthesis and recovery of ZIFs crystals from the fresh solution, the mother liquor (ML) was separated and reused for the synthesis of next generation of ZIF crystals. Before reuses, the first and second mother liquors were modified to arrange composition of the synthesis solution. This modification involves only pH arrangement and addition of metal ion to produce second and third generations of ZIFs crystals.

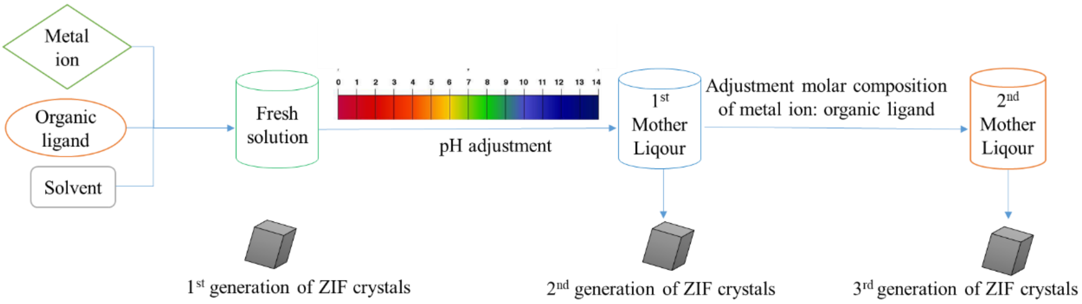

Figure 8. Schematic expression of recycle mother liquor

1.4.2 Statement of the Problem and Significance of Vapor/Gas Separation

Vapor/ gas separation systems has been studied since 1990s. The first application for vapor/gas separation system had been established by Membrane Technology Research group in 1996 (Norman N Li et al. 2008). Since then, new systems have been developed in the chemical process industry worldwide. By the end of 2006, nearly 400 membrane-based separation units were installed in the world (Peinemann 2006).

VOCs are commonly removed from air by adsorption process in the many chemical processes. Columns following the adsorption period are regenerated by increasing temperature, decreasing pressure or using high flux sweeping gases (mostly nitrogen). The VOC swept from the adsorption column are cooled down to condense and fed to the distillation units to recover and separate the VOC mixture into its components. VOCs recovery process are also employed in food-packing printing industry (Figure 9). In this process, solvent containing air’s volumetric flow rate is 100 000 m^3/h that contains approximately 5 -10 g-solvent /m^3. The solvent/air passes through a carbon adsorption bed, which has hydrophobic character. The solvents adsorbed until the bed reaches saturation. At this point, the system closes the flow of solvent leaned air. Subsequently, nitrogen with a volumetric flow rate of 20000 m^3/h starts to flow on the bed and nitrogen strips solvents form the adsorption bed and is fed to a condenser. The condensed solvent mixture are separated into its components by a set of distillation columns.

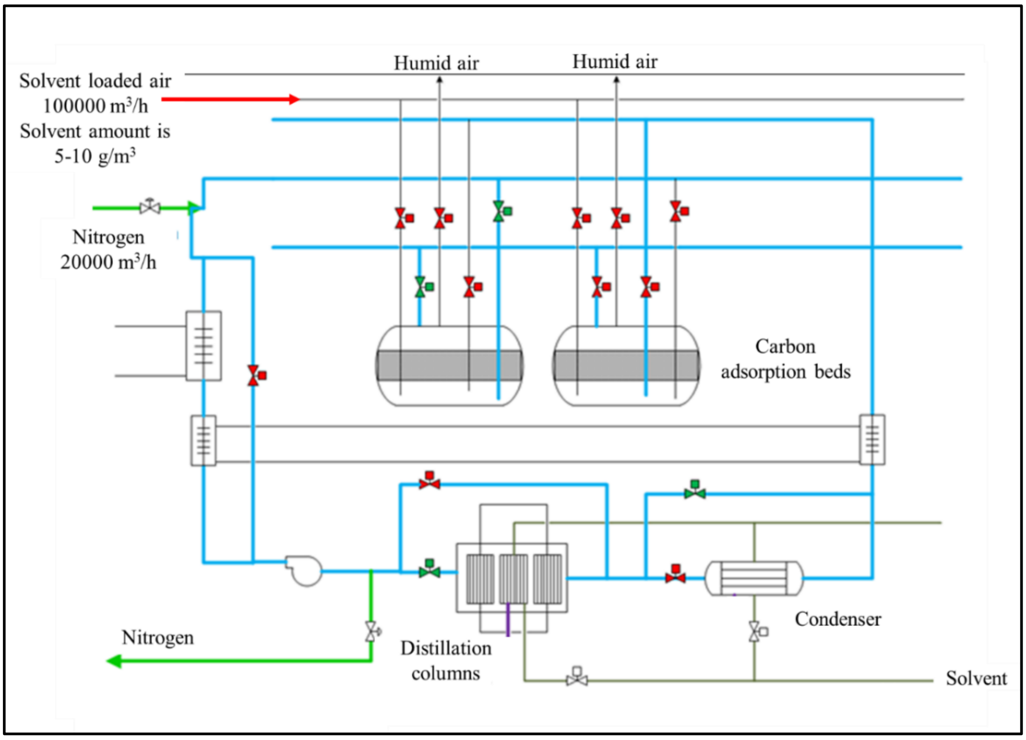

Figure 9. Schematic representation of VOCs recovery system in food-packing printing industry

Nevertheless, low partial pressure of solvent vapors in nitrogen requires cryogenic condensation, which is difficult and expensive. The efficiency of solvent recovery processes can be enhanced by increasing the partial pressure of VOC so that condensation is likely to be easier and more economical. In this study, ZIF filled PDMS mixed matrix membranes, which selectively permeated solvent vapors (VOCs) while rejecting nitrogen and water vapor, were developed. The membrane can be mounted between adsorption columns and condenser as shown in Figure 10. Hence the VOCs concentration at the permeate side of membrane, which is then fed to condenser, will be higher and more condensable. For instance, the dew point of feed stream is equal to -11.8 °C when and N_2: VOCs molar composition is 0.996:0.0036. If the membrane permeates VOCs with ~5 % of the N_2, the dew point is expected to increase up to 77 °C.

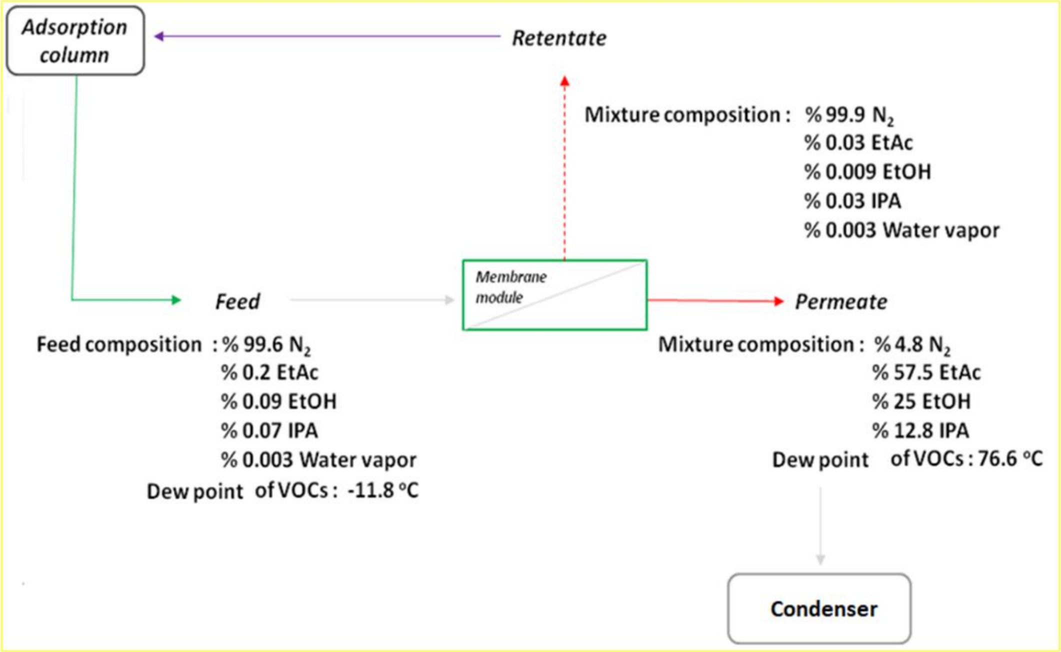

Figure 10. A representative method of membrane-based separation process

CHAPTER 2

LITERATURE REVIEW

2.1 Synthesis of ZIFs

ZIFs are synthesized by copolymerization reaction of metal ion with an organic linker (Park et al. 2006). In this reaction, metal ions are the limiting reactants whereas the organic ligands are the excess ones. Table 5 shows 10 members of ZIF family. Molar composition of reactants and unit cell formulas of those ZIFs indicate that there are still unreacted organic linkers in the reaction medium after crystallization reaction. For instance, 1 mol of Zn $(NO_3).H_2O$ is reacted with 2 moles of Hmim in order to synthesized ZIF-1. However, there are 6 moles of Hmim in the reaction medium at the beginning of the reaction. It is essential to consume almost all organic linkers due to economic loss and environmental issue.

Some methods exist for increasing the product yield of ZIF-8 in the literature. Polyzoidis et al. used a continuous micro reactor to synthesis ZIF-8. The yield of the reaction was only 54 % (Polyzoidis et al. 2016). Nordin et al. synthesized ZIF-8 in the different concentration of triethylamine by solvothermal method at room temperature. They reported that the yield of ZIF-8 was 90 % but they did not mention about the applicability of this method to the other ZIFs. Some research groups increased the amount of organic ligand in the reaction medium. They claimed that the product yield of ZIF-8 could increase by diluting $Zn(NO_3)_2$ in the reaction medium (Cravillon et al. 2012; Pan et al. 2011). The molar composition of $Zn(NO_3)_2$: Hmim varied from 1:23 to 1:70 in those study. They defined yield of the ZIF-8 based on the amount of zinc salt and they obtained yield up to 100 % . On the other hand, they caused a rise for unreacted Hmim at the end of the crystallization reaction. The micro-wave-assisted method has been used for fast crystallization reaction under hydrothermal operating conditions (Bhattacharjee et al. 2014). Besides higher yield, this method requires high energy consumption (Gross et al. 2012).

Table 5. Metal sources, organic linker sources, molar composition of metal ion: organic ligand and unit cell formula

ZIF-n	Metal sources	Organic linker sources	Molar composition of metal ions:organic linker	Unit Cell Formula
ZIF-1 [a]	$Zn(NO_3)_2\cdot 4H_2O$	Hmim	1: 6	$Zn(IM)_2$
ZIF-3 [a]	$Zn(NO_3)_2\cdot 4H_2O$	Hmim	1: 12	$Zn(IM)_2$
ZIF-4 [a]	$Zn(NO_3)_2\cdot 4H_2O$	Hmim	1: 3	$Zn(IM)_2$
ZIF-7 [a]	$Zn(NO_3)_2\cdot 4H_2O$	H-PhIM	1: 6	$Zn(PhIM)_2$
ZIF-8 [b]	$Zn(NO_3)_2\cdot 6H_2O$	Hmim	1: 8	$Zn(MeIM)_2$
ZIF-10 [a]	$Zn(NO_3)_2\cdot 4H_2O$	Hmim	1: 12	$Zn(IM)_2$
ZIF-11 [a]	$Zn(NO_3)_2\cdot 4H_2O$	H-PhIM	1: 15	$Zn(PhIM)_2$
ZIF-12 [a]	$Co(NO_3)_2\cdot 6H_2O$	H-PhIM	1: 7	$Co(PhIM)_2$
ZIF-67 [c]	$Co(NO_3)_2\cdot 6H_2O$	Hmim	1: 58	$Co(MeIM)_2$
ZIF-L [d]	$Zn(NO_3)_2\cdot 6H_2O$	Hmim	1: 8	$Zn(PhIM)_2$

[a] Park et al. (2006) ; [b] Keser, et al. (2014) ; [c] Qial et al. (2012);

[d] Chen et al. (2013)

In our research group, second and third generation of ZIF-8 crystals were acquired by recycling the mother liquors. The product yield of the ZIF-8 increased from 38 % to 80 % (Keser Demir et al. 2014). The recycling method do not required neither diluted metal salt nor unfavorable energy consumption. This method based on the pH adjustment of the 1st mother liquor and metal ion addition to the 2nd mother liquor. In this study, it was aimed to show the potential of the recycling method for increasing the product yield with consuming most of the organic ligands.

105 different ZIFs crystals were reported (Phan et al. 2010) , hence it is not possible to apply this method to all of them. In this PhD thesis, five distinct ZIF crystals were chosen ZIF-8, ZIF-L, ZIF-67 and ZIF-7. The product yield of those ZIFs are given in Table 6 which demonstrate the necessity of the recycle method. Those ZIFs were chosen to representative the rest.

Table 6. Yield of the ZIF-8, ZIF-L, ZIF-67 and ZIF-7 with respect to literature

	Yield (%)	References
ZIF-8	38 - 80	(Keser Demir et al. 2014; Pan et al. 2011; Cravillon et al. 2012; Lee et al. 2015)
ZIF-L	80	(Chen et al. 2013)
ZIF-67	53 -75	(Lin & Chang 2015; Li et al. 2016)
ZIF-7	83- 94	(X. Wang et al. 2016; He et al. 2013)

The ZIFs were synthesized with solvothermal methods by combining different metal sources and organic ligands. Those ZIFs have different crystals structure (Figure 11) different zeolite topology, and different pore metrics (Table 7). Thus, density of metal atom per unit volume (T/V^f) is varied . Either 2-methylimizidazole (mIM) or benzimidazole (bIM) are chosen as an organic ligand, SOD or RHO topologies are obtained, respectively. The difference between them is position of IM (4 or 5).

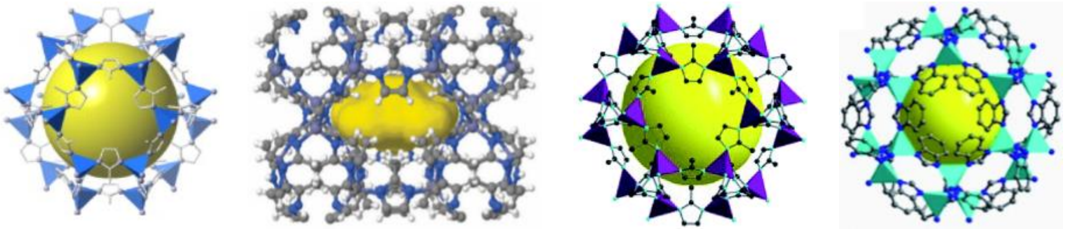

(a) (b) (c) (d)

Figure 11. ZIF structure (a) ZIF-8 (Park et al. 2006) (b) ZIF-L (Zhong et al. 2015) (c) ZIF-67 (Daojun et al. 2013) (d) ZIF-7 (Yunpan et al. 2013)

Table 7. Zeolite topology, density of metal atoms per unit volume (T/V^f), diameter the largest pore through which a sphere can pass (d_a^g) , the diameter of the largest sphere which can fit into the framework (d_p^h) (Banerjee et al. 2008; Park et al. 2006)

	Zeolite code	T/V^f (T/nm^3)	$d_a^g\,(A)$	$d_p^h(A^o)$
ZIF-8	SOD	2.45	3.4	11.6
ZIF-L	Semi- SOD			817*
ZIF-67	SOD	2.46	3.4	11.6
ZIF-7	SOD	2.49	2.9	4.31
ZIF-71	RHO	2.06	4.2	16.5
* $(A^o)^3$				

2.2 Application of PDMS Based MMMs for Vapor/Gas Separation

PDMS (Figure 12) is one of the most studied silicon-based polymers due to excellent membrane performance for separation of vapors from permanent gas (S.A.Stern 1995). It is preferred due to some inherent characteristic properties such as; high chain flexibility, constant physical properties over wide range of temperature, high stability resistance to weather and ozone, excellent physiological inertness, rotational mobility, large free volume, low glass transition temperature (-123 °C), and a hydrophobicity (Smallwood 2002; Yeom et al. 2002a; Lue et al. 2010; Fang et al. 2015a; Norman N Li et al. 2008).

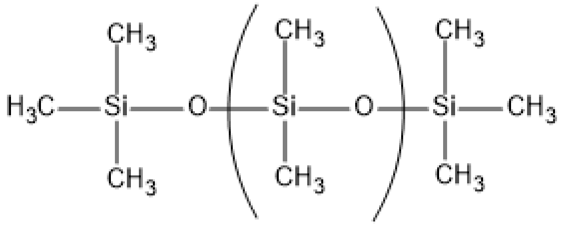

Figure 12. Scheme of PDMS

PDMS easily swell in the presence of vapors and gas which results in a high permeability and leads to higher diffusion coefficients. This phenomenon is a good example of enhancing vapor-gas selectivity by increasing vapor-gas diffusivity (Cen & Lichtenthaler 1995). VOCs/N_2 selectivity of PDMS-based membranes are given in Figure 13. A length of the bar represents mean selectivity by single measurement at ambient temperature with 1μm thick pure PDMS membrane. The selectivity of hydrocarbons changes between 10 and 100.

VOCs/gas separation performance of PDMS-based membrane is donated in Table 8. Air, N_2 ,and H_2 are the off-gases while high-value organic vapors are alcohols, ester, gasoline etc. Some researchers claimed that VOCs and gas display reverse temperature dependence because of different enthalpies of sorption and diffusion (Leemann et al. 1996; Pinnau & He 2004).

Some researchers have focused on the effect of multi-component system and VOCs concentration on organic vapor permeability through PDMS membrane (Table 8). Permeability and selectivity of toluene-ethyl acetate vapor mixtures were less than the single vapor systems by ~ 10 % (Leemann et al. 1996). It was pointed out that permeation and selectivity of VOCs depend of both VOCs content in feed and condensability of VOCs (Yeom et al. 2002b).

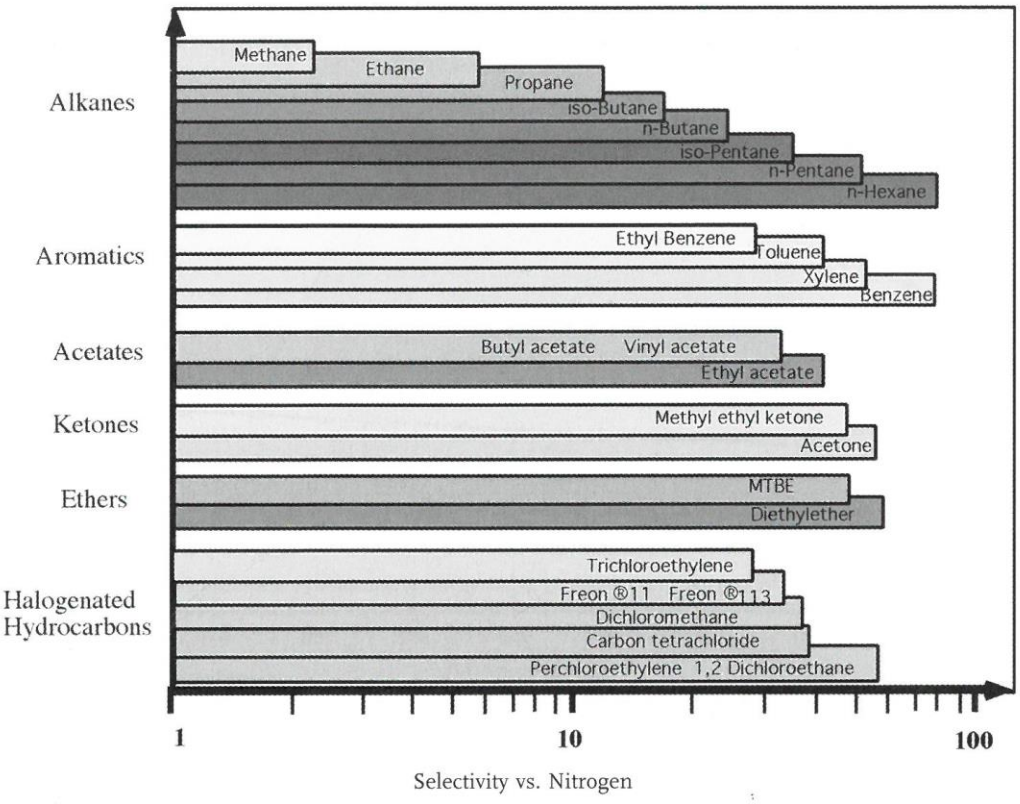

Figure 13. Selectivities of varioous VOCs over nitrogen by 1 μm PDMS composite membranes (Peinemann 2006)

Yeom et al. found that N_2 permeability was suppress below pure nitrogen permeability by sorption of VOCs into PDMS membrane and this effect was more outstanding when VOCs are more condensable. Pinnau et al. said that PDMS chain mobility increased in the event of increasing concentration of the organic vapor, so diffusivity and permeability increase too (Pinnau & He 2004). In this case, permeability of condensable vapors was higher than permanent gas. It was reported in the literature that the permeance, selectivity and permeate of VOCs were rich at high VOCs level in feed stream due to swelling of PDMS layer (Majumdar et al. 2003; Gales et al. 2002).

Table 8. Literature for PDMS based membrane for separation of vapor from gas

Vapor	Gas	Membrane	Selectivity	Permeability (barrer)	References
Propane	N_2	ZIF-8/PDMS MMMs	Propane /N_2	N_2: 200 barrer	(Fang et al. 2015)
			24.5 -19.7	Propane: 4170 barrer	
Pxylene	Air	PDMS capilary membrane	77.8	70000	(Leemann et al. 1996)
Butyl acetate			111.1	100000	
Toluene			33.3	30000	
Ethyl acetate			44.4	40000	
Methyl ethyl ketone			27.8	25000	
Water			16.7	15000	
Ethanol			10.0	9000	
Oxygen			1.3	1200	
Nitrogen			1.0	900	
Methylene chloride	N_2	Pure PDMS Membrane	150-135	250-450	(Yeom et al. 2002)
Chloroform			170-160	250-480	
1,2- dichloroethane			250-210	300-700	
1,1,2-trichloroethane			300-370	290-1000	
Toluen /N_2	N_2	PDMS hollow fiber membrane	Methanol/acetone		(Obuskovic et al. 2003)
Methanol /N_2			60-100		
Acetone /N_2			Toluene: 200-250		

Table 8 continue

Vapor	Gas	Membrane	Selectivity	Permeability (barrer)	References
Propane	H_2	Pure PDMS Membrane	*a) 35* ^{o} *C*		(Pinnau et al. 2004)
Ethane			√ Ethane/Methane= 3	*35* ^{o} *C*	
Methane			√ Propane/Methane= 5.7	Propane= 7400	
n-Butane			√ Ethane/H_2= 4	Ethane =3900	
			√ Propane/H_2= 7.5	Methane=1300	
			b) Minus 20 ^{o} *C*	H_2 = 980	
			√ Ethane/Methane= 4.5		
			√ Propane/Methane= 39		
			√ Ethane/H_2= 9.1		
			√ Propane/H_2= 78		
Acetone	Air	PDMS hollow fiber membrane	Acetone : 1947 to 8526	Acetone : 37 000 to 162 000	(Gales et al. 2002)
Ethyl acetate			Ethanol : 1947 to 4148	Ethanol : 37 000 to 78 810	
Ethanol			Ethyl acetate 10710 to 15902	Ethyl acetate: 203 500 to 286 750	
		Pure PDMS Membrane	Acetone : 60 to 86	Acetone : 22 200 to 31820	
			Ethanol : 72 civarı	Ethanol : 26 650 civarı	
			Ethyl acetate: 72 to 213	Ethyl acetate: 31 820 to 78 810	
				N_2 : 370	

Table 8 continue

Vapor	Gas	Membrane	Selectivity	Permeability (barrer)	References
Toluene	N_2	Pure PDMS Membrane	Pre : CA = 10:1	Pre : CA = 10:1	(Lue et al. 2010)
		Pre : CA = 10:1	16 - 1480	324 ±18	
		Pre : CA = 10:2.5	Pre : CA = 10:2.5	Pre : CA = 10:2.5	
			110-1170	178 ± 11	
Methane	N_2	Pure PDMS Membrane	3.15	0.00486	(Javaid. 2005)
Propane			18.65	0.0287	
Ethylene			8.18	0.0126	
Ethane			9.81	0.0151	
Acetone	Air	Pure PDMS Membrane	11-25		(Noble et al.1995)
Toluene			83		
1,2-Dicloromethane			142		
1,2-Dicloroethane			103		

ZIF-8/PDMS MMMs were synthesized to separate propane from N_2 (Fang et al. 2015a). It was reported that separation selectivity of propane/N_2 enhanced by 38 % according to pure PDMS MMMs with 10 wt % ZIF-8 loading. The research on ZIF/PDMS MMMs to separate VOCs from N_2 is limited to the best of our knowledge. ZIF/PDMS MMMs are mostly used for pervaporation recovery of solvents. For instance, ZIF-7/PDMS MMMs, ZIF-67/PDMS MMMs, ZIF-71/PDMS MMMs and ZIF-8/PDMS MMMs were used separation of various solvents from aqueous solution (Wang et al. 2016; Khan et al. 2018; Y. Li, Lik H. Wee, Martens & Ivo F. J. Vankelecom 2014; Bai et al. 2013).

2.3 Hansen Solubility Parameter

Hilde-brand and Scott offered the solubility parameters in 1950. Fifty year later, Hansen published the Hansen solubility parameters (HSP) (Charles 2000). HSP depends on dispersion, polar and hydrogen bonds that occur if cohesive bonds in a liquid is broken down by an evaporation process. Dispersion (d) forces are deal with the van der Waals bonds between molecules. Polar (p) interactions define degree of dipolar interaction while hydrogen bonds (h) is a special case of polar interaction.

HSP are applicable for practical applications such as prediction of interaction between solute-solute molecules, solvent-solvent molecules and solvent-solute molecules. It expresses the degree of “like” by defining the solvent and solute by three parameters: δ_d : dispersion solubility parameter; δ_p: polar solubility parameter δ_h : hydrogen bonding solubility. Total solubility parameter (δ_t) is equal to square root of summation (Eq 4). If a solvent and a solute have close δ_t value, this means that the solvent more likely to solve the solute.

$$\delta_t^2 = \delta_d^2 + \delta_p^2 + \delta_h^2 \quad (Eq\ 4)$$

Hansen solubility parameter has different meaning for polymers. It defines degree of swelling when a solvent interact with the polymer. PDMS is one of the most preferable polymer in the industry. It has low dispersion energy and zero polar and zero hydrogen bonding with HSP values like [12, 0, 0]. It's solubility parameter versus the logarithm of the linear swelling ratio is figured out with various solvents (Dam 2006). Dotted vertical line in Figure 14 expressed solvents that have very close HSP value with PDMS. Those solvents cause the highest degree of PDMS swelling.

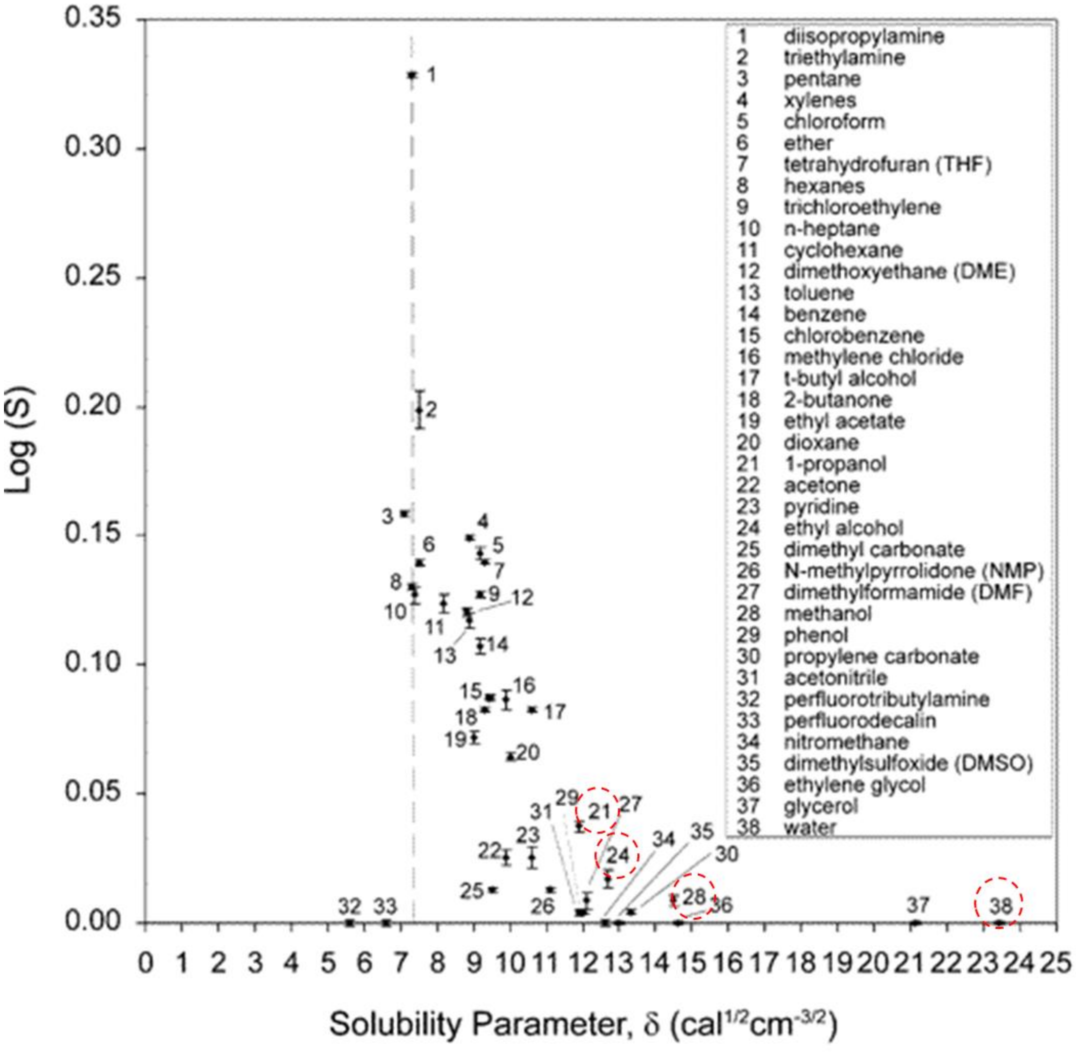

Figure 14. PDMS swelling ratio with solvent vapors (Dam 2006)

The distance between two molecules is called as "Ra ". This is also indicator of polymer-solvent likeness and it can be calculated by Eq 5 where p and s indicate the polymer and solvent contribution. If the distance between polymer and solvent is small, they are more likely to be compatible.

$$Ra = \sqrt{4\left(\delta_{dp} - \delta_{ds}\right)^2 + \left(\delta_{pp} - \delta_{ps}\right)^2 + \left(\delta_{hp} - \delta_{hs}\right)^2} \qquad (Eq\ 5)$$

The swelling degree may enable to predict VOCs/non-condensable gas separation performance of PDMS based membrane. It is known that non-condensable gas (i.e. N_2 and O_2) permeability shows inverse effect with swelling of PDMS polymer. However, it has not given satisfactory information for solvent-solvent separation performance. Rumens et al. evaluated swelling ratio in terms of both weight and volume by expose PDMS elastomers to 15 different solvent vapors (Rumens et al. 2015). In this study, their aim was to associate Ra value with experimental data. They found that solvents that had the closest Ra value to PDMS results in the greatest swelling value. However, they found that if two solvent have closed Ra value to each other, their swelling ratio might be different. They explained this situation with Fickion diffusion. Solvent vapor diffusion rate may be smaller than PDMS chain mobility, so changeable swelling ratio will observe. They added that vapor pressure and molecule size have also impact on swelling ratio of PDMS. Unfortunately, physical properties of PDMS networks in the presence of any solvent has not been predictable yet (Masaro & Zhu 1999).

CHAPTER 3

SYNTHESIS ZEOLITIC IMIDAZILE FRAMEWORKS

3.1 Introduction

Zeolitic imidazolate frameworks (ZIFs) are porous crystalline materials consisting of well-ordered pores. They have high surface area, specific adsorption capacities and often exhibit high thermal, chemical and hydrothermal stability (Bhattacharjee et al. 2014; Phan et al. 2010). These properties make them attractive materials for many applications such as gas storage, separation, catalysis, drug delivery and chemical sensors (Pan et al. 2011; Phan et al. 2010; Keser Demir et al. 2014; Bhattacharjee et al. 2014; Li et al. 2010).

The properties, types and structures of ZIFs depend mainly on different combinations of different imidazole linkers and metal ions (Park et al. 2006; Kida et al. 2013). A great number of ZIFs structures have been reported in the literature, which can be synthesized by using different transition metals (e.g., Zn and Co), imidazole linkers (e.g., 2-methylimidazole, benzimidazole) and solvents such as water, dimethylformamide (DMF), diethylformamide (DEF), ethanol and methanol (Pan et al. 2011; R. Chen et al. 2013; Qian et al. 2012). ZIFs can be synthesized by solvothermal or hydrothermal synthesis methods at temperatures between 298 – 423 K generally using excess amount of imidazole (Banerjee et al. 2008; Bhattacharjee et al. 2014). Recently, research has also been devoted to the development of more efficient methods that increase the chemical yield and reduce the environmental effects (Yao et al. 2015).

ZIF-8 synthesized by solvothermal methods in methanol and DMF has an average particle size of 3-5 μm and 150-200 μm, respectively (Lee et al. 2015). On the other hand, Pan et al. [1] successfully synthesized ZIF-8 nanocrystals (<100 nm) in aqueous solutions containing excess amount of imidazole linker. High imidazole to metal ion molar ratio leads to smaller ZIF-8 crystals since the crystal growth was sterically hindered by excess amount of ligand molecules. Therefore, there is still necessity to develop green synthesis methods for the synthesis of nanosize ZIF materials.

We recently reported the synthesis of ZIF-8 from recycled the mother liquors (Keser Demir et al. 2014). Following the crystallization, the mother liquor contains significant amount of unreacted metal ions, imidazole linkers, possibly intermediate precursor species and large amount of methanol, which was used as solvent. Hence the mother liquor can be recycled for the synthesis of new generation of ZIF-8 crystals. Three different procedures have been developed to recycle the mother liquor. In the first one, only initial amount of Zn^{2+} was added to one-day aged mother liquor. In the second one, the pH of the mother liquor was firstly increased from 7 to 9 by adding NaOH, and then consumed amount of Zn^{2+} was added. In the last one, procedure two was followed but the initial amount of Zn^{2+} was added to the mother liquor instead of consumed amount. The recycling process was repeated four times so that almost all imidazole ligand in the solution was depleted. Total yield increased from 38 % to 80 % by recycling the mother liquors.

In the present study, we showed that different ZIFs can also be synthesized by recycling the mother liquor of the synthesis solution and highlighted the versatility of the previously developed recycling approach. For this purpose, four different ZIFs (ZIF-8, ZIF-L, ZIF-67 and ZIF-7) were selected considering the type of reactants (type of metal ion and imidazolate linker) and solvents (water or organic solvents) necessary for the crystallization. ZIF-8, ZIF-L, and ZIF-67 have been synthesized in aqueous solutions with HMIM (2-methylimidazole), whereas ZIF-7 was prepared in DMF (dimethylformamide) by using Bim (benzimidazole) as imidazole linker. Zinc nitrate hexahydrate ($Zn(NO_3)_2.6H_2O$) was used for ZIF-8, ZIF-L and ZIF-7, on the other hand cobalt nitrate hexahydrate ($Co(NO_3)_2.6H_2O$) was used for ZIF-67. All these ZIFs were synthesized from fresh solutions and recycled mother liquors. The products were characterized by measuring BET equivalent surface area, XRD crystallinity and determining the crystal morphology and thermal stability. The expensive and environmentally undesired imidazole species and organic solvents will be recycled with a small amount of make-up to produce different ZIFs continually. Therefore, this method is expected to reduce the synthesis cost and the environmental impact of ZIF synthesis substantially.

A systematic study carried out and published in order to synthesized ZIF-8, ZIF-L, ZIF-67 and ZIF-7 (Şahin, F.; Topuz, B.;Kalıpçılar 2018). ZIF-71 crystals were synthesized after publishing this article. They only used for as a filler to synthesized ZIF-71/PDMS mixed matrix membrane that mentioned in Chapter 4.

3.2 Experimental Study

3.2.1 Materials

Zinc nitrate hexahydrate ($Zn(NO_3)_2.6H_2O$), 2- methylimidazole (Hmim) ($C_4H_6N_2$), methanol, N,N-dimethyl formamide (DMF), sodium hydroxide (NaOH), potasyum hydroxide (KOH), zinc acetate, 4,5-dichloroimidizole and benzimidazole (Bim) were purchased from Sigma–Aldrich. Cobalt nitrate hexahydrate ($Co(NO_3)_2.6H_2O$) was obtained from MCB. All chemicals were used as purchased.

3.2.2 Synthesis of ZIFs Crystals from Fresh Solution

ZIF-8 synthesis was carried out by using water as solvent at room temperature. In a typical synthesis, 2.34 g $Zn(NO_3)_2$ was dissolved in 16 g deionized (DI) water; and 45.4 g Hmim was dissolved in 160 g DI water. Both solutions were mixed to obtain crystal mixture with a molar composition of Zn^{2+}: Hmim: H_2O=1:70:1243. The crystallization mixture was stirred 30 minutes at room temperature (23 ±2 ^oC). The product, named as ZIF-8.0, was recovered by centrifugation (at 2655 relative centrifugal force (RCF) for 30 min) and rinsed with methanol. This purification step repeated twice. The product was dried at 80 ^oC overnight.

The synthesis of ZIF-L was carried out from fresh solution with a molar composition of Zn^{2+}: Hmim: H_2O=1:8:2240 as follows (R. Chen et al. 2013) . The zinc nitrate solution (0.59 g of $Zn(NO_3)_2$ in 40 g DI water) and imidazole solution (1.3 g of Hmim in 40 g DI water) were prepared separately and then mixed. After stirring for 4 h at room temperature, the product was recovered by centrifugation (at 2655 RCF, for 45 min) and then washed with water twice and methanol twice subsequently. This powder, named as ZIF-L.0, was dried at 70 ^oC overnight.

ZIF-67, called as ZIF-67.0, was also synthesized in aqueous medium. Typically, 2.704 g cobalt nitrate hexahydrate and 44.24 g Hmim were dissolved in 24 g and 160 g DI water, respectively. These two solutions were then mixed to obtain a mixture with a molar composition of Co^{2+}: Hmim: H_2O =1:58:1100. The crystallization was performed at room temperature by stirring for 6 h. The product was recovered by centrifuging at 2655 RCF for 30 min and washed with water three times and methanol three times subsequently. Afterwards, the product was dried at 70 ^oC overnight.

Zinc nitrate (1.269 g) and benzimidazole (3.231 g) were mixed, and this solid mixture was dissolved in 398.16 g DMF at room temperature for the synthesis of ZIF-7. The molar composition of fresh solution was Zn^{2+}: Bim: DMF=1:6:1277 . The synthesis was carried out at 50 ^oC for 46 h. The synthesis mixture was centrifuged (at 2655 RCF for 10 min) to recover ZIF-7 which was then washed with methanol three times. The ZIF-7 protected from fresh solution was called as ZIF-7.0.

ZIF-71 was synthesized by following the reported procedure (Y. Li, Lik H Wee, Martens & Ivo F J Vankelecom 2014). Zinc acetate (0.73 g) and 4,5-dichloroimidizole (2.2 g) in 150 ml of methanol were prepared separately. The crystallization mixture stirred 30 minutes and left static for 24h at room temperature. After removing methanol, crystal precipitation were soaked in chloroform for two days to remove remaining methanol. Finally, ZIF-71 crystals recovered by centrifugation.

3.2.3 Synthesis of ZIFs Crystals from Recycled of Mother Liquors

After synthesis of ZIFs, mother liquor (ML) was separated by centrifugation for use in the synthesis of next generation of ZIF crystals. The new synthesis solution was formulated by adding NaOH or KOH, metal ion, and imidazole to the mother liquor. The amount of chemicals added to the ML is shown in Table 9 for each type of ZIF and for each recycling. Table 10 presents the molar ratio of synthesis solution, ML and modified ML based on metal salt/organic ligand/solvent. The crystallization time, temperature, centrifugation conditions and the molar compositions of synthesis solutions were also shown in Table 10. In those tables ZIF-X.0, ZIF-X.1 and ZIF-X.2 denote the crystals synthesized from fresh solution, first recycled and second recycled mother liquors, respectively. The first recycled ML implies the solution remained from the synthesis with fresh solution and the second recycled ML implies the solution remained from the synthesis with first ML.

Table 9. Amount of components used for the synthesis of ZIFs. Superscripts indicate the type of metal ion, organic linker and solvent used for the synthesis of a particular ZIF. Aging was carried out at room temperature overnight.

Sample Name	Metal ion (g)	Organic Linker (g)	Solvent (g)	NaOH [g] or KOH [h] (g)	Mother Liquor (g)	Aging
ZIF-8.0	2.34 [a]	45.4 [c]	176 [e]	x	x	x
ZIF-8.1	x	x	x	0.44 [g]	221.82	√
ZIF-8.2	1.81 [a]	x	x	x	220.64	x
ZIF-L.0	0.59 [a]	1.3 [c]	80 [e]	x	x	x
ZIF-L.1	0.337 [a]	x	x	0.132 [g]	81.19	√
ZIF-L.2	0.463 [a]	0.435 [c]	x	x	81.09	x
ZIF-67.0	2.704 [b]	44.24 [c]	184 [e]	x	x	x
ZIF-67.1	x	x	x	0.49 [g]	229.27	√
ZIF-67.2	1.90 [b]	x	x	x	229.04	x
ZIF-7.0	1.269 [a]	3.231 [d]	398.16 [f]	x	x	x
ZIF-7.1	0.52 [a]	x	x	0.243 [h]	401.5	√
ZIF-7.2	0.53[a]	0.625[d]	x	x	401.3	x

(a) $Zn(NO_3)_2.6H_2O$ or (b) $Co(NO_3)_2.6H_2O$; (c) Hmim or (d) Bim; (e) Water or (f) DMF

3.2.4 Characterization of ZIFs

Phase identification was carried out by Bruker X-ray diffractometer operating at 40 kV and 40 mA with Cu Kα radiation. The relative crystallinities were calculated based on the peaks of ZIFs at Bragg angles between 7 and 25°. For each type of ZIF, the one produced from fresh synthesis solution (ZIF-X.0) was designated as the reference with 100% crystallinity and the relative crystallinities of all other samples were determined with regard to the reference sample (Park et al. 2006; R. Chen et al. 2013; Gross et al. 2012).

Table 10. Crystallization time and temperature of the ZIFs synthesized from fresh and recycled solution, and centrifugation period (at 2655 RCF) to recover ZIF crystals; molar compositions of synthesis solution, remaining mother liquor by mass balance and modified mother liquors. The solution composition is given in the order of metal ion: organic ligand: solvent

Sample name	Crystallization		Centrifugation period (min)	Synthesis solution	Mother liquor	Modified mother liquor
	t (h)	T (^{o}C)				
ZIF-8.0	0.5	23	30	1:70:1243	1:222:4015	1:222:4015
ZIF-8.1			40	1:222:4015	1:318:5902	1:70:1275
ZIF-8.2			30	1:70:1275	1:162:3070	
ZIF-L.0	4	23	45	1:8:2240	1:36:13562	1:8:3045
ZIF-L.1			70	1:8:3045	1:25:10287	1:8:2240
ZIF-L.2			45	1:8:2240	1:17:6054	
ZIF-67.0	6	23	30	1:58:1100	1:166:3236	1:166:3236
ZIF-67.1			45	1:166:3236	1:198:3875	1:58:1116
ZIF-67.2			30	1:58:1116	1:79:1562	
ZIF-7.0	46	50	10	1:6:1277	1:11:2594	1:6:1420
ZIF-7.1			30	1:6:1420	1:8:2197	1:6:1277
ZIF-7.2			10	1:6:1277	1:7:1568	

The yield was defined as the ratio of the amount of solid product obtained from 100 g of synthesis mixture to the maximum possible amount of ZIF that can be produced from 100 g of synthesis mixture if all limiting reactant is consumed. The unit cell formula of ZIF-8, ZIF-L, ZIF-67 and ZIF-7 are $Zn_6N_{24}C_{48}H_{60}$ (Keser Demir et al. 2014) , $C_{10}H_{16}N_5O_{3/2}$ Zn (R. Chen et al. 2013), $Co_6N_{24}C_{48}H_{120}$ and $C_{56}H_{64}N_{16}O_{12}Zn_4$ (Park et al. 2006) , respectively.

Crystal morphology and size was determined by using QUANTA 400F Field Emission series scanning electron microscopy. The average particle size was determined by counting at least 50 particles on each SEM image. For particle size determination, three samples synthesized at different times were used. This approach was followed for all samples. Thermal behavior of ZIFs was determined by TGA (Shimadzu DTG-60H) with a heating rate of 10^{o}C/min under a continuous-flow of air between 40 and 800 ^{o}C. The N_2 adsorption-desorption isotherms were obtained by using Micromeritics Tristar II instruments at 77 K. The CO_2 adsorption-desorption isotherms were obtained by the same instrument at 0 ^{o}C. The ZIF-8, ZIF-L, ZIF-67 and ZIF-7 were degassed at 135 ^{o}C (24 hours), 110 ^{o}C (24 hours), 200 ^{o}C (24 hours) and 150 ^{o}C (16 hours) in vacuum, respectively.

3.3 Results and Discussion

3.3.1 Synthesis of ZIFs from Fresh Crystallization Solution

ZIF-8.0, ZIF-L.0, ZIF-67.0 and ZIF-7.0 were synthesized using molar ratios given in the literature (Pan et al. 2011; R. Chen et al. 2013; Qian et al. 2012; Liu et al. 2011). XRD patterns of the as-synthesized ZIFs from fresh solutions are shown in Figure 15, which also includes the patterns from the literature as reference. The relative intensities and the peak positions of each sample match well with the corresponding reference (Park et al. 2006; R. Chen et al. 2013; Gross et al. 2012; Yin et al. 2017). There is no evidence for the formation of any other crystalline phases in the samples.

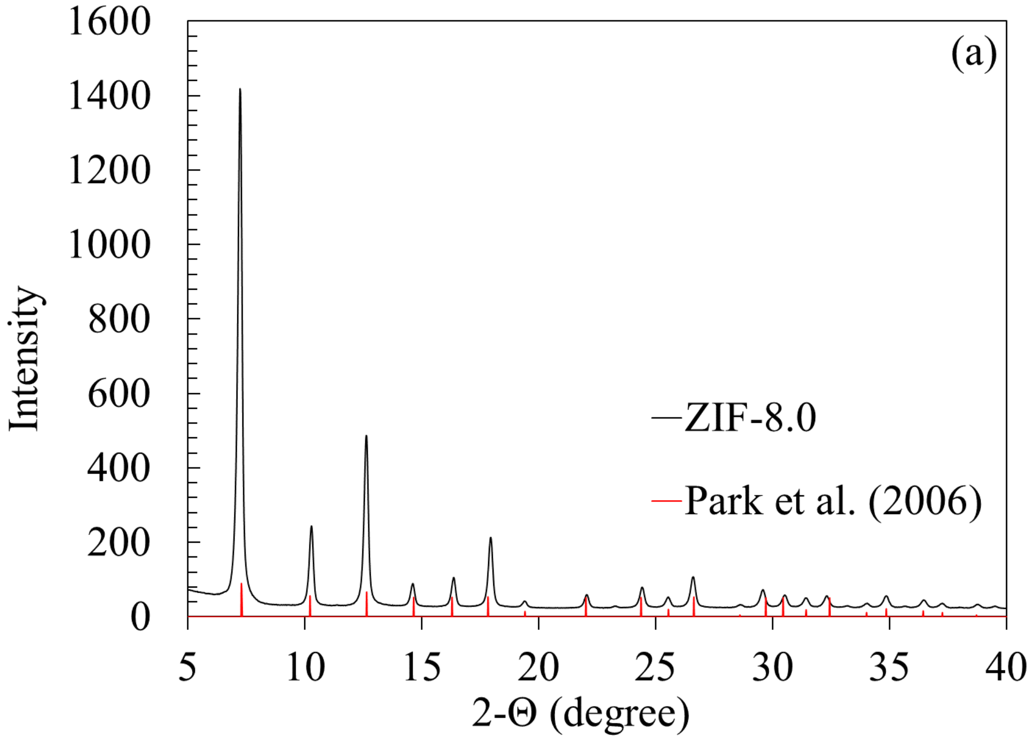
(a)
Intensity
0
200
400
600
800
1000
1200
1400
1600
5
10
15
20
25
30
35
40
2-Θ (degree)
ZIF-8.0
Park et al. (2006)

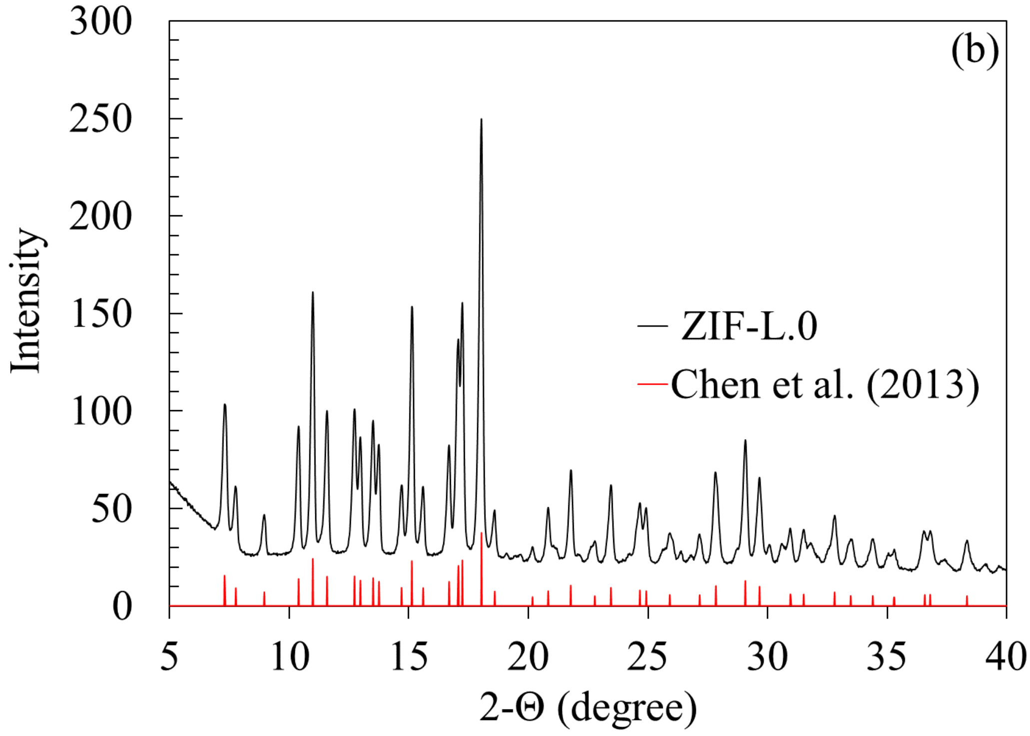
(b)
Intensity
0
50
100
150
200
250
300
5
10
15
20
25
30
35
40
2-Θ (degree)
ZIF-L.0
Chen et al. (2013)

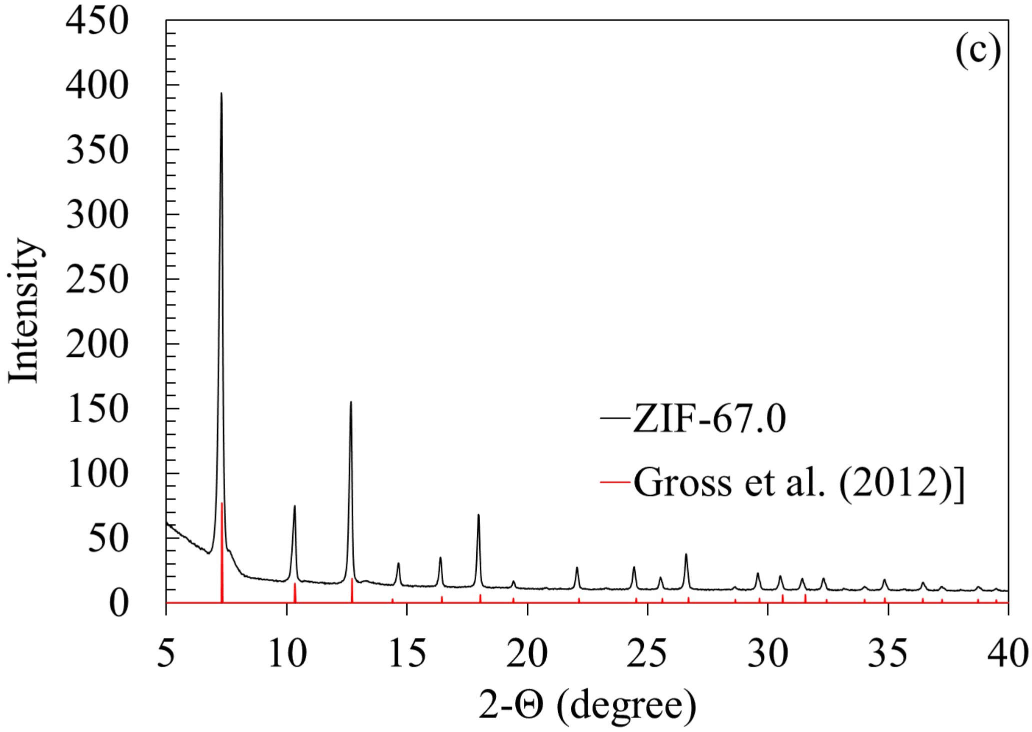
(c)
Intensity
0
50
100
150
200
250
300
350
400
450
5
10
15
20
25
30
35
40
2-Θ (degree)
ZIF-67.0
Gross et al. (2012)]

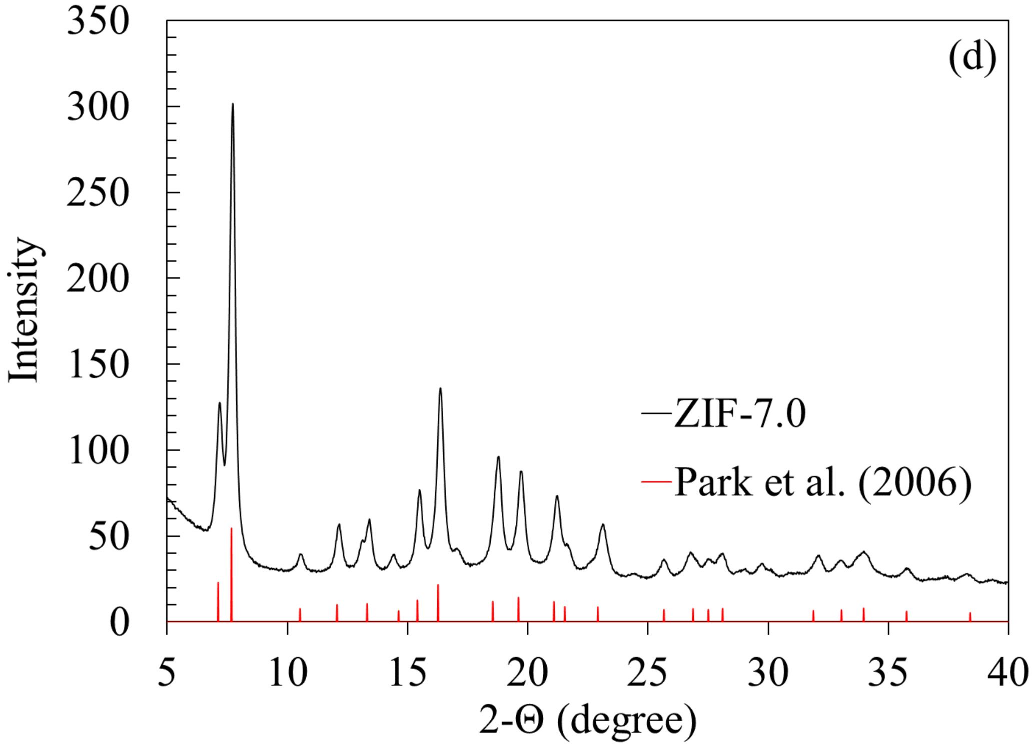
(d)
Intensity
0
50
100
150
200
250
300
350
5
10
15
20
25
30
35
40
2-Θ (degree)
ZIF-7.0
Park et al. (2006)

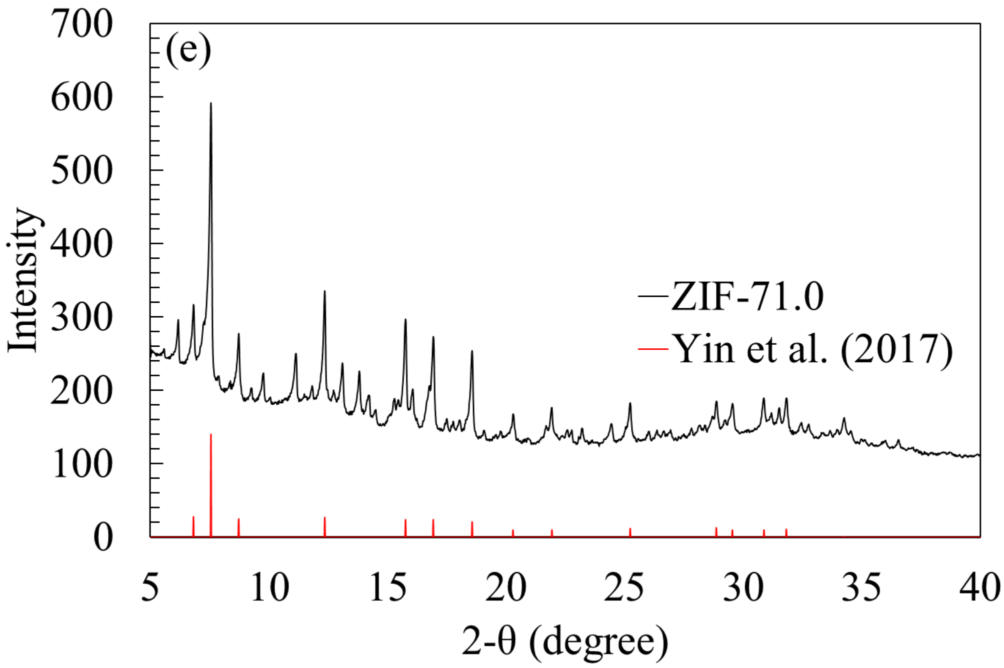

Figure 15. XRD patterns of ZIFs produced from fresh synthesis solution; (a) ZIF-8.0 (b) ZIF-L.0 (c) ZIF-67.0 (d) ZIF-7.0 (e) ZIF-71.0. The red line shows the reference patterns.

3.3.2 Synthesis of ZIFs from Recycled Mother Liquor

Recently, Pan et al.(Pan et al. 2011) has shown the synthesis of ZIF-8 in water, which is an environmental friendly and cheaper solvent than organic solvents. However, the molar ratio of Hmim/Zn^{2+} is significantly higher in the water route (Pan et al. 2011) than in the methanol route (Keser Demir et al. 2014; Surendar R. Venna et al. 2010). If the molar ratio of Hmim/Zn^{2+} is reduced, other types of ZIF crystals such as ZIF-L are obtained. Therefore, recycling is essential for efficient and environmental friendly synthesis of not only ZIF-8 but also all ZIFs. For instance, DMF, which is a very hazardous aprotic solvent, is the only solvent used in the synthesis of another type of ZIF called ZIF-7. It is crucial to reuse this solvent to synthesize ZIF-7 crystals again.

Following the crystallization from fresh solutions, ML (mother liquor) for each ZIF was also recovered and recycled to synthesize new generation of ZIFs as described in the experimental section. Figure 16 presents the XRD patterns for ZIF crystals produced from fresh solution (ZIF-X.0), the first recycled mother liquor (ZIF-X.1) and the second recycled mother liquor (ZIF-X.2). All patterns obtained from the recycled solutions perfectly matched with the pattern of respective ZIF obtained from the fresh solution.

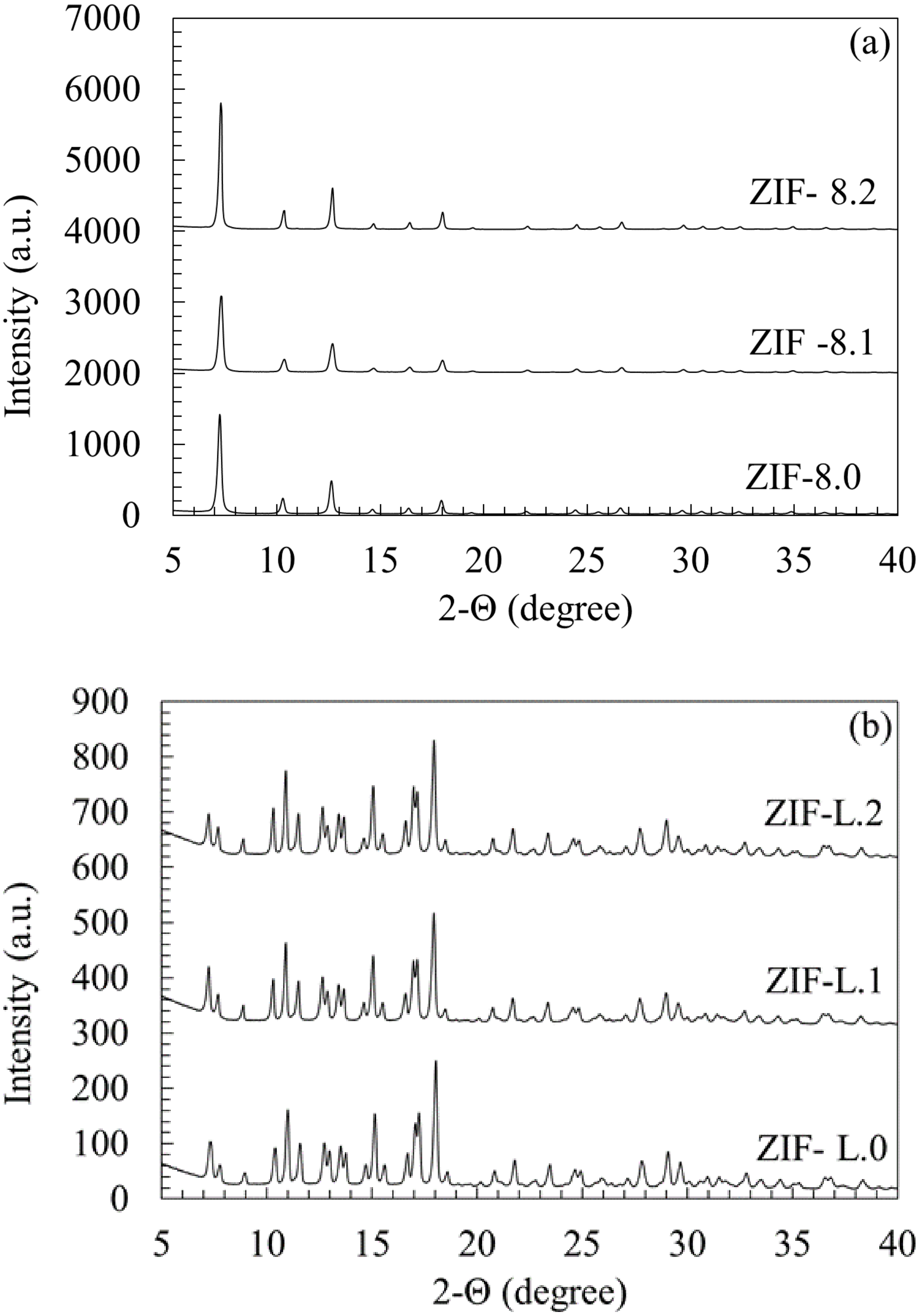

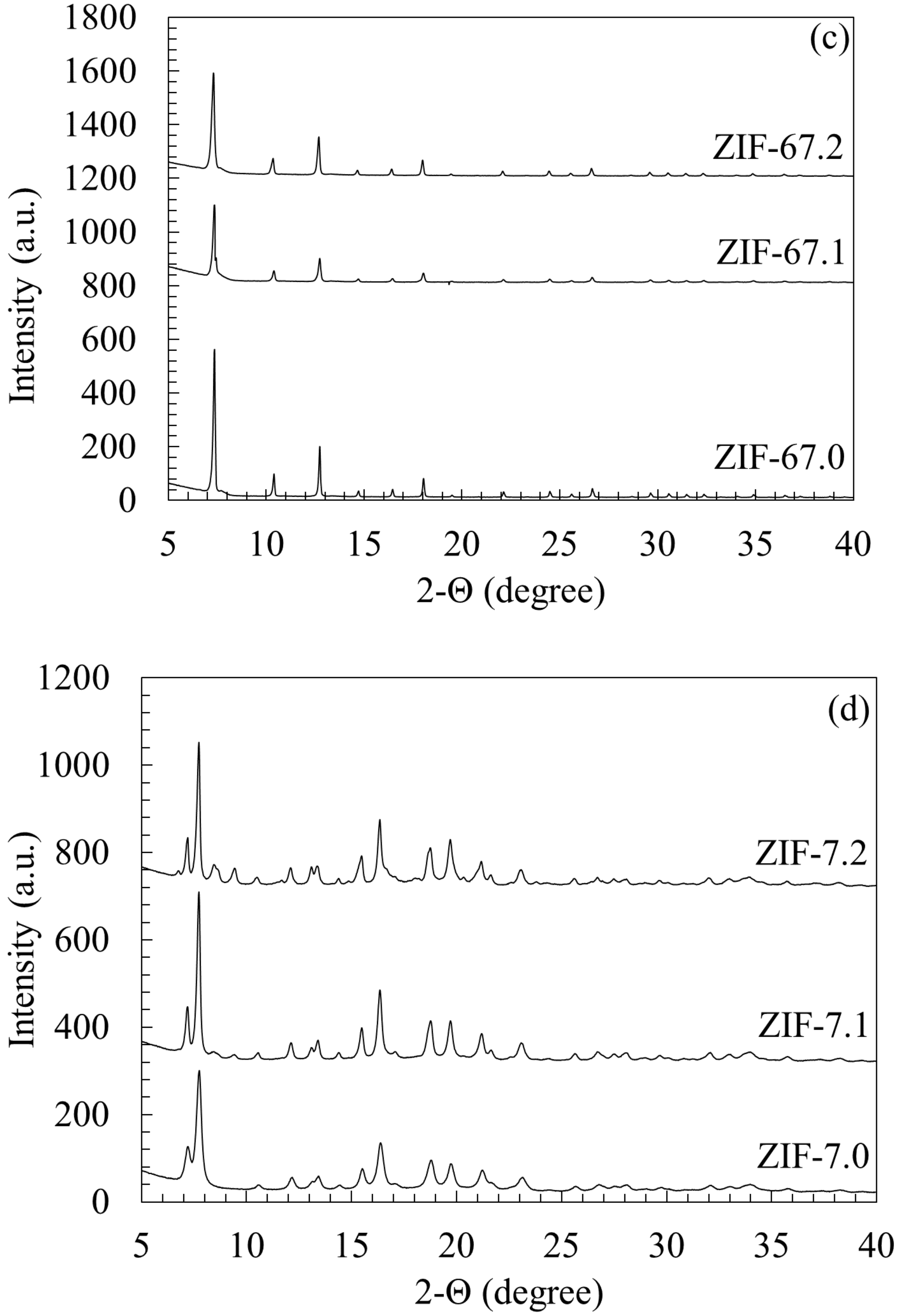

Figure 16. XRD patterns of ZIFs synthesized from fresh solutions and mother liquors (a) ZIF-8 (b) ZIF-L (c) ZIF-67 (d) ZIF-7. ZIF-X.0 synthesis from fresh solution, ZIF-X.1 synthesis from first mother liquor, and ZIF-X.2 synthesis from second mother liquor.

To show the reproducibility of synthesis and recycling process, each type of ZIF was synthesized at least five times starting with the fresh solution. The results clearly indicated that the mother liquor can be recycled and successfully used to produce new generations of different types of ZIFs. X-Ray diffraction of ZIF that were synthesized from different batch is given in Appendix Part A (A1- A4).

The relative crystallinities of ZIF-X.1 and ZIF-X.2 are calculated with reference to the crystallinity of ZIF-X.0, which is assumed to be 100 % (Table 11). All results are given in Appendix Part B (B1-B4). The crystallinity of ZIF-8.1 and ZIF-67.1 dropped to 70% and 63%, respectively. ZIF-8.1 and ZIF-67.1 were synthesized in the solutions with Zn^{+2}:Hmim ratio of 1:222 and 1:166 respectively. In addition, the synthesis mixtures were diluted with solvent after first recycling such that the Zn^{+2}:H_2O ratio was 1:4015 for ZIF-8 and 1:3236 for ZIF-67 (Table 10). The lower crystallinity of ZIF-X.1 can be attributed to decrease in the relative amount of metal ions and to dilution of synthesis medium. The addition $Zn(NO_3)$ to the second ML have endorsed the crystallization so that ZIF-8.2 and ZIF-67.2 had more crystallinity than ZIF-8.1 and ZIF-67.1.

Table 11. The yield and crystallinity ZIFs obtained from fresh and recycled mother liquors

ZIFs crystal	Yield (%)	Crystallinity (%)
ZIF-8.0	68 ± 2	100
ZIF-8.1	35 ± 7	70 ± 4
ZIF-8.2	62 ± 3	85 ± 17
ZIF-L.0	84 ± 1	100
ZIF-L.1	70 ± 2	90 ± 4
ZIF-L.2	26 ± 8	96 ± 9
ZIF-67.0	66 ±1	100
ZIF-67.1	17 ± 3	63 ± 11
ZIF-67.2	27 ± 4	74 ± 13
ZIF-7.0	51 ±1	100
ZIF-7.1	35 ±5	125 ± 17
ZIF-7.2	19 ±1	117 ± 14

For recycling of ZIF-7 and ZIF-L, the composition of mother liquor was arranged in such a way that its metal:organic linker ratio was the same as the fresh solution with some dilution (Table 10). Apparently, the metal: organic linker ratio has more impact on the crystallization. Therefore, no considerable change was observed in the crystallinity of ZIF-L with increasing the number of recycling while a slight increase was observed for ZIF-7.

Though, the recycling had a strong influence on the yield, which was calculated by assuming that all solid recovered from the synthesis mixture is ZIF, which was also supported by XRD patterns. Calculated yield of each crystallization reaction is given in Appendix Part C (C1- C4). The yield obtained from the crystallization in fresh solution was always higher than the crystallization in first and second ML. For ZIF-8, the yield was greater than 60 % when the synthesis was carried out with fresh solution and dropped to 35 % in the synthesis with first recycled ML due to substantial depletion of Zn^{2+} in the synthesis solution. Prior to synthesis from second recycled ML, Zn^{+2} was added to the mother liquor, and as expectedly, the yield increased to 62 %. On the other hand, the yield decreased constantly for other types of ZIFs. No more recycling was performed after the synthesis in the second recycled solution, since the amount of Hmim in the mother liquor was anticipated to be very low based on the material balance carried out using the yield.

SEM images of the different types of ZIFs and their average particle sizes were shown in Figure 17 to Figure 21 and Tablo 10, respectively. All ZIFs exhibited their characteristic morphology regardless of whether the fresh or recycled solution was used for synthesis. ZIF-8 crystals synthesized in the fresh solution had hexagonal facets (Figure 17) with an average size of 77 nm. Synthesis from recycled solutions resulted in a small change in the average particle size. In all samples, ZIF-8 crystals exhibited a narrow distribution, which is in a good agreement with several reports using the same preparation protocol of fresh solution (Pan et al. 2011).

ZIF-L had two dimensional leaf-shaped-morphology as reported previously (Figure 18) (Low, Razmjou, et al. 2014; Q. Liu et al. 2014; R. Chen et al. 2013). There are bright lines are seen in SEM image since some ZIF-L crystals are standing upright or fractured . Aspect ratio of ZIF-L.0, ZIF-L.1 and ZIF-L.2 is approximately 2 (Table 12) which was similar to ZIF-L crystals prepared by Chen et al. (R. Chen et al. 2013), who produced crystals with a length and width of 5µm x 2µm. On the other hand, the thickness of ZIF-L crystals, which is approximately 150±39 nm, is very small compared to its length and width. Those particles are semi-transparent hence; the underneath ZIF-L particles can also be seen in the SEM images.

ZIF-67 had polyhedral shape (Qian et al. 2012; H. Li, Hong Ma, Wang, Jin Gao, et al. 2014) (Figure 19) and exhibited a tendency to aggregate into larger particles. The average crystal size of ZIF-67.0 was 281 nm and considerably increased with recycling. The SEM pictures show that the ZIF-7 particles have a well-defined shape and narrow size distribution (Figure 20) . The average particle size was around 65 nm for ZIF-7.0, and much larger particles were obtained by synthesis in the recycled ML.

Table 12. The average particle size based on SEM images and BET-equivalent surface area of ZIFs obtained from fresh and recycled mother liquors.

ZIFs crystal	Average particle size	BET surface area (m^2/g)
ZIF-8.0	77 ± 4 nm	1424
ZIF-8.1	79 ± 19 nm	1293
ZIF-8.2	98 ± 4 nm	1383
ZIF-L.0	3.68 ± 0.98 x 1.56 ± 0.41 μm	289
ZIF-L.1	3.77 ± 1.45 x1.70 ± 0.45 μm	263
ZIF-L.2	2.03 ± 0.71 x1.02 ± 0.2 μm	301
ZIF-67.0	281 ± 24 nm	1329
ZIF-67.1	560 ± 37 nm	1090
ZIF-67.2	452 ± 44 nm	1322
ZIF-7.0	65 ± 3 nm	75
ZIF-7.1	220 ± 26 nm	
ZIF-7.2	173 ± 21 nm	
ZIF-71.0	2.08 ± 1.85 μm	650

The morphology of ZIF-71 crystals that are cubic-shaped had determined via SEM images (Figure 21). The average particle size of ZIF-71 is nearly 2.08 μm with a standard deviation of 1.85 μm.

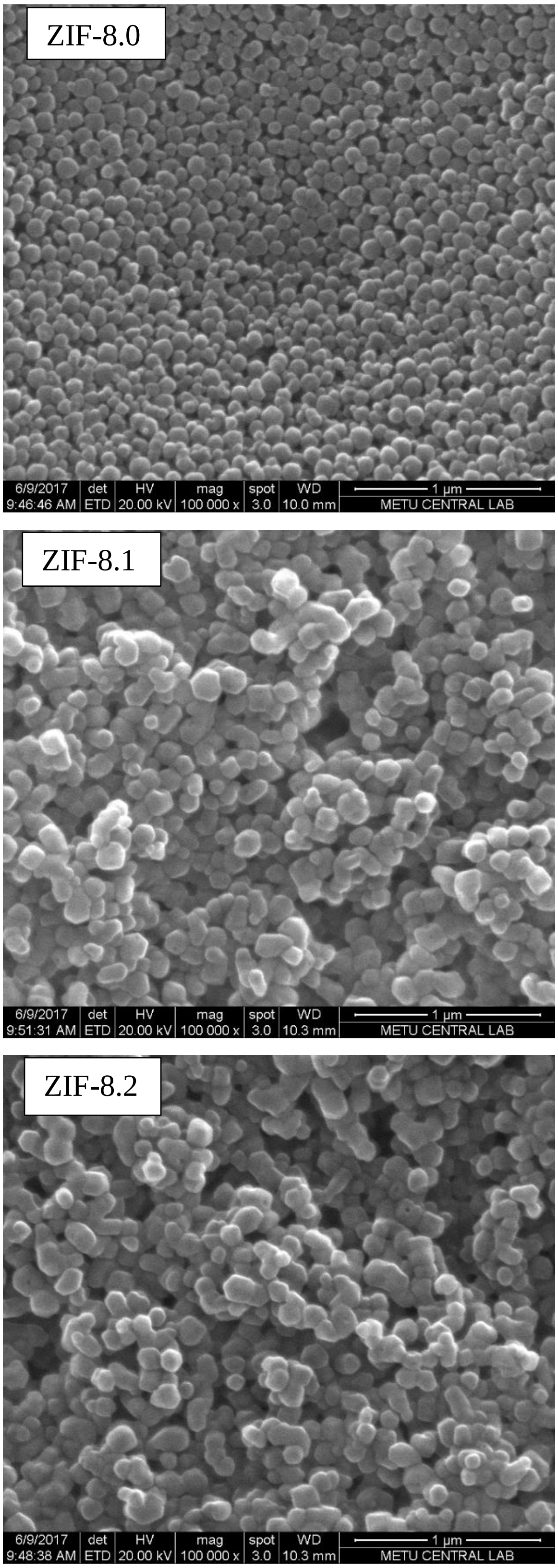

Figure 17. SEM images of ZIF-8.0, ZIF-8.1 and ZIF-8.2, which are synthesized from fresh solutions and mother liquors.

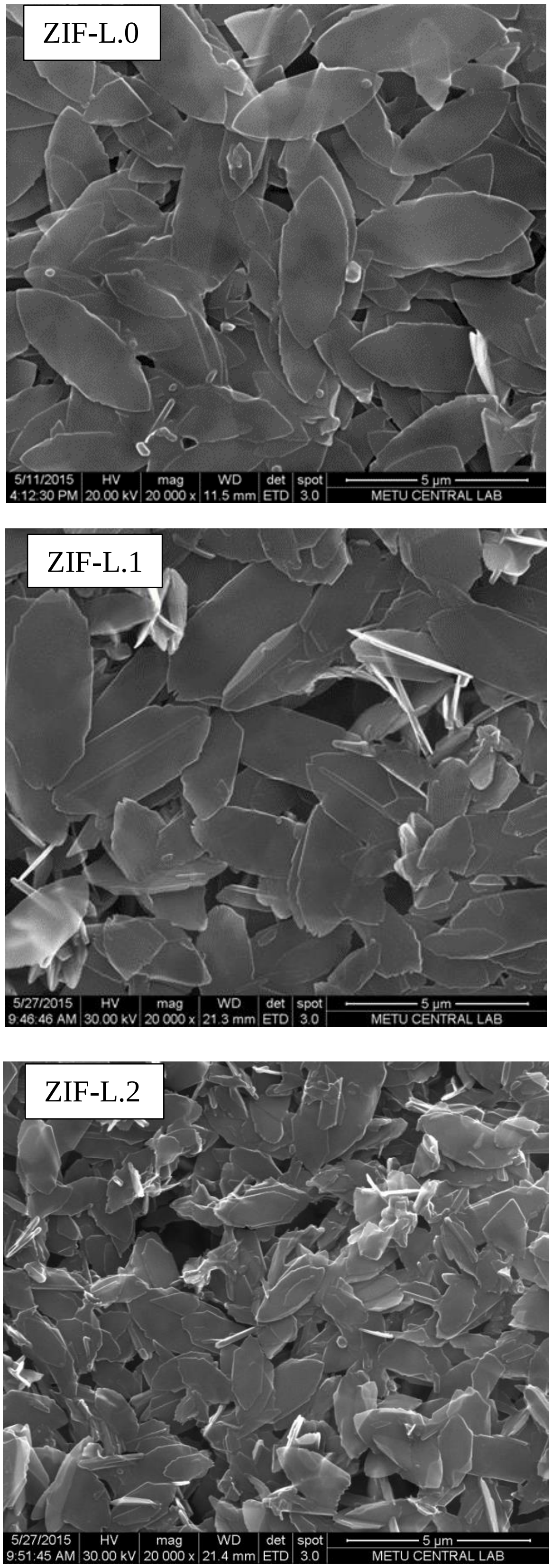

Figure 18. SEM images of ZIF-L.0, ZIF-L.1 and ZIF-L.2, which are synthesized from fresh solutions and mother liquors.

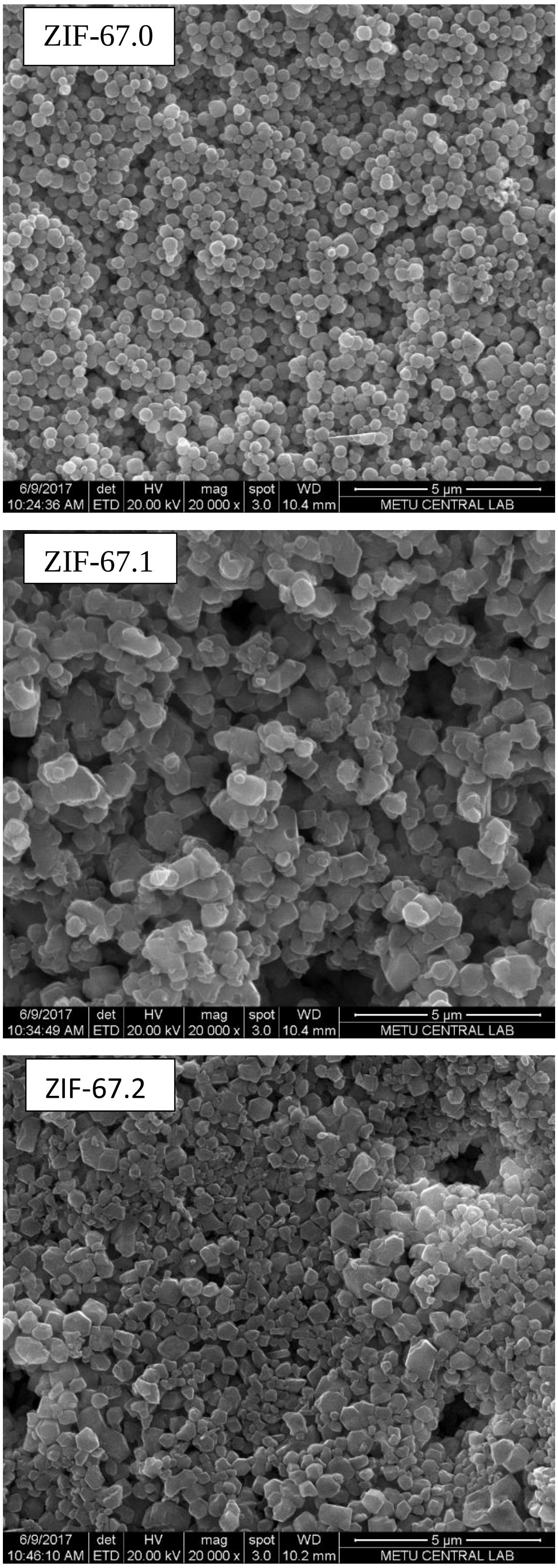

Figure 19. SEM images of ZIF-67.0, ZIF-67.1 and ZIF-67.2, which are synthesized from fresh solutions and mother liquors.

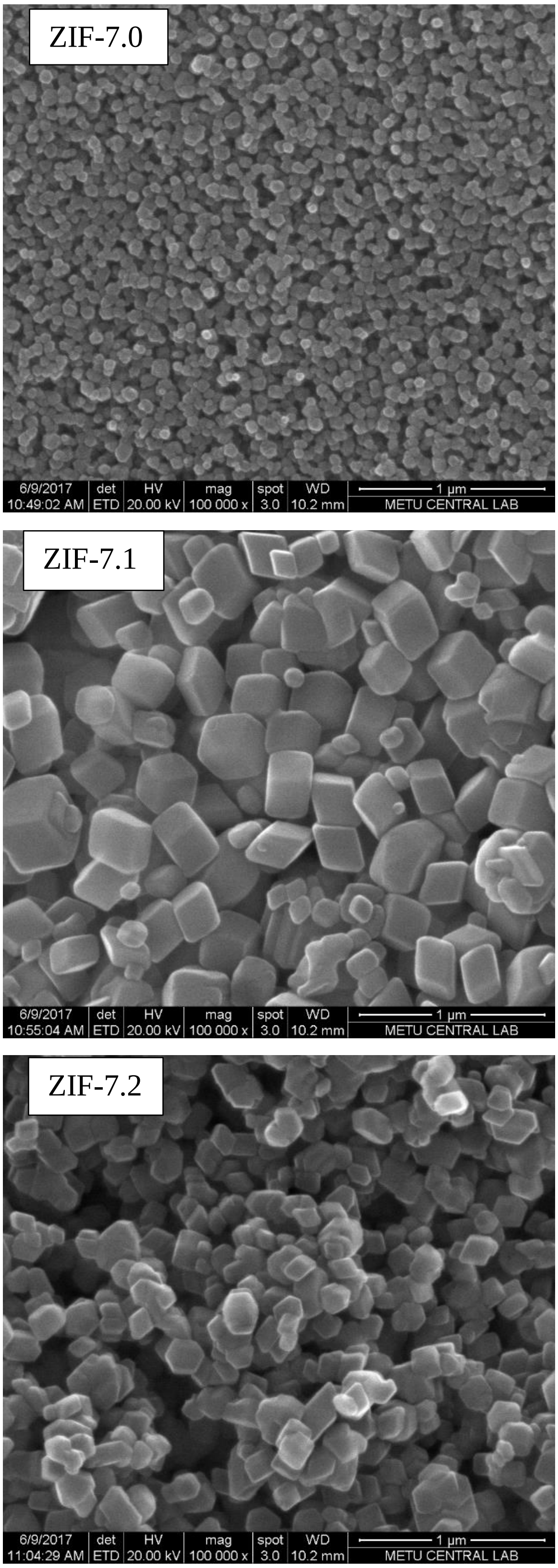

Figure 20. SEM images of ZIF-7. ZIF-7.0, ZIF-7.1 and ZIF-7.2, which are synthesized from fresh solutions and mother liquors.

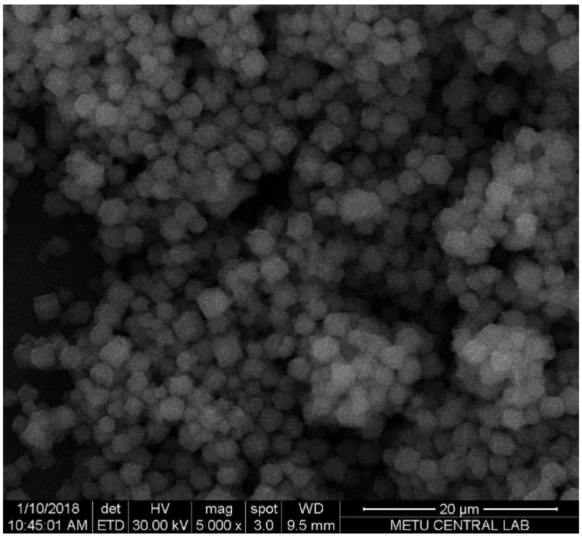

Figure 21. SEM images of ZIF-71.0

ZIF-8, ZIF-L and ZIF-67 showed Type I-N_2 adsorption isotherms at 77 K with no hysteresis, which is characteristic to microporous materials (Figure 22 a,b and c) (Pan et al. 2011; Keser Demir et al. 2014; Qian et al. 2012; Li et al. 2012; R. Chen et al. 2013). The respective N_2 adsorption capacity was approximately 480 cm^3STP/g, 100 cm^3STP/g and 440 cm^3STP/g for ZIF-8, ZIF-L and ZIF-67 regardless of the synthesis method.

Li et al. reported that N_2 adsorption capacity of ZIF-7 was nearly 150 cm^3 STP/g, whereas Bergh et al.(Bergh, Johan; Gücüyener, Canan;Pidko, Evgeny;Hensen, Emiel;Gascon, Jorge;Kapteijn 2011) and Thompson et al.[22] observed no N_2 adsorption on ZIF-7 due to its small pore opening. In the present study, the volume adsorbed was approximately 50 cm^3 STP/g for ZIF-7.0 and almost no adsorption was observed on ZIF-7.1 and 7.2 (Figure 22. d). Therefore, ZIF-7 was also characterized by CO_2 adsorption at 273 K (Figure 23). CO_2 adsorption isotherm of all samples were similar to those reported by Wu et al. (Wu et al. 2006) , and Wang et al (Wang et al. 2014). All isotherms clearly illustrated that ZIFs produced from fresh and recycled mother liquors have similar pore structure.

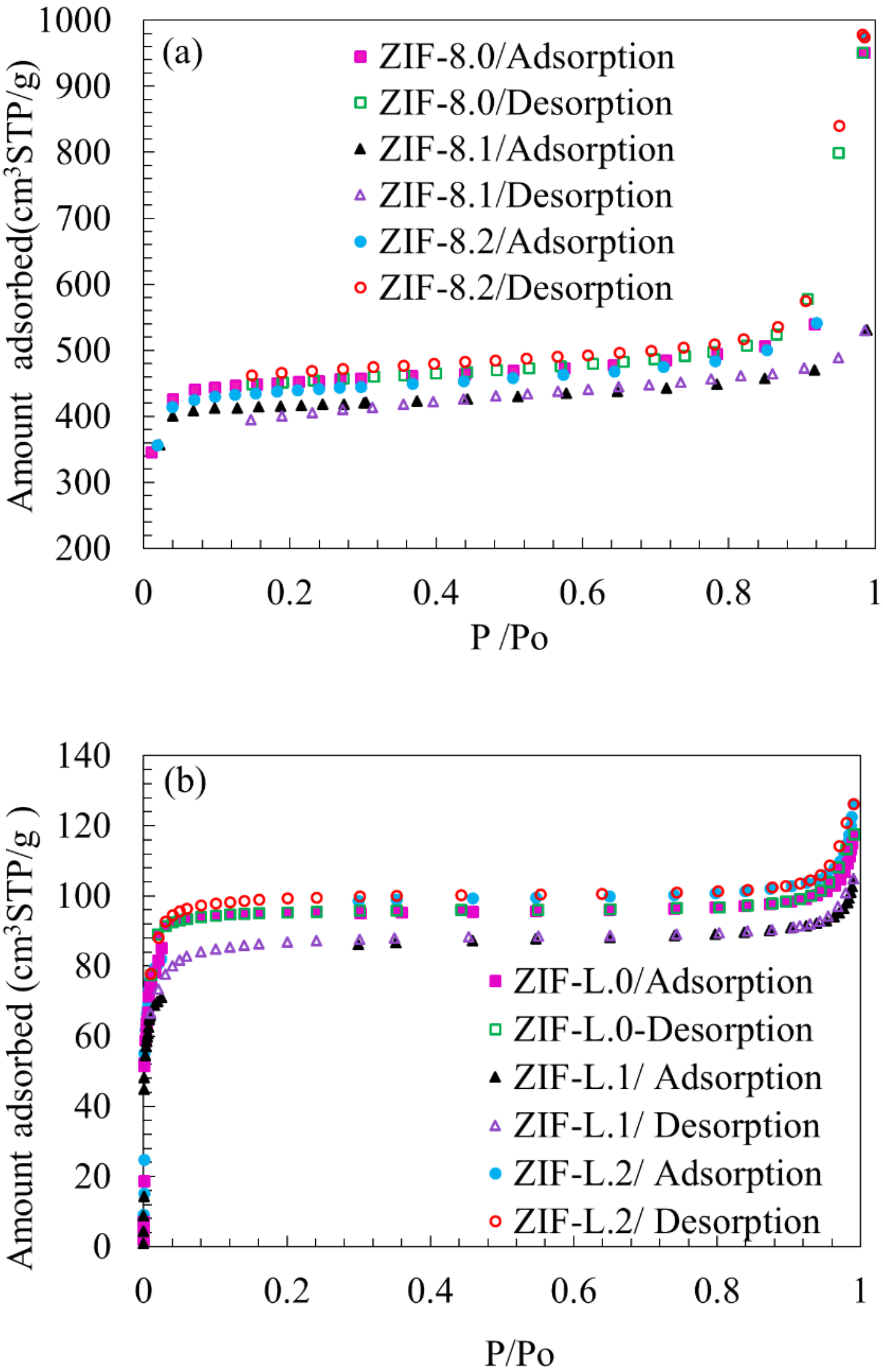
(a)
ZIF-8.0/Adsorption
ZIF-8.0/Desorption
ZIF-8.1/Adsorption
ZIF-8.1/Desorption
ZIF-8.2/Adsorption
ZIF-8.2/Desorption
Amount adsorbed(cm3STP/g)
1000
900
800
700
600
500
400
300
200
0
0.2
0.4
0.6
0.8
1
P /Po
(b)
ZIF-L.0/Adsorption
ZIF-L.0-Desorption
ZIF-L.1/ Adsorption
ZIF-L.1/ Desorption
ZIF-L.2/ Adsorption
ZIF-L.2/ Desorption
Amount adsorbed (cm3STP/g)
140
120
100
80
60
40
20
0
0
0.2
0.4
0.6
0.8
1
P/Po

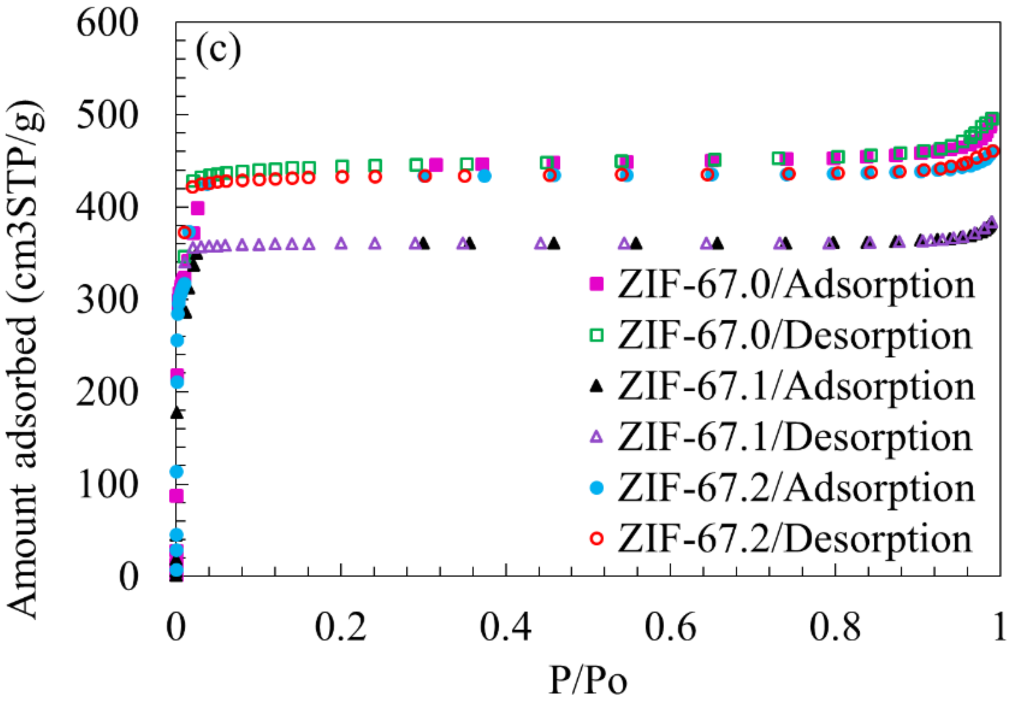
(c)
Amount adsorbed (cm3STP/g)
600
500
400
300
200
100
0
0
0.2
0.4
0.6
0.8
1
P/Po
ZIF-67.0/Adsorption
ZIF-67.0/Desorption
ZIF-67.1/Adsorption
ZIF-67.1/Desorption
ZIF-67.2/Adsorption
ZIF-67.2/Desorption

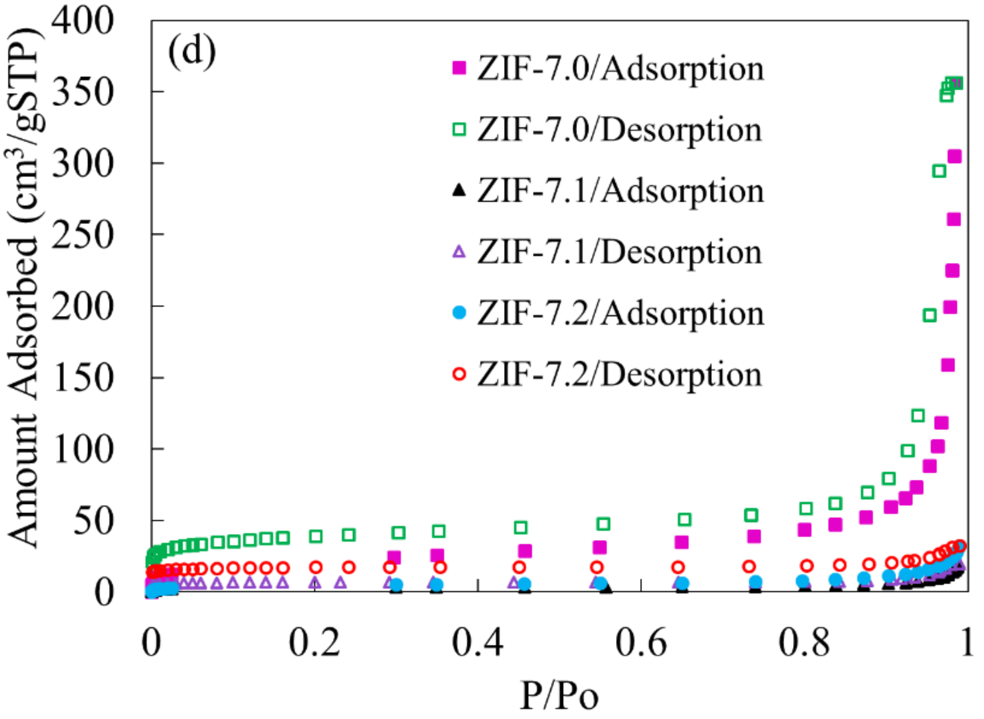
(d)
Amount Adsorbed (cm^3/gSTP)
400
350
300
250
200
150
100
50
0
0
0.2
0.4
0.6
0.8
1
P/Po
ZIF-7.0/Adsorption
ZIF-7.0/Desorption
ZIF-7.1/Adsorption
ZIF-7.1/Desorption
ZIF-7.2/Adsorption
ZIF-7.2/Desorption

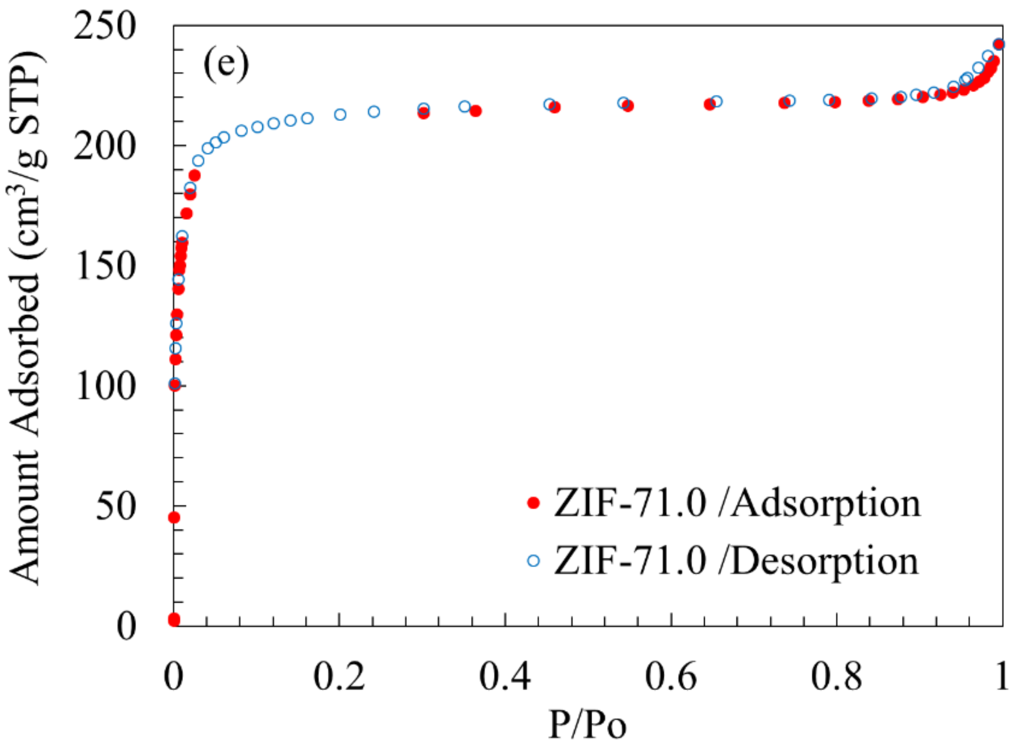

Figure 22. N_2 adsorption/desorption isotherms of (a) ZIF-8 (b) ZIF-L (c) ZIF-67 (d) ZIF-7 (e) ZIF-71synthesized from fresh solutions and mother liquors.

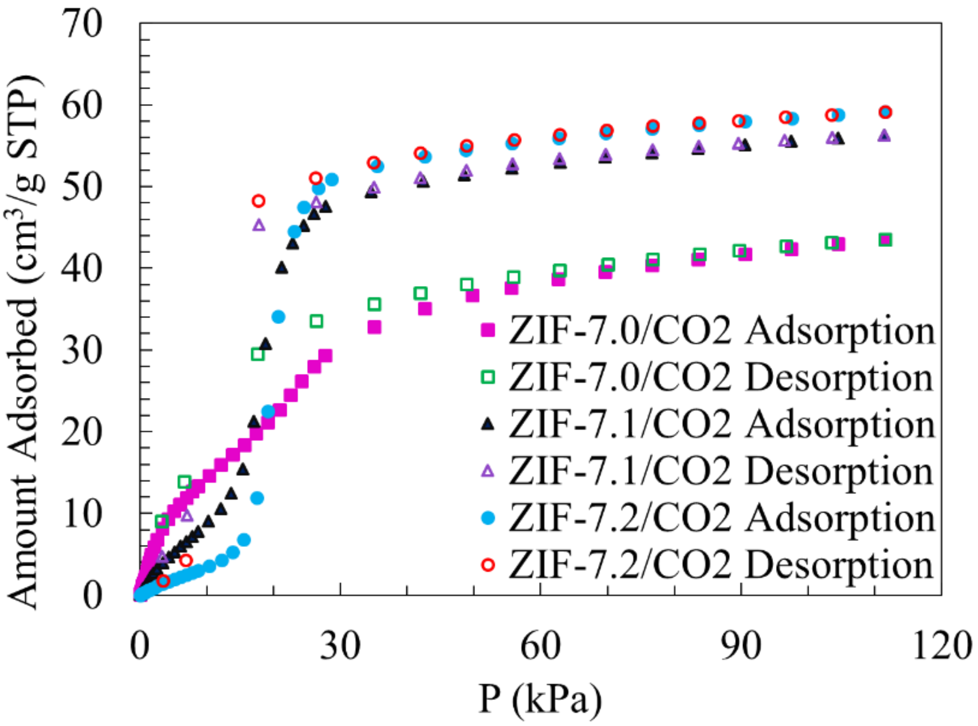

Figure 23. CO_2 adsorption/desorption isotherms of ZIF-7.0, ZIF-7.1 and ZIF-7.2, which are synthesized from fresh solutions and mother liquors.

BET equivalent surface area of ZIFs are shown in Table 12. ZIF-8 samples have BET equivalent surface area of approximately 1300 m^2/g, which is in good agreement with the literature (Keser Demir et al. 2014; Pan et al. 2011; Kida et al. 2013). Surface area of ZIF-8 synthesized in aqueous system is reported between 1079 m^2/g and 1500 m^2/g (Gross et al. 2012; Kida et al. 2013; Keser Demir et al. 2014). In the literature, ZIF-L with a BET equivalent surface area of 160-250 m^2/g (Q. Liu et al. 2014; R. Chen et al. 2013) were reported. ZIF-L particles synthesized in the current study has a BET equivalent surface area of 290 m^2/g, which is slightly greater than the values in the literature. Our BET equivalent surface area results showed that surface area of ZIF-67 samples are over 1200 m^2/g. In the literature, BET equivalent surface area of ZIF-67 was reported in a very wide range from 316 m^2/g to 2380 m^2/g (Qian et al. 2012; H. Li, Hong Ma, Wang, Jin Gao, et al. 2014; Lin & Chang 2015a; Gross et al. 2012). Due to low adsorption capacity of ZIF-7.0 for N_2, the BET equivalent surface area was found as only 75 m^2/g. As synthesized ZIF-71 crystals, N_2 adsorption capacity was approximately 220 cm^3 STP/g and it showed Type-I adsorption isotherms with no hysteresis at 77 K.

Figure 24 shows the TGA curves of ZIFs. All thermograms exhibited approximately 10% weight-loss at low temperatures, which was often attributed to the removal of solvent, either water or DMF (Keser Demir et al. 2014; R. Chen et al. 2013; Q. Liu et al. 2014; Lin & Chang 2015b). Between 400 and 600°C, a sharp decrease in the weight was observed for ZIF-8, ZIF-67 and ZIF-7 due to the decomposition of organic framework. The residue was about 30% for these types of ZIF. The residue is expected to be ZnO for ZIF-8 and ZIF-7 (Pan et al. 2011; Keser Demir et al. 2014), and Co_3O_4 (Gross et al. 2012) for ZIF-67 with a theoretical amount of 36%, 23 % and 32% respectively. TGA curves for ZIF-L (Figure 24.b) displayed a step-wise decrease under air flow, a similar trend had been reported by Chen et al. (2013) and Liu et al. (2014). Weight loss is approximately 12% up to 280 °C that can be ascribed to the removal water from ZIF-L and desorption of unreacted ligand (e.g. Hmim) (Q. Liu et al. 2014). ZIF-L crystals TGA studied done under air atmosphere gives 27.5 wt% of residue (alike the value calculated) and it is characterized to be ZnO (R. Chen et al. 2013).

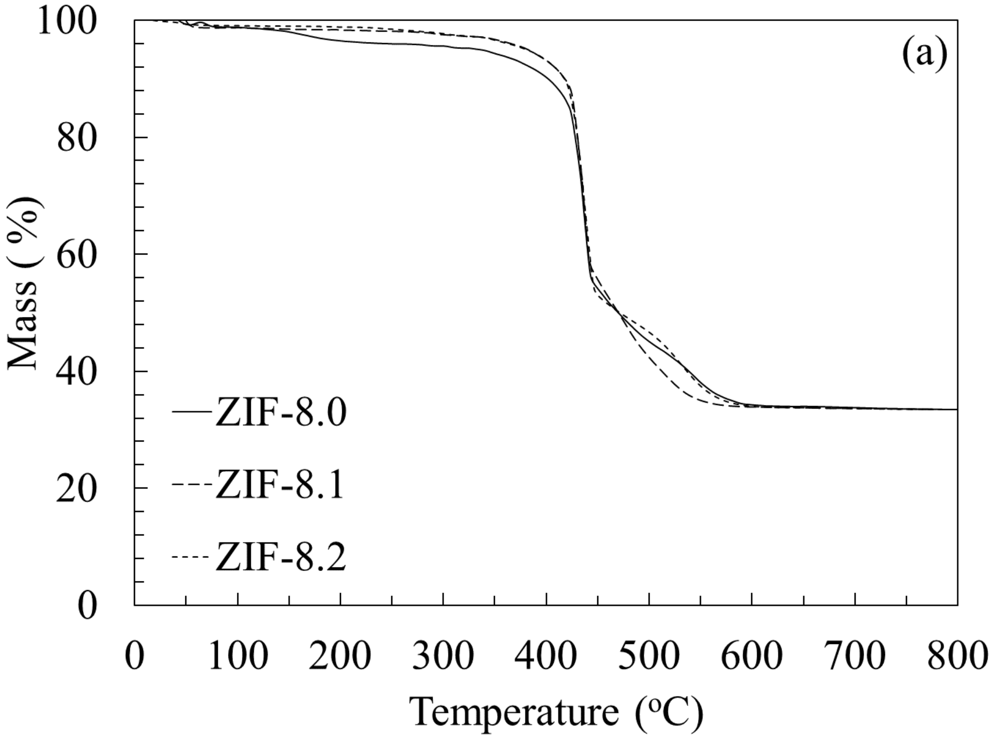

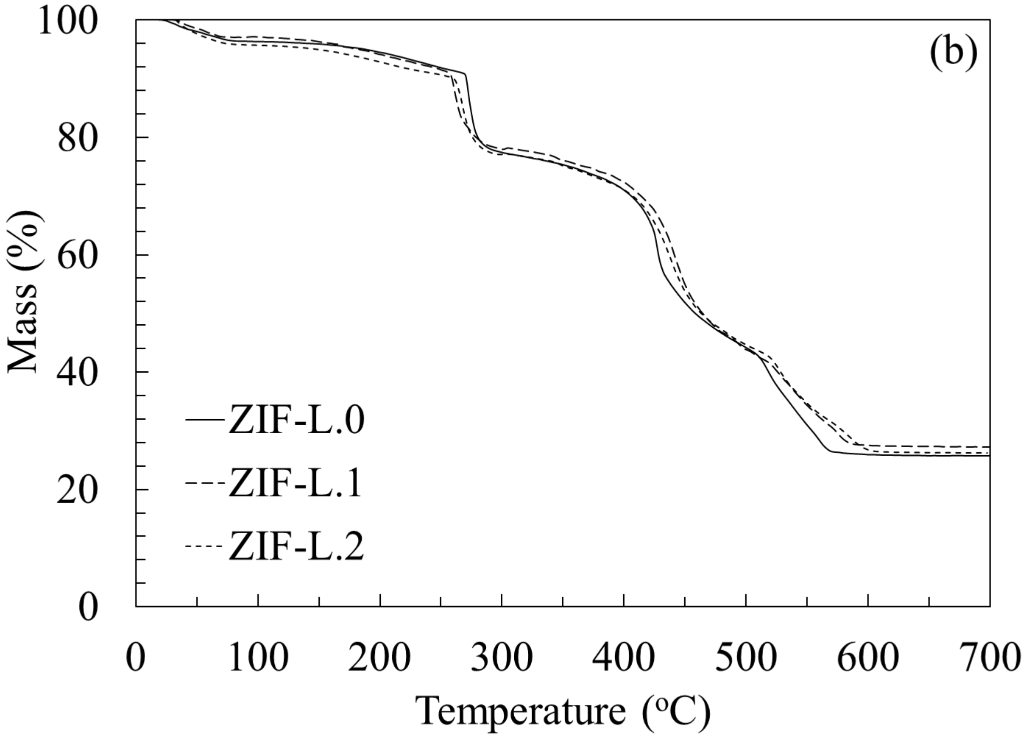
(b)
Mass (%)
100
80
60
40
20
0
0
100
200
300
400
500
600
700
Temperature (oC)
ZIF-L.0
ZIF-L.1
ZIF-L.2

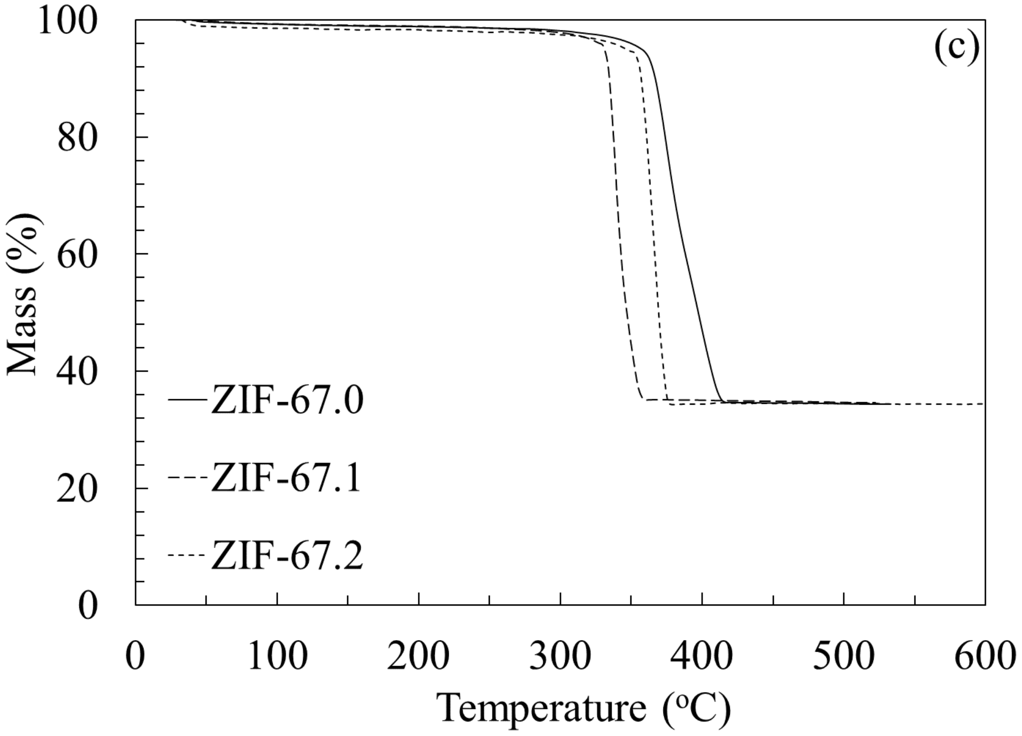
(c)
Mass (%)
100
80
60
40
20
0
0
100
200
300
400
500
600
Temperature (oC)
ZIF-67.0
ZIF-67.1
ZIF-67.2

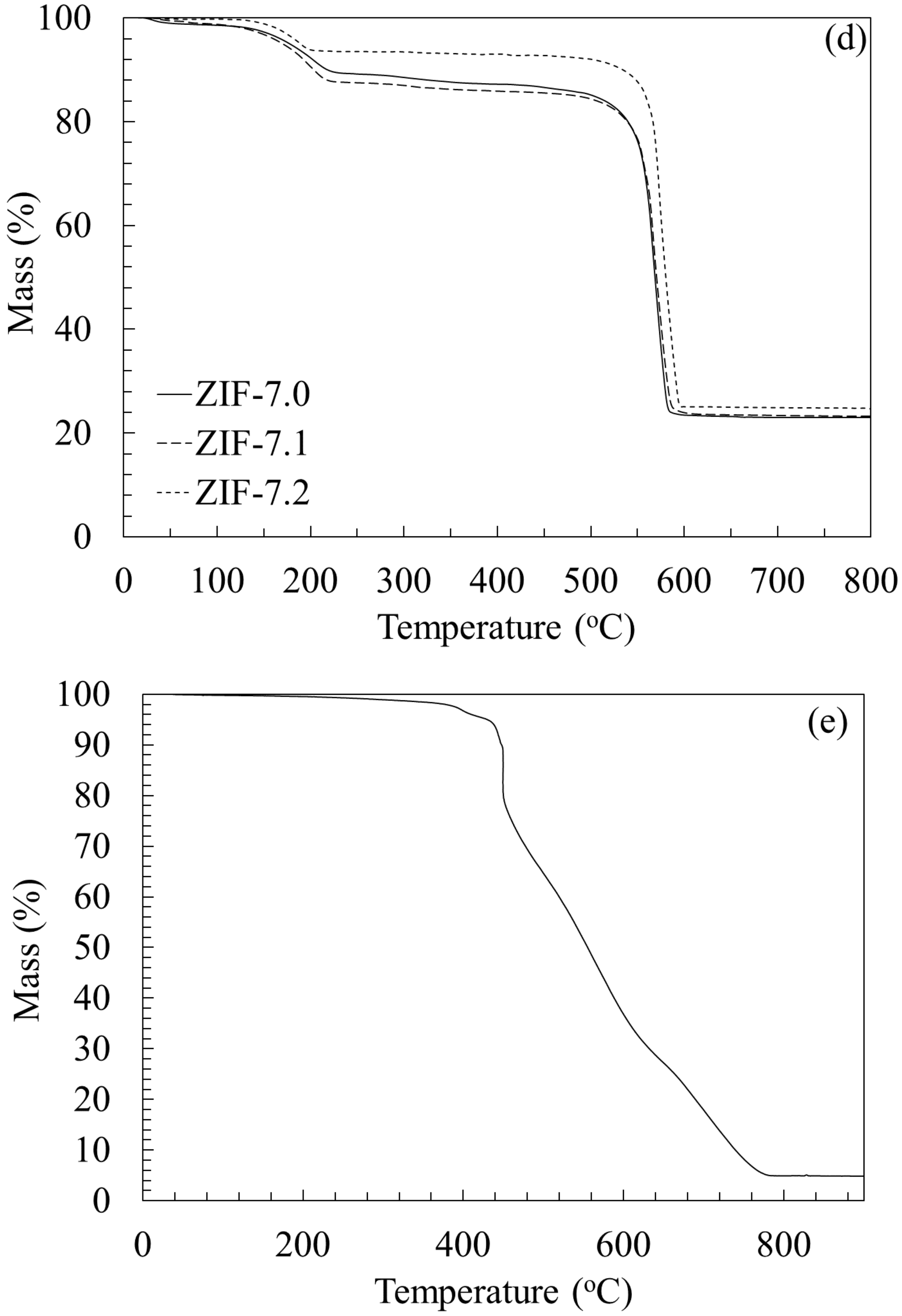

Figure 24. TGA curves (a) ZIF-8 (b) ZIF-L (c) ZIF-67 (d) ZIF-7 (e) ZIF-71 synthesized from fresh solutions and mother liquors.

Figure 24.e shows the TG curve of ZIF-71 crystals. There is no weight loss between 40 °C and 200 °C which ruling out the absence of liquid in the pore. This is an evidence of the hydrophobic properties of ZIF-71. A residual mass of 4.8 % corresponds to the decomposition of ZIF-71 crystals structure with results in the formation of ZnO.

3.3.3 Assessment of the Recycling Procedures

The pH of the synthesis medium was monitored as a function of synthesis time during the synthesis of ZIF-8, ZIF-L and ZIF-67, which were carried out in aqueous solutions (Figure 25) . The representative reactions for the synthesis of those ZIFs and ZIF-7 are shown below.

ZIF-8 : $Zn(NO_3)_2 \,.6H_2O + C_4H_6N_2 \rightarrow \mathrm{Zn(MeIM)}_2 + H^+ + NO_3{}^- + H_2O$

ZIF-L : $Zn(NO_3)_2 \,.6H_2O + C_4H_6N_2 \rightarrow \mathrm{Zn(MeIM)}_{2.5} + H^+ + NO_3{}^- + H_2\,O$

ZIF-67 : $Co(NO_3)_2 \,.6H_2O + C_4H_6N_2 \rightarrow \mathrm{Co(MeIM)}_2 + H^+ + NO_3{}^- + H_2O$

ZIF-7 : $Zn(NO_3)_2 \,.6H_2O + C_7H_6N_2 \rightarrow \mathrm{Zn(PhIM)}_2 + H^+ + NO_3{}^- + H_2O$

All reactions are anticipated to produce nitric acid so that the pH of the medium decreases as the crystallization proceeds. Figure 25 shows the change of pH through the course of crystallization. This decrease was particularly clear in the synthesis from the fresh solutions.

Organic linkers may exist in two forms during the crystallization: a linker unit in its deprotonated form and a stabilizing unit in its neutral form (Cravillon et al. 2012). Those coexist in the reaction medium at equilibrium. The concentration of deprotonated linker decreases with the pH of synthesis solution (Surendar R. Venna et al. 2010). The decrease in pH stabilizes the neutral linker and then terminate the crystal growth in the synthesis from the fresh solution. In the current study, NaOH or

KOH were added to the first mother liquor to increase the pH to a value closed to the pH of fresh solution and to stimulate the crystallization in the mother liquor. The OH^- source neutralizes H^+, which induces the deprotonation of excess neutral organic imidazole. Thus we can conclude that OH^- promotes the nucleation and inspires the crystal growth during the synthesis from first mother liquor.

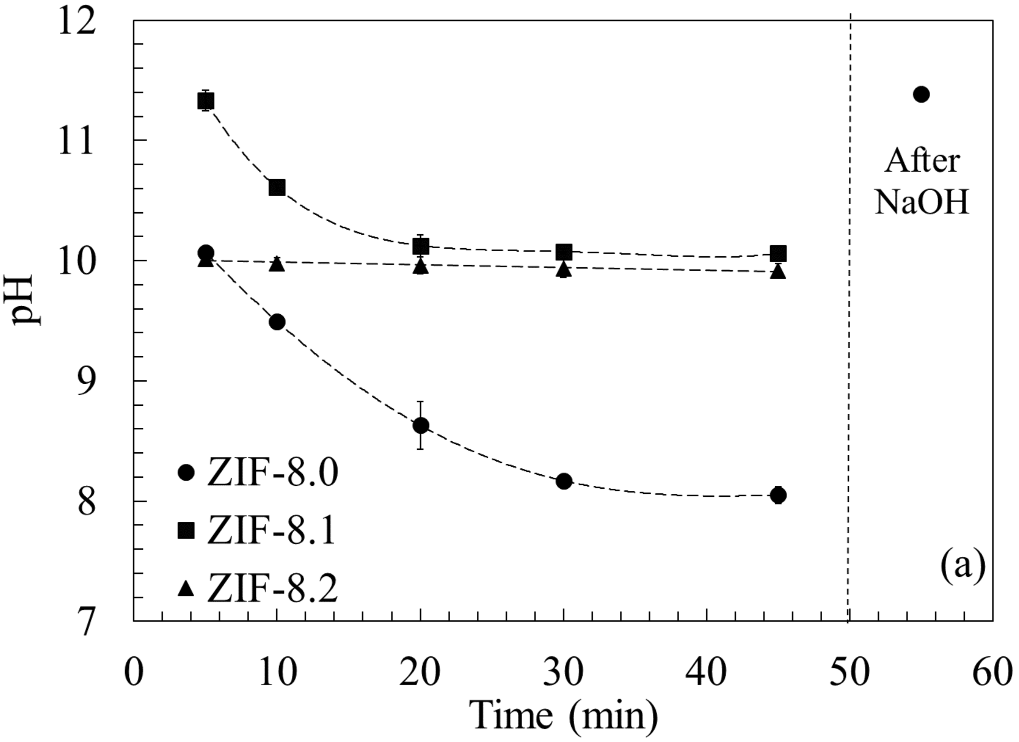

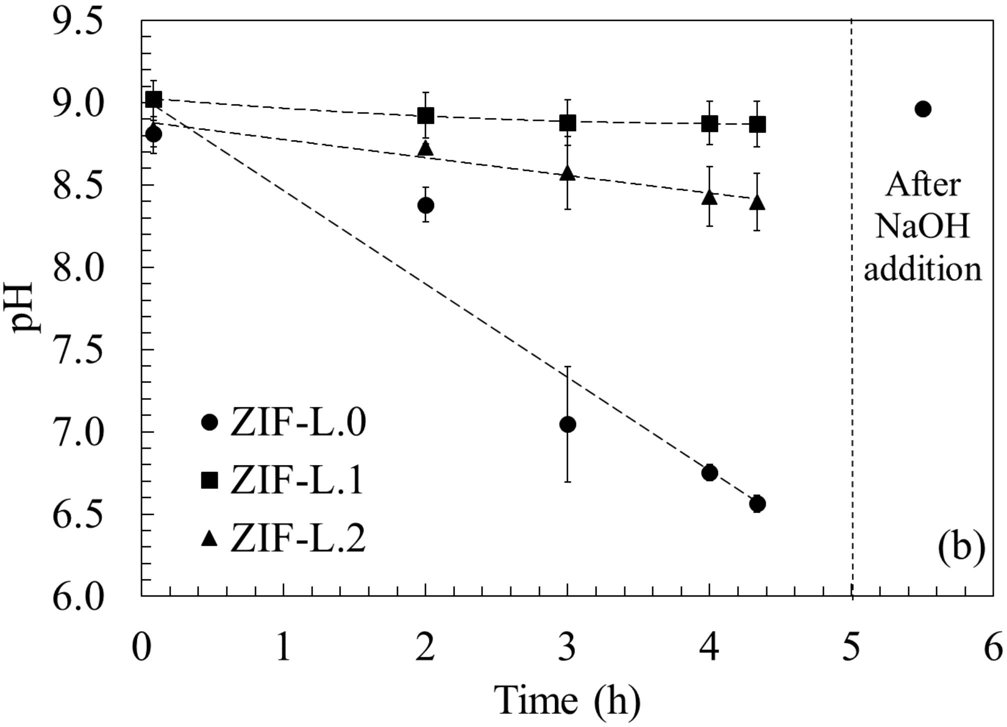

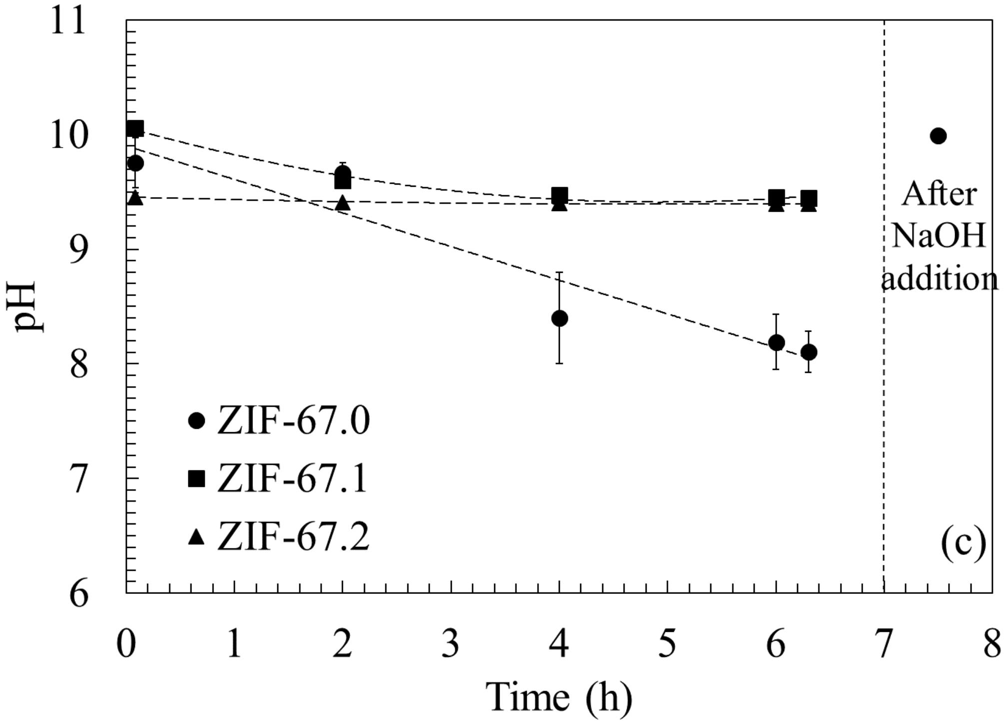

Figure 25. pH change of fresh solution during the course of crystallization of ZIFs in fresh and recycled solutions (a) ZIF-8 (b) ZIF-L (c) ZIF-67.

On the other hand, neither $NaNO_3$ nor KNO_3 salts was observed in the solid samples from XRD patterns, probably, they remained dissolved in the synthesis solution.

The pH change of ZIF-7 was not measured since the reaction was carried out in DMF. Though, the same pH adjustment procedure was applied to its mother liquors and ZIF-7 was also obtained from the recycled solutions.

The procedures, which has been developed to recycle the mother liquor remained after the synthesis, yield ZIFs without any lost in their desirable properties. The XRD patterns of samples obtained by recycling processes showed that no amorphous or any other phases exists, besides the relative crystallinities of the samples are comparable to those synthesized from fresh solutions. The SEM images show pure crystals with well-defined shapes in all steps of the recycling procedure. Moreover, the BET equivalent surface area and thermal stabilities of all recycle products are very similar to those obtained from the fresh synthesis solutions.

The developed procedures introduce many advantages in ZIF production from the standpoint of production efficiency and environment. Table 13 shows the amount of ZIF produced per amount of organic linker. For example, 0.16 g of ZIF-7 was produced from 1 g of BIM after synthesis from fresh solution. Following the recycling procedure, 0.36 g of ZIF-7 was totally produced from 1 g of BIM. The amount of ZIF produced per gram of organic linker almost doubled for all types of ZIFs. It should also be noticed that no solvent was added to the synthesis medium throughout the recycling processes. The results clearly showed the improvement in the efficiency of ZIF synthesis and reduction in the amount of organic linkers disposed to the environment by recycling the synthesis solution.

Table 13. The efficiency of single step synthesis from fresh solution and three step synthesis using two mother liquors. The efficiency is defined as total amount of ZIF produced per total amount of organic linker used throughout the process.

	Total amount ZIF produced/total amount organic linker used (g/g)	
Sample name	Fresh solution synthesis	Recycle synthesis
ZIF-8	0.028	0.054
ZIF-L	0.38	0.67
ZIF-67	0.032	0.049
ZIF-7	0.16	0.36

3.4 Conclusion

ZIF-8, ZIF-L, ZIF-67 and ZIF-7 were successfully synthesized from fresh and recycled synthesis solutions with high purity and yield. The adjustment of pH and the metal ion to organic linker molar ratio of the mother liquor were crucial for the synthesis of next generation of the ZIF crystals through the recycling procedure. The crystals produced from recycled solutions had similar morphological and structural properties with those produced from fresh synthesis solutions. Those ZIFs represent synthesis using different metal ions, organic linkers and solvents, therefore it is concluded that the procedures developed for recycling of synthesis solution can be adapted to many types of ZIFs.

CHAPTER 4

ZIF -X /PDMS MMMs FOR SEPARATION OF SOLVENTS FROM NITROGEN

4.1 Introduction

The production in petroleum refining, food, printing, paints, gluing, pharmaceutical and coating process often release waste air streams containing a large amount of volatile organic compounds (VOCs) (Lue, Chen, et al. 2008; Obuskovic et al. 2003). VOCs are highly reactive hydrocarbons. It is essential to recover the VOCs from waste gas streams in an industrial process due to environmental issues and recover high value compounds.

Ethyl acetate (EtAc), ethanol (EtOH), isopropanol (IPA), methanol (MeOH), and propanol are widely used as solvents in defense, electronic, textile and rubber industries. One of the industries that uses large amounts of solvents is packing-printing industry. EtOH and IPA are common solvents used for thinning paint. They evaporate from the surface of the polymeric packing films during drying process. The solvent vapors should be swept away to improve the indoor air quality. The VOCs in air rather either disposed to atmosphere or recovered from air by adsorption-based processes and recycled.

Current VOCs recovery processes are commonly based on activated carbon filled adsorption columns. Following the adsorption period, the columns are regenerated by increasing temperature, decreasing pressure or using high flux sweeping gases (mostly nitrogen). The VOCs swept from the adsorption column cool down to condense and fed to the distillation processes to separate the VOC mixture into its components. Nevertheless, condensation in solvent – recovery process is an expensive step because it often requires cryogenic temperatures due to low partial pressure of VOCs in N_2. The efficiency of solvent recovery processes can be enhanced by increasing the partial pressure of VOCs. Membrane-based separation process is an effective way to increase the VOCs partial pressure in nitrogen. It is also an environmentally friendly and cost-effective method.

Mixed matrix membranes (MMMs) have many advantages such as combining desirable properties of polymers – economical, easy scalability and fabrication - and high selectivity of inorganic filler materials (Chung et al. 2007; Fang et al. 2015a). In most cases, polydimethylsiloxane (PDMS) based membranes are preferred due to high selectivity and permeability for VOCs over non-condensable gases such as O_2 and N_2 (Yeom et al. 2002a; Obuskovic et al. 2003; Baker 2006). In addition , PDMS has connatural characteristic features like high resistance to weather and ozone, constant thermal properties, and hydrophobic nature.

Zeolitic imidazolate frameworks (ZIFs) are crystalline microporous materials with a large surface area, chemical and thermal stability (Surendar R Venna et al. 2010; Keser Demir et al. 2014) besides they exhibit high compatibility with rubbery membranes owing to their organic backbone. These properties make them attractive candidates for the selective separation process.

PDMS can easily swell in the presence of VOCs that enhance permeability. Therefore, PDMS based-membranes have analyzed for allocation of VOCs from waste gas streams by many researchers. ZIF-8/PDMS MMMs were synthesized to separate propane from N_2 (Fang et al. 2015a). The propane/N_2 selectivity of 10 wt % 10 ZIF-8/PDMS membrane was higher by 38 % than that of pure PDMS membrane. However, the research on the preparation of ZIF/PDMS membranes for separation of VOCs from N2 is very limited and required further investigation. The MMMs used for vapor separation are usually prepared using rubbery polymers and zeolite like zeolite A and silicate (Birgül Tantekin-Ersolmaz et al. 2001; Chandak et al. 1998; Kim et al. 2009) as fiilers. In recent years, metal organic frameworks (MOF) and ZIFa as a subset of MOF are often used in preparation of MMMs.

In this study, PDMS based MMMs that selectively permeate solvent vapors (VOCs) over nitrogen and water vapor were developed. VOCs concentration at the permeate will be higher and condensable at temperature over 0^oC. As a result, the condensation in the solvent recovery process is expected to economically more feasible.

4.2 Experimental

4.2.1 Materials

4,5-dichloroimidizole, benzimidazole (Bim), 2- methylimidazole (Hmim) ($C_4H_6N_2$), N,N-dimethyl formamide (DMF), sodium hydroxide (NaOH), potasyum hydroxide (KOH), methanol (MeOH), hexane and benzimidazole (Bim) were purchased from Sigma–Aldrich. Zinc nitrate hexahydrate ($Zn(NO_3)_2$) and that were purchased from Acros respectively. Cobalt nitrate hexahydrate ($Co(NO_3)_2.6H_2O$) was obtained from MCB. All chemicals used as purchased while synthesizing ZIF crystals.

Polydimethylsiloxane (PDMS) purchased from Dow Corning and used as received. Polyethersulfone (PES) ultrafiltration support membrane, NADIR® RM UP150 P, was purchased from Microdyn-Nadir. Nitrogen (N_2, 99.999 vol %) was also used in the separation processes.

4.2.2 Synthesizes of ZIFs

ZIFs were synthesized based on the procedure described in Chapter 3 section 3.2.2. ZIF-71 was synthesized by following the procedure reported by Y. Li, Lik H Wee, et al. 2014 . Zinc acetate (0.73 g) and 4,5-dichloroimidizole (2.2 g) in 150 ml of methanol were dissolved separately. The zinc acetate solution was added over imidazole solution at room temperature under vigorous mixing. The crystallization mixture was then stirred for 30 minutes and kept without mixing for 24h at room temperature. After removing methanol with pipet , crystal precipitation were sucked in chloroform for two days to remove remaining methanol. Finally, ZIF-71 crystals recovered by centrifugation.

Pore size, zeolite topology and unit cell formula of the ZIFs are represented in Table 14.

Table 14. Pore size, topology and unit cell formula of ZIFs

	Pore Size (nm)	Zeolite code	Unit Cell Formula
ZIF-7	0.29	SOD	$Zn\ (PhIM)_2$
ZIF-8	0.34	SOD	$Zn\ (MeIM)_2$
ZIF-67	0.34	SOD	$Co\ (MeIM)_2$
ZIF-71	0.42	RHO	$Zn(dcIM)_2$
ZIF-L	0.34	Semi-SOD	$Zn\ (MeIM)_{2.5}$

4.2.3 Membrane Preparation

In the present study, all ZIF- X /PDMS MMMs were prepared with 20 wt % loading of ZIF- X (X: ZIF-8, ZIF-L, ZIF-67, ZIF-7, and ZIF-71). The ZIF-X loading of a membrane was defined as mass fraction ZIF-X in the PDMS.

PDMS has two portion: pre-polymer and cross-linker agent (CA). Firstly, 1 g ZIF-X and 4 g pre-polymer were dissolved in 16 g hexane. Hexane was used to decrease viscosity of pre-polymer thus; ZIF-X could dispersed in pre-polymer. The mixture was stirred overnight at room temperature to obtain a homogenous mixture. While stirring, hexane evaporated and removed from the pre-polymer and ZIF-X mixture. The cross-linking procedure was inhibited in the presence of hexane. After removing hexane, 0.4 g CA was added to the mixture. The resulting solution was stirred for 3 hours at 35 ^{o} C. The air bubbles were removed from final solution by vacuum evacuation. The solution was casted on PES ultra-filtration membrane at room temperature. The membrane dried at room temperature overnight and then cured at 130 ^{o} C for 6 hours. The membrane thicknesses, which were measured by a micrometer, were between 17 and 75 µm.

Pure PDMS membranes were synthesized by following a procedure similar to ZIF- X/PDMS MMMs without adding any ZIF crystals.

4.2.4 Characterization

ZIFs were characterized by Philips PW 1840 X-ray diffractometer (XRD) operating at 40 kV and 40 mA with Cu Kα radiation. The N_2 adsorption-desorption isotherms of ZIFs were obtained by using Micromeritics TriStar-II 3020 instruments at 77 K. Before test, ZIFs were evacuated as describe Chapter 3, section 3.2.4. Scanning electron microscopy (SEM) micrographs of ZIFs and membranes were obtained by using QUANTA 400F. Thermogravimetric analysis (TGA) of ZIFs and membranes were made with Shimadzu DTG-60H with a heating rate of 10^{o}C/min under a continuous-flow of air.

4.2.5 Membrane Permeation Test

The membrane permeation test of single gas and VOCs/N_2 mixture were performed a set up schematically shown in Figure 26. Membrane sealed in the membrane module had an effective membrane area for permeation was 12.5 cm^2. The membrane module was in an oven to keep temperature constant throughout the test. The total feed rate was adjusted as 22 ml/min with a mass flow controller $_1$. There were two mass flow controllers (MFC) in the set up and their calibration curves are given in Appendix Part D. The feed pressure was modulated with backpressure valve $_1$. A vacuum was applied before each experiment to clear out.

Single gas (N_2 or CO_2) permeation test utilizing a constant pressure –variable volume method. The flow rate of the permeate gas was measured by a soap flow meter. CO_2 permeation test was performed at 2 bar and 35 ^{o}C , whereas N_2 permeation test was performed at different pressures (0.5 bar - 4 bar) and temperatures (35 ^{o}C- 90 ^{o}C). Permeability (J) was calculated by Equation 6 where Q is the volumetric flow rate; ΔP is transmembrane pressure; A is effective membrane area and ℓ is the thickness of the membrane.

$$J = \frac{Q\,\ell}{A\,\Delta P} \quad (Eq\ 6)$$

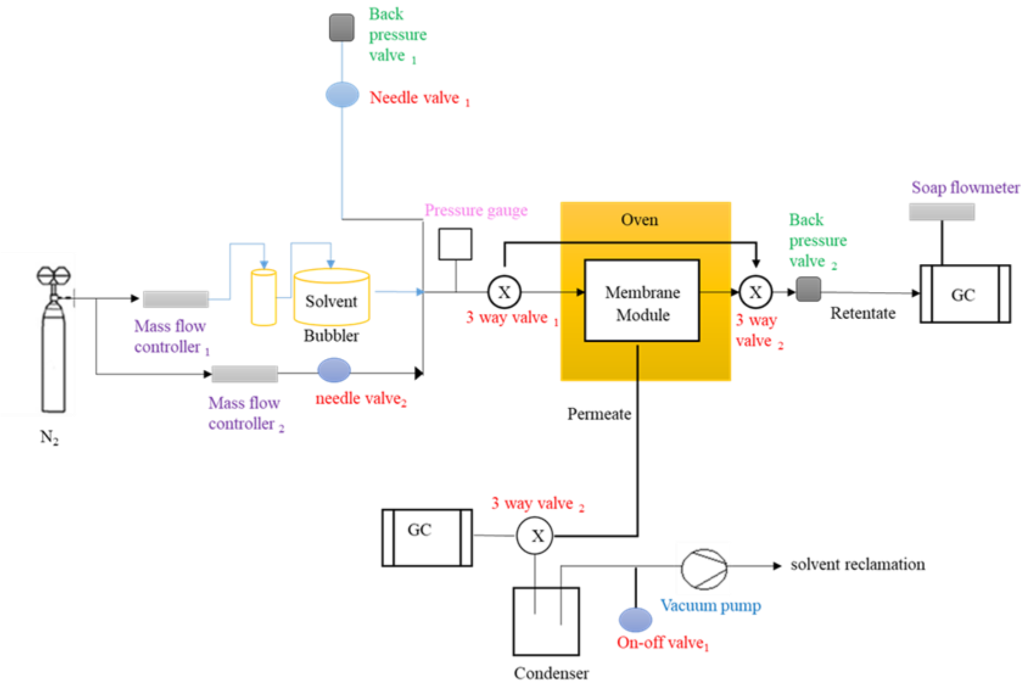

Figure 26. Schematic representation of VOCs permeation system

The feed that was a mixture of VOCs and N_2 were generated by bubbling nitrogen at 2 bar through a solvent tank with a flow rate of 22 ml/min. Three way-valve $_1$ was turned to the side of three way-valve $_2$ to analyze VOCs and N_2 concentration in the feed. If VOCs concentration in the feed was high, MFC_2 was opened to dilute it. Composition of the feed was evaluated via gas chromatography (GC). GC calibration curve of VOCs and N_2 are given in Appendix Part E. The detector of GC , Varian Capillary Column CP-Wax 57 CB, was maintained at 190 ^{o} C. Helium was used as a vector gas.

Three way-valve $_1$ was turned to the side of membrane module after adjusting feed composition. The feed was conducted with the membrane while a vacuum was applied on the permeate side. The VOCs permeated through the membrane were collected in a cold trap and then weighed using a digital balance. Each test took 2 hours, so that the mass flow rate of VOCs could been calculated at the end of each experiment.

VOCs permeability was calculated with Equation 7 where J_i is the permeability, Q is the volumetric flow rate of VOCs at permeate side , y_i the mole fraction of component *i* in the permeate side , A is the effective membrane area, and ΔP_i is the partial pressure difference of component *i* across the membrane. $\Delta P_i = P_h x_i - P_i y_i$, where P_h and P_i are the VOCs pressure in the feed and permeate, respectively, and x_i is the mole fraction of component *i* on the feed side.

$$J_i = \frac{Q\,\ell\,y_i}{A\,\Delta P_i} \quad (Eq\ 7)$$

N_2 permeability values were calculated with respect to VOCs' ones. The calculation was done by using permeate side composition of VOCs and N_2 that were obtained via GC analysis. The permeability was expressed in the unit of Barrer (1 Barrer = $1*10^{-10}$ cm^3 cm cm^{-2} s^{-1} $cmHg^{-1}$).

The membrane performance was also characterized in terms of selectivity. Throughout the test, composition of permeate and retentate side were analyzed by GC. The molar composition of N_2: VOCs was used to calculate VOCs/N_2 selectivity with Equation 8.

$$\alpha_{i/N_2} = \frac{(\frac{n_i}{n_{n_2}})_P}{(\frac{n_i}{n_{n_2}})_R} \quad (Eq\ 8)$$

4.3 Results and Discussion

4.3.1 ZIFs characterization

Figure 27 shows the XRD patterns of ZIFs which were synthesized based on the procedures described previously in Chapter 3, section 3.2.2. The reference pattern for each type of ZIF is also shown as bar graph in the figure. The peak positions and intensities match completely with the corresponding reference patterns (ZIF-8 : (Park et al. 2006) ; ZIF-67 (Gross et al. 2012) ; ZIF-71 (Yin et al. 2017); ZIF-7 (Park et al.

2006); ZIF-L (R. Chen et al. 2013)), indicating that the ZIFs were synthesized with high crystallinity and purity for use in mixed matrix membranes as microporous filler.

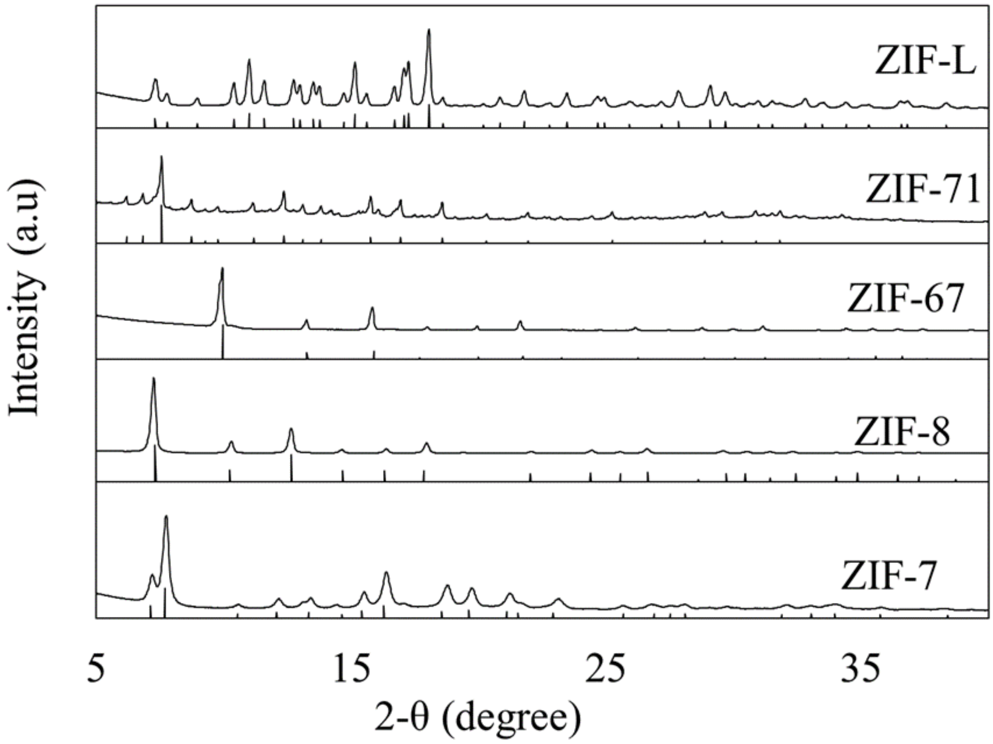

Figure 27. XRD patterns of ZIFs (The bar graph bellowed each pattern represent the references pattern).

Figure 28 shows SEM images of as-synthesized ZIFs. Each type of ZIF has its own characteristic morphology. ZIF-8 and ZIF-67 have hexagonal shape (Figure 28.a and c) (Keser Demir et al. 2014), ZIF-L has leaf-shaped morphology (Figure 28.b) (R. Chen et al. 2013) and ZIF-7 has cubic morphology (Figure 28.d). Lively et al. (Lively et al. 2011) stated that ZIF-71 has an undefined morphology although it looks like cubes. Ortiz et al. (Ortiz et al. 2014) has, therefore, defined the morphology of ZIF-71 as rhombic dodecahedron. In our study, the shape of ZIF-71 was defined rhombic dodecahedron like Ortiz et al. (Figure 28.e).

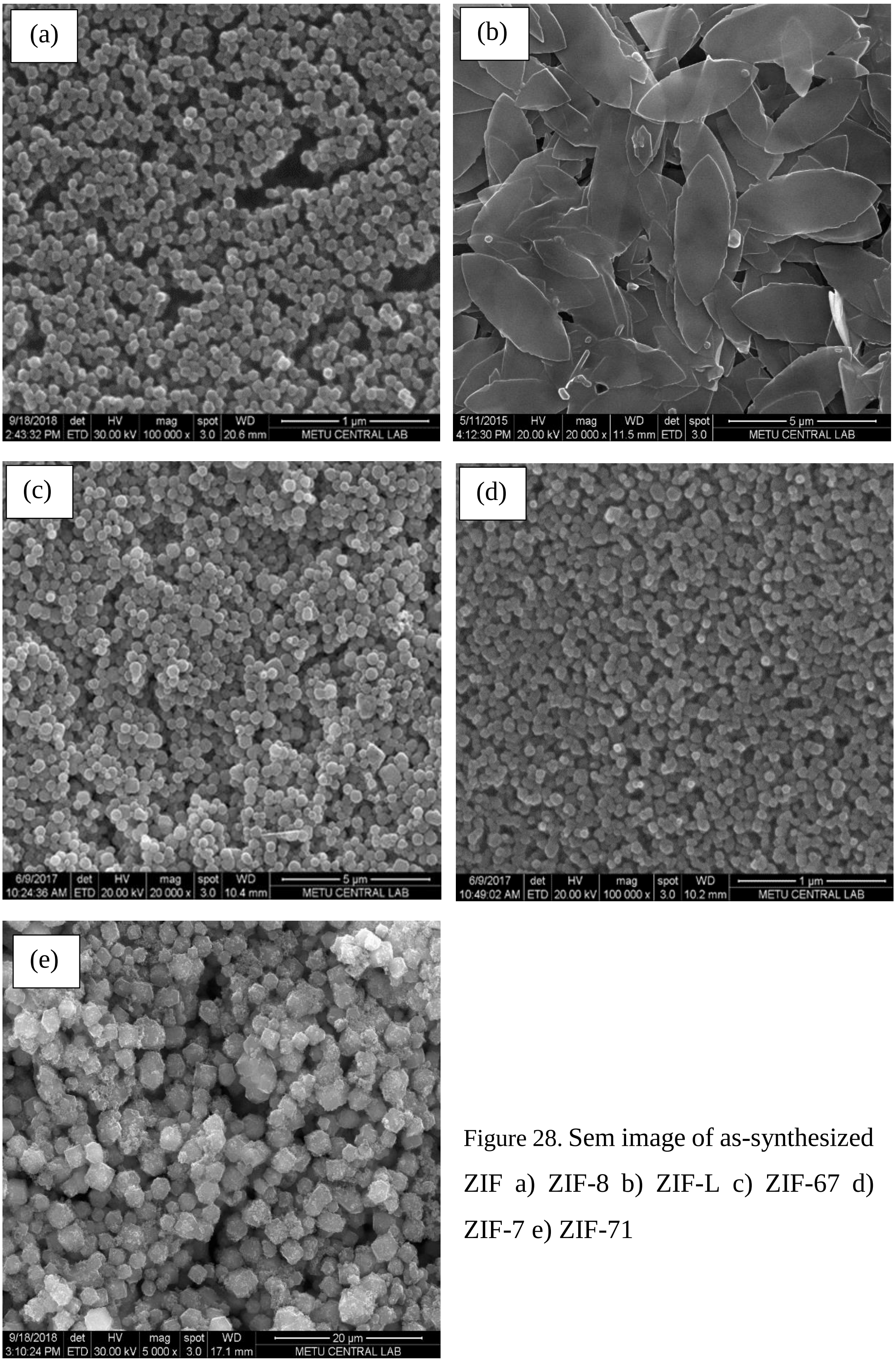

Figure 28. Sem image of as-synthesized ZIF a) ZIF-8 b) ZIF-L c) ZIF-67 d) ZIF-7 e) ZIF-71

The average particle size of each ZIF was determined using the SEM images. For this purpose, three different samples were synthesized for each type of ZIF, and at least 90 particles were counted (Table 15). The average particle size changes from nano- to micron sizes in a wide range, which allows us to investigate the effect of particle size on the membrane morphology and performance.

The N_2 adsorption isotherms of the synthesized ZIFs are depicted in Figure 29. ZIF-8, ZIF-L, ZIF-67 and ZIF-71 showed Type I-N_2 adsorption isotherms at 77 K that is characteristic of microporous materials (Keser Demir et al. 2014; R. Chen et al. 2013; Qian et al. 2012; Y. Li, Lik H. Wee, Martens & Ivo F.J. Vankelecom 2014). However, ZIF-7 exhibited Type II-N_2 adsorption isotherms, which is characteristic to non-porous materials. Li et al. [11] suggested that ZIF-7 has Type-I isotherm, although Johan et al. [12] and Thompson et al. [13] has claimed that the pore aperture of ZIF-7 is too small so that ZIF-7 behaves like non-porous materials during N_2 adsorption at 77 K. The N_2 adsorption capacities and BET surface area of ZIFs (Table 15) are in the range of those reported in the literature (Li et al. 2013; R. Chen et al. 2013; Q. Liu et al. 2014; Keser Demir et al. 2014; Şahin, F.; Topuz, B.;Kalıpçılar 2018; Qian et al. 2012; Gross et al. 2012; Y. Li, Lik H Wee, Martens & Ivo F J Vankelecom 2014).

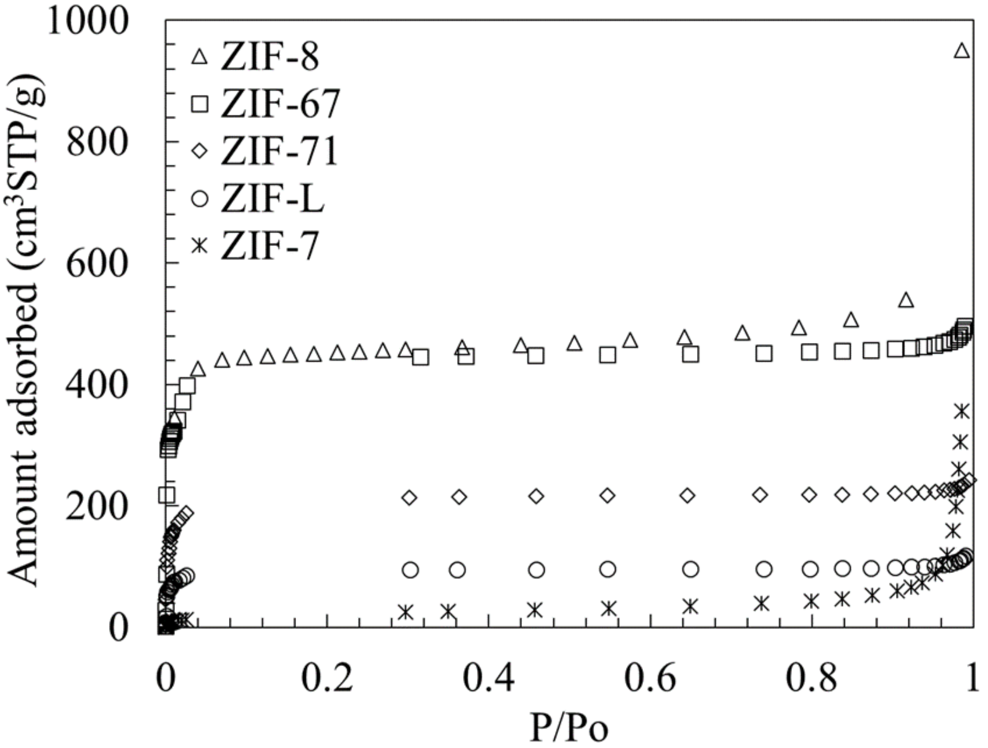

Figure 29. N_2 adsorption isotherms of ZIFs crystals

Table 15. Average particle size, N_2 adsorption amount and BET surface area of ZIFs

	Average particle size	Adsorption of N_2 (cm^3STP/g)	BET surface area (m^2/g)	BET surface area in the literature (m^2/g)	Adsorption of N_2 in the literature (m^2/g)
ZIF-7	65 ± 3 nm	32	75	No area * - 362	10 - 150
ZIF-8	73 ± 10 nm	480	1424	1019 - 1500	240 - 450
ZIF-67	281 ± 24 nm	440	1329	316 - 2380	100 - 500
ZIF-71	2500 ± 600 nm	220	650	782 - 1186	250 - 280
ZIF-L	3.8 ± 0.98 µm x 1.56 ± 0.41 µm x 150 ±39 nm	100	289	160-250	50

* No BET area based on N_2 adsorption of 77 K

4.3.2 Morphology of ZIF-X/PDMS MMMs

Five different types of ZIFs were chosen as filler to prepare MMMs. All ZIFs are hydrophobic (Keser Demir et al. 2014; R. Chen et al. 2013; Low, Yao, et al. 2014; Li et al. 2012; Qian et al. 2012; Gücüyener et al. 2010; Ortiz et al. 2014), which may improve the compatibility between ZIFs and hydrophobic PDMS. However, they have different characteristic regarding their pore structure, crystal morphology, particle size and shape. In addition, ZIFs with two different metal ions (Zn^{+2} and Co^{+2}) and three different organic ligand sources (Hmim, Bim and 4,5-dichloroimidazole) were used for membrane preparation. Hence, ZIFs with different diffusion and adsorption characteristics were used to prepare ZIF-X/PDMS MMMs for the separation of organic vapors from nitrogen.

The cross-sectional SEM image of a pure PDMS membrane is shown in Figure 30. All membranes cast on commercial ultrafiltration (UF) membranes (shown with white dash line on the figure), which has a non-woven supporting layer with a thickness of 180 ± 5 µm. A polymer intermediate layer with finger-like pores is above the non-woven and below the separating PES layer. The PES separating layer, with a molecular weight-cut-off 15000 Da and thickness of approximately 10 µm, is also shown on Figure 30. PES UF membrane is not anticipated to contribute to the separation of VOC from N_2 owing to its large pore size. The pure PDMS membrane with thickness of approximately 15 µm was cast uniformly over the UF membranes as shown in Figure 30 by a solid vertical line. The interface between PDMS and PES layers, can be clearly seen on the images, suggests good adhesion between two polymers.

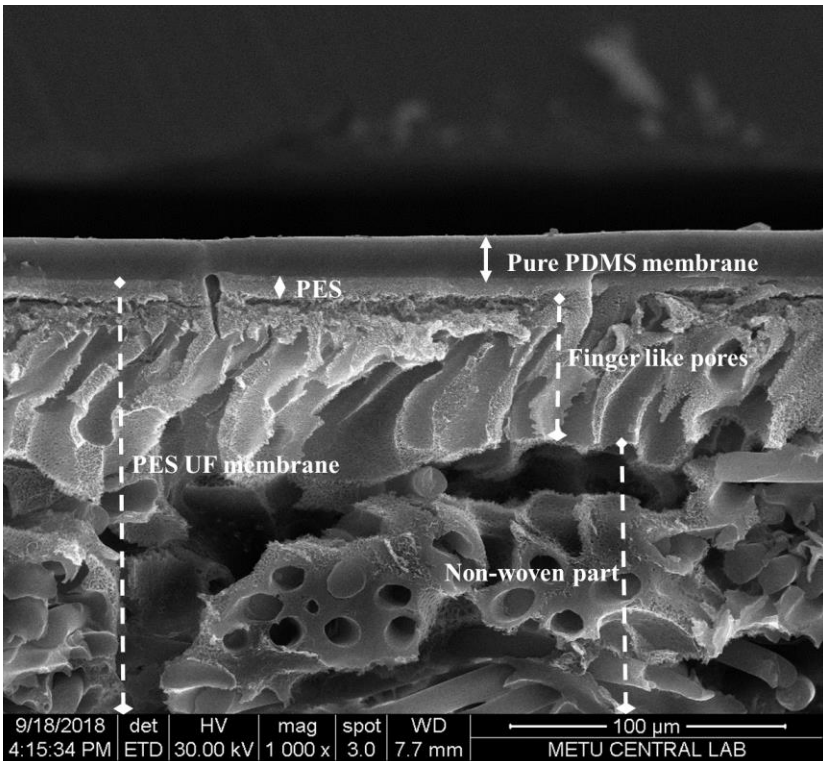

Figure 30. SEM image of pure PDMS membrane

Figure 31 shows the cross-sectional SEM images of 20 wt % ZIF-X loaded PDMS mixed matrix membranes. All MMMs were uniformly cast over UF membrane with a thickness of less than 60 µm (Table 16). The thickness of at least two membranes, which were prepared at different times, were measured for each type of ZIF-X loaded membrane. All membranes had similar thicknesses indicating the reproducibility in membrane casting. Besides the adhesion between PES and PDMS layers were excellent and not influenced from the incorporation of ZIFs into the membrane formulation.

The SEM images (Figure 31. a - e) shows homogeneous dispersion of ZIFs without forming large agglomerates in the PDMS matrix. The adhesion between PDMS and ZIF particles were excellent so that the ZIF particles can be barely seen on the SEM images even at high magnifications. The hydrophobic nature of ZIFs and flexible rubbery nature of PDMS (Fang et al. 2015a) may resulted in good compatibility and yielded defect free MMMs.

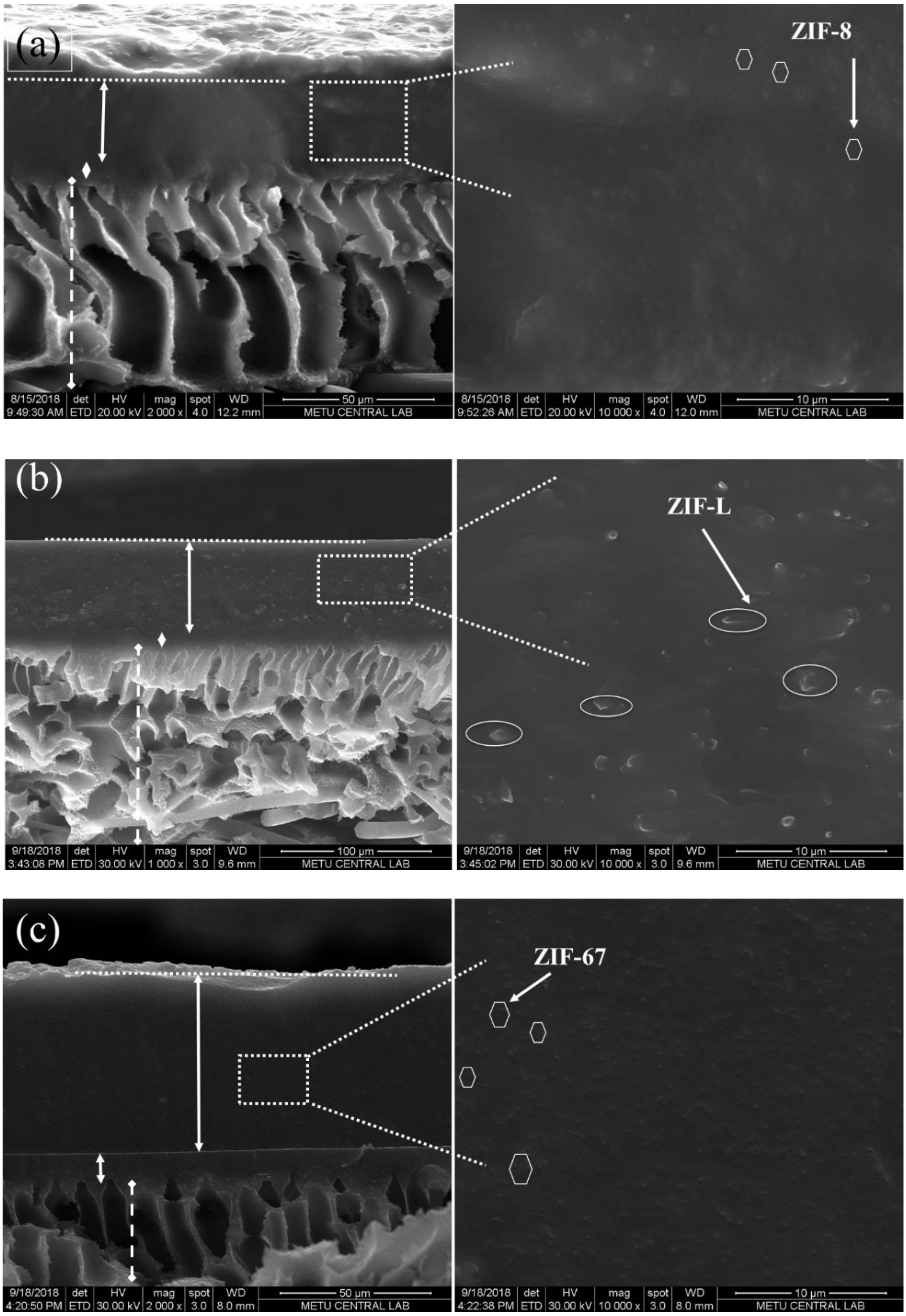
(a)
ZIF-8
8/15/2018 9:49:30 AM | det ETD | HV 20.00 kV | mag 2 000 x | spot 4.0 | WD 12.2 mm | 50 µm | METU CENTRAL LAB
8/15/2018 9:52:26 AM | det ETD | HV 20.00 kV | mag 10 000 x | spot 4.0 | WD 12.0 mm | 10 µm | METU CENTRAL LAB
(b)
ZIF-L
9/18/2018 3:43:08 PM | det ETD | HV 30.00 kV | mag 1 000 x | spot 3.0 | WD 9.6 mm | 100 µm | METU CENTRAL LAB
9/18/2018 3:45:02 PM | det ETD | HV 30.00 kV | mag 10 000 x | spot 3.0 | WD 9.6 mm | 10 µm | METU CENTRAL LAB
(c)
ZIF-67
9/18/2018 4:20:50 PM | det ETD | HV 30.00 kV | mag 2 000 x | spot 3.0 | WD 8.0 mm | 50 µm | METU CENTRAL LAB
9/18/2018 4:22:38 PM | det ETD | HV 30.00 kV | mag 10 000 x | spot 3.0 | WD 8.0 mm | 10 µm | METU CENTRAL LAB

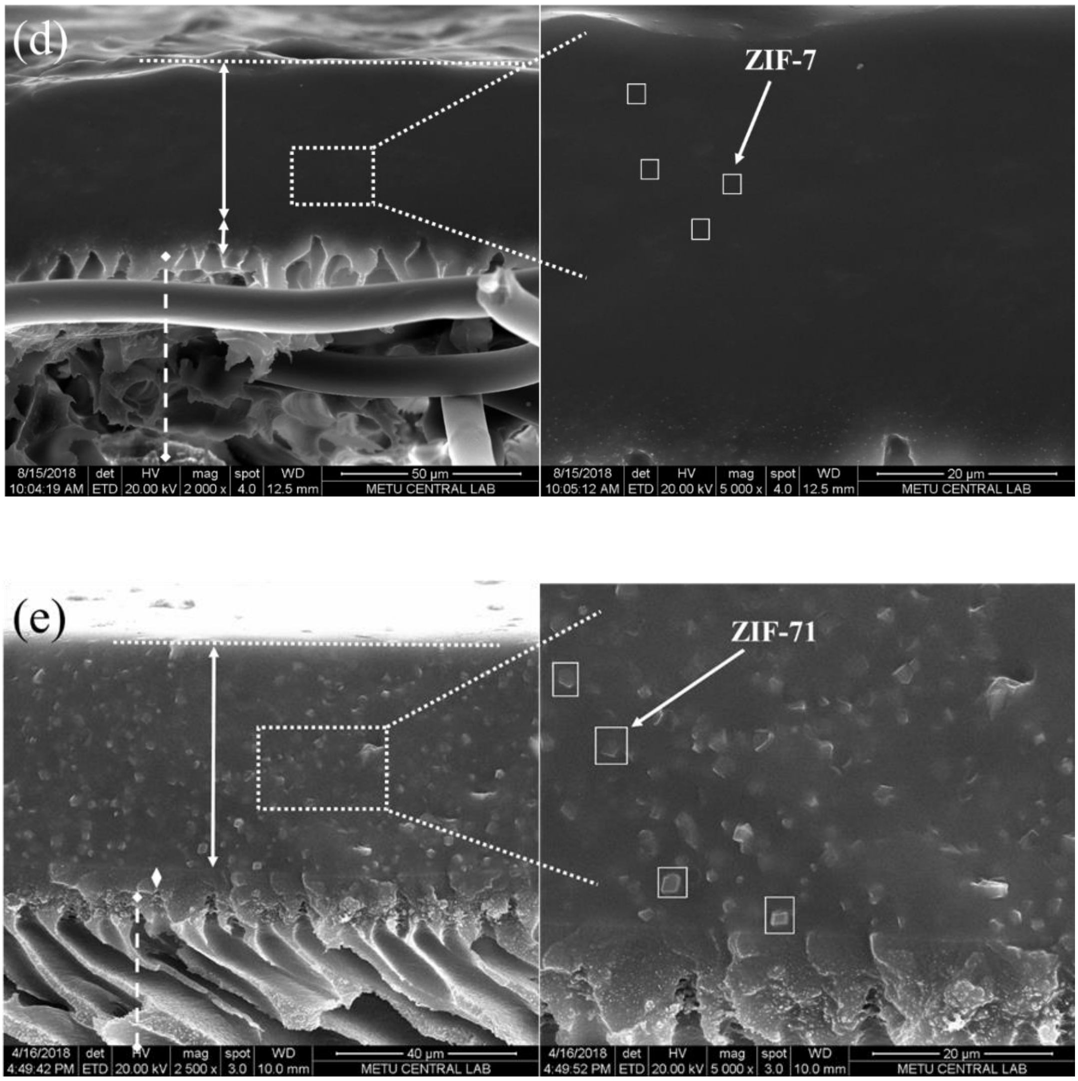

Figure 31. SEM image (a) 20 % ZIF-8 PDMS MMMs (b) 20 % ZIF-L PDMS MMMs (c) 20 % ZIF-67 PDMS MMMs (d) 20 % ZIF-7 PDMS MMMs (d) 20 % ZIF-71 PDMS MMMs

Table 16. Thickness of the membrane

	Thickness (μm)
Pure PDMS Membrane	15.2 ± 1.1
20 % ZIF-8 PDMS MMMs	27.7 ± 0.9
20 % ZIF-L PDMS MMMs	58.5 ± 1.2
20 % ZIF-67 PDMS MMMs	59.2 ± 1.2
20 % ZIF-7 PDMS MMMs	47.0 ± 0.8
20 % ZIF-71 PDMS MMMs	50.3 ± 0.8

The dispersion of ZIF-L (20% by weight) in the PDMS was further determined by EDX analysis (Figure 32). The blue dots represents Si in PDMS while the yellow ones are for Zn^{+2} ions in ZIF-L. The image shows the homogeneous dispersion of yellow dots in blue dots, suggesting uniform distribution of ZIF-L in PDMS matrix.

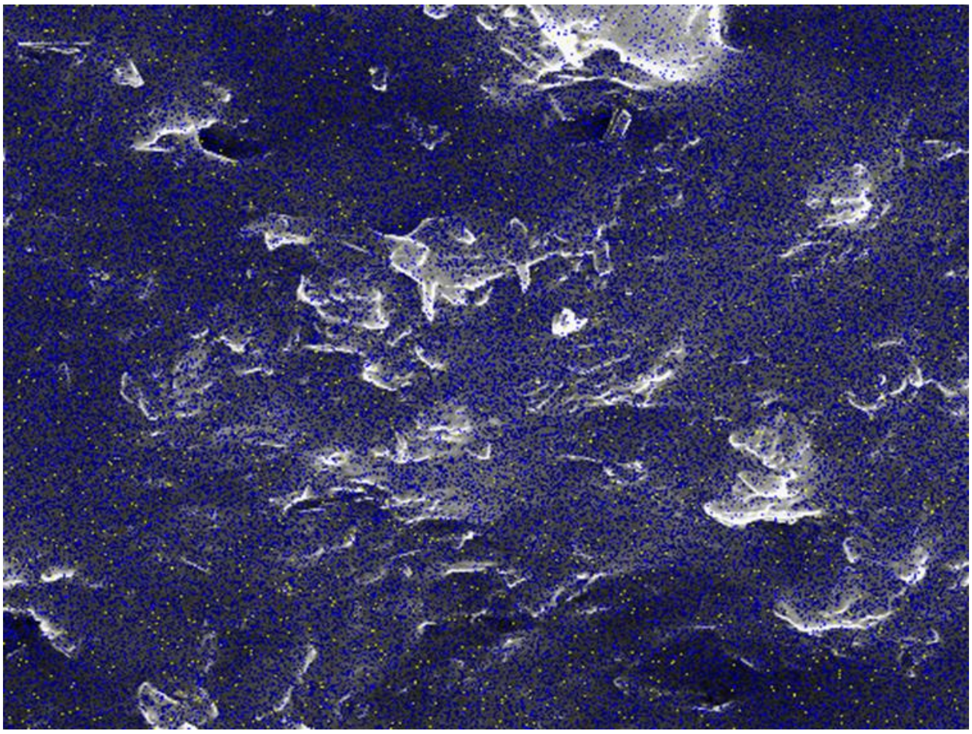

Figure 32. EDX Analyzed of 20 % ZIF-L/PDMS MMMs (blue dots: Si and yellow dots: Zn^{+2})

The average dispersion of ZIFs in the entire membrane was also determined by TGA. For this purpose, five pieces from different positions in a MMMs (Figure 33) was analyzed by TGA in air atmosphere. The total weight of five pieces analyzed by TGA is approximately 13% (by weight) of the whole membrane. The residual solid is expected to be a mixture of SiO_2 from the oxidation of PDMS and ZnO from the oxidation of ZIFs. Their relative amounts, therefore, show the average dispersion of ZIFs throughout the polymer matrix. For this purpose, UF membrane, pure PDMS coated membrane and pure ZIF-X powder were analyzed to determine the amount of residual solids (Figure 34). No solid remained after thermal treatment of UF membrane at 600°C. The percentage residual (SiO_2) was 18.3% after oxidizing of pure PDMS membrane. The percentage residual solids of pure ZIFs are shown in Table 17. Based on the analysis of those materials, the expected percent residual for a MMMs can be predicted as follows:

$$\% \text{ residual in MMMs} = (1-y)*18.3+y*(\% \text{ residual of ZIF-X})$$

where y is the percent ZIF-X in a MMMs. For example, the percent residual of a 20% ZIF-L containing is expected to be 19.9 %. Table 17 lists the predicted percent residuals for each MMMs.

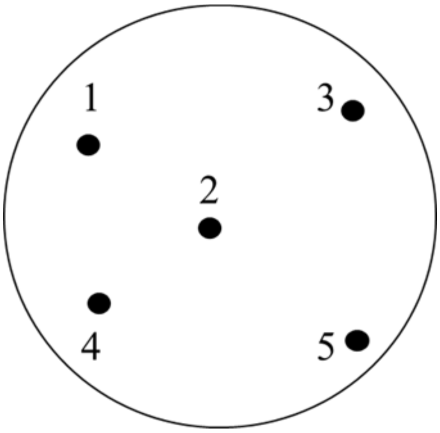

Figure 33. Schematic representation of parts that analyzed by TG

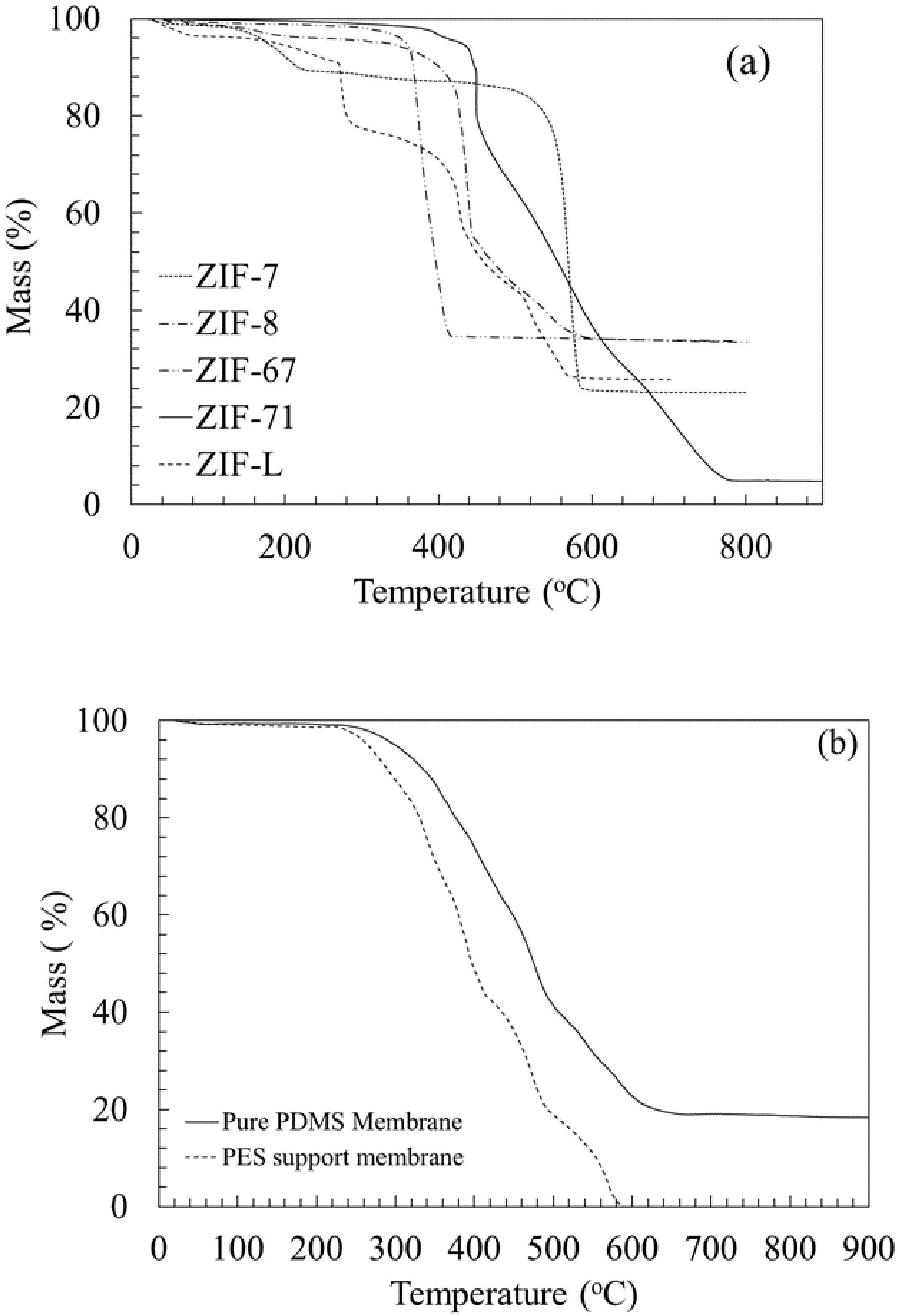

Figure 34. TGA curves of (a) ZIFs (b) Pure PDMS and PES support membrane

Table 17. Residual weight percentages after TGA

	Experimental residual amount (%)		Theorical residual amount (%)
ZIF-8 crystals	33.8		
ZIF-L crystals	25.7		
ZIF-67 crystals	34.0		
ZIF-7 crystals	23.0		
ZIF-71 crystals	4.8		
Pure PDMS Membrane		18.3	
% 20 ZIF-8 PDMS MMMs		19.6± 1.2	21.5
% 20 ZIF-L PDMS MMMs		20.1± 0.8	19.9
% 20 ZIF-67 PDMS MMMs		17.1± 0.4	21.5
% 20 ZIF-7 PDMS MMMs		18.3 ± 0.7	19.3
% 20 ZIF-71 PDMS MMMs		14.5± 1.3	15.6

Figure 35 shows the TGA of membrane pieces that were cut from 20% ZIF-L/PDMS MMMs. All membrane pieces showed very similar thermographs. The average percent residual of membrane pieces was 20.1% with a standard deviation of 0.8 %. The close average percent residual to the predicted one and small standard deviation indicate the homogenous distribution of ZIF-L crystals in the MMMs. The TGA of other membranes also suggest similar results. The TGA results of 20 % ZIF-X/PDMS MMMs are given in Appendix F.

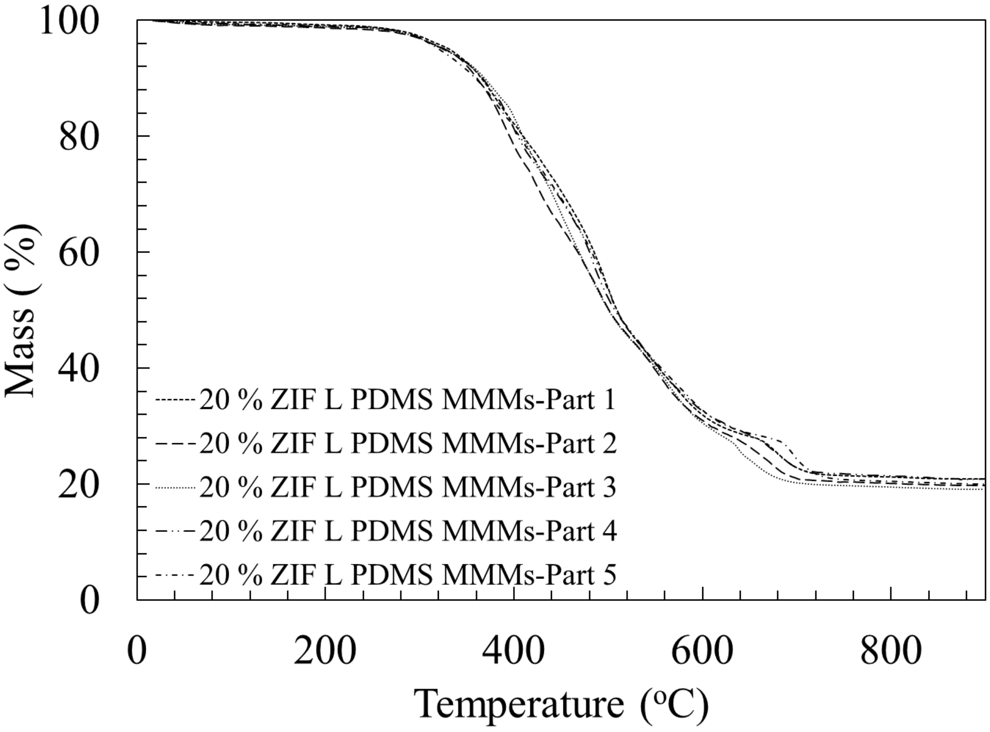

Figure 35. TGA curves of 20 % ZIF-L PDMS MMMs' pieces

4.3.3 Nitrogen permeation through pure PDMS membrane

The N_2 permeability of pure PDMS membrane was measured at 35°C and 2.92 bar feed pressure and compared with the PDMS permeabilities reported in the literature (Table 18). The N_2 permeability of the membrane prepared in this study was 266 Barrer, which is very similar to the permeabilities reported in the literature. Those results indicate the successful coating of PES support with PDMS for use as gas separation membrane.

Table 18. Pure PDMS N_2 permeability comparison with literature

T (^{o}C)	Permeability (barrer)	Source
35	266	This work
20	200	Fang et al., 2015
28	245	Rebollar-Pérez et al., 2012
35	210	Yeom et al., 2002
40	280	Jong et al., 2006
25	340	Choi et al., 2007
20	280	Leeman et al., 1996
28	245	Singh et al., 1998
40	220	Richard et al., 1987

As the objective of this study is to develop membranes for printing industry, in which the temperature of VOC/N_2 stream stripped from the adsorber can be as high as 150^{o}C and at several bars. Figure 36 shows the effect of permeation temperature and pressure on the N_2 permeability of pure PDMS membrane. The N_2 permeability increases with temperature, which is consistent with the literature (Figure 36.a). The results suggest the PDMS membranes are stable at moderately high temperatures and can be used for VOC separation at temperatures similar to industrial VOC recovery process. On the other hand, the N_2 permeability was nearly independent of pressure (Figure 36.b). In the literature, the N_2 permeability was reported to nearly independent of pressure (Rao et al. 2007; Choi et al. 2007; C K Yeom et al. 2000) or slightly increased with pressure (Shi et al. 2006). Therefore, the membranes produced throughout this thesis were tested at a feed pressure of 2.92 bar.

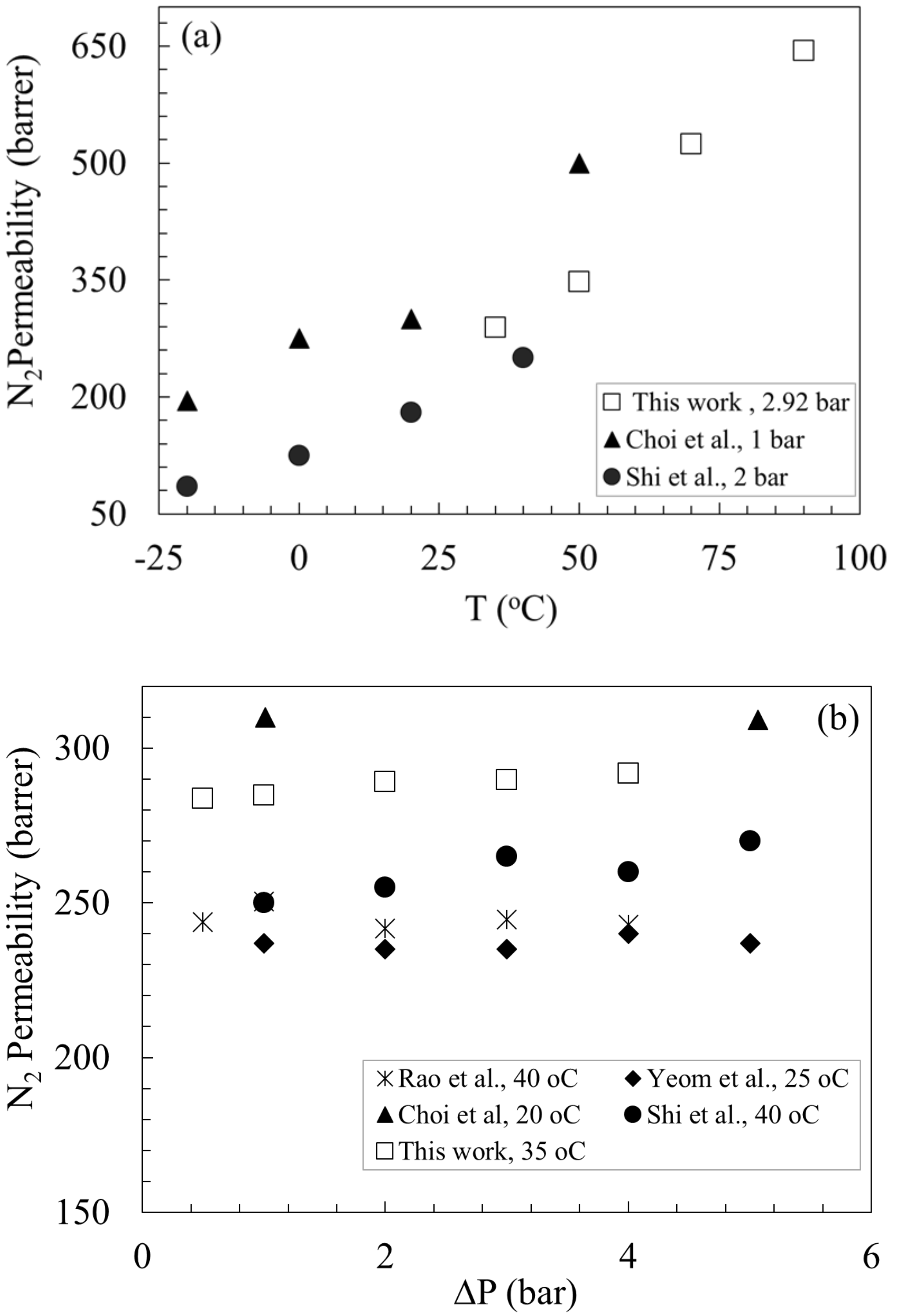

Figure 36. N_2 permeability of pure PDMS membrane (a) at different temperature (P_{feed} = 2.92 bar) (b) at different feed pressure (T = 35 ^{o}C)

4.3.4 Single gas permeation through ZIF-X/PDMS MMMs

The gas separation performance of MMMs were determined by measuring single gas permeabilities of CO_2 and N_2 at 35°C and 2.92 bar before testing VOC/N_2 mixtures. This was a quick method for determining membrane performance.

CO_2/N_2 ideal selectivity value of the synthesized membranes were between 7 and 10.5 while CO_2 permeability values were between 1100 barrer and 3700 barrer (Figure 37). In the literature, CO_2 sorption amount of ZIFs are given as 0.75-0.87 mmol/g; 0.90-0.94 mmol/g; 0.70-0.75 mmol/g; 2.30-2.50 mmol/g; and 0.4 mmol/g for ZIF-8, ZIF-L, ZIF-67, ZIF-7 and ZIF-71 respectively (McEwen et al. 2013; Cacho-Bailo et al. 2016; Abdelhamid & Zou 2018; Pera-Titus & Farrusseng 2012; Ding & Yazaydin 2013; Ding et al. 2018). According to those values, CO_2 loading of ZIFs can be sorted as ZIF-7 > ZIF-L > ZIF-8 > ZIF-67 > ZIF-71. Despite this, it was observed that 20 % ZIF-71/PDMS MMMs has the highest CO_2 permeability value. This situation may be the result of the relationship between kinetic diameter of the gas and aperture pore size of the ZIF. A gas molecule can diffuse thorough the pores of ZIFs that is larger than its kinetic diameter unless ZIFs are flexible (Zhang et al. 2013; Du et al. 2017). The kinetic diameters of N_2 and CO_2 are in order of 0.36 nm and 0.34 nm (Du et al. 2017). The aperture sizes of ZIFs are given in Table 14. According to this, both N_2 and CO_2 can penetrate through the pores of ZIF-71, 0.42 nm. This may be the reason of obtaining the highest N_2 and CO_2 permeability values with 20 wt % ZIF-71 loaded PDMS MMMs.

Pure PDMS membrane has a higher N_2 and CO_2 permeability than 20 % ZIF-8/PDMS MMMs, 20 % ZIF-67/PDMS MMMs, 20 % ZIF-L/PDMS MMMs and 20 % ZIF-7/PDMS MMMs. Those ZIFs have smaller pore size than kinetic diameter of the gases. Neither N_2 nor CO_2 can easily diffuse through the pores of those ZIFs. The addition of ZIF-8, ZIF-67, ZIF-L and ZIF-7 may cause local chain rigidity and decrease free volume in the polymeric phase to transport (Merkel et al. 2002; G. Liu et al. 2014) . Besides, ZIF-L has the same pore diameter with ZIF-8 and ZIF-67 (0.34 nm), 20 % ZIF-L/ PDMS MMMs had the lowest N_2 and CO_2 permeability value. This may be explained with orientation of ZIF-L crystals in the PDMS polymer matrix. If ZIF-L crystals are aligned perpendicular to the gas flow, filler arrangement in the polymer matrix look like “ brick and mortar” (Lape et al. 2004). According to SEM micrograph of 20 % ZIF-L/PDMS MMMs (Figure 38), ZIF-L crystals approximately align vertical to gas flow. Either N_2 or CO_2 should have to pass around the crystals. ZIF-L orientation may increase the pathway of the permeate gas which results in a higher time-lag and lower permeability value (Kim et al. 2018; Barrer et al. 1963). 20 % ZIF-7/PDMS MMMs have the second smallest N_2 and CO_2 permeability values. The gases may difficultly permeate through the pores of ZIF-7 due to having the smallest pore diameter, 0.29 nm.

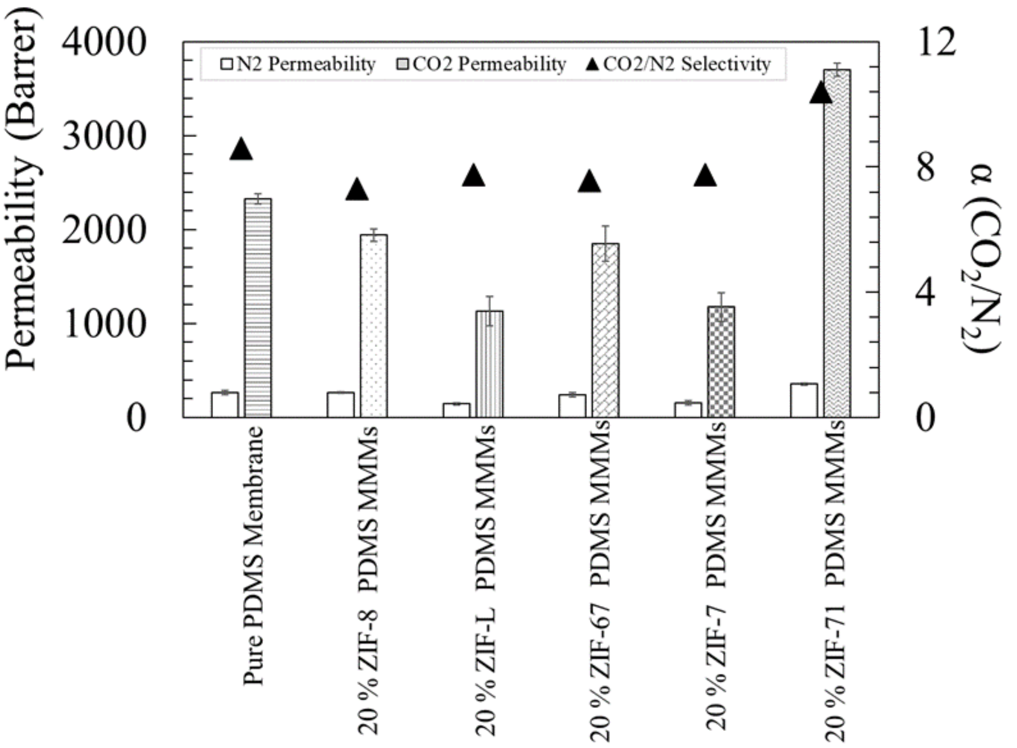

Figure 37. N_2, CO_2 permeability and CO_2/N_2 selectivity of the synthesized membranes

(Pure gas, P_{feed}: 2.92 bar and 35 ^{o}C)

20 % ZIF-L/PDMS MMMs reduced N_2 permeability by % 55 according to pure PDMS membrane regarding to experimental data. This is the desired situation in this study due to aiming VOCs selective MMMs over N_2.

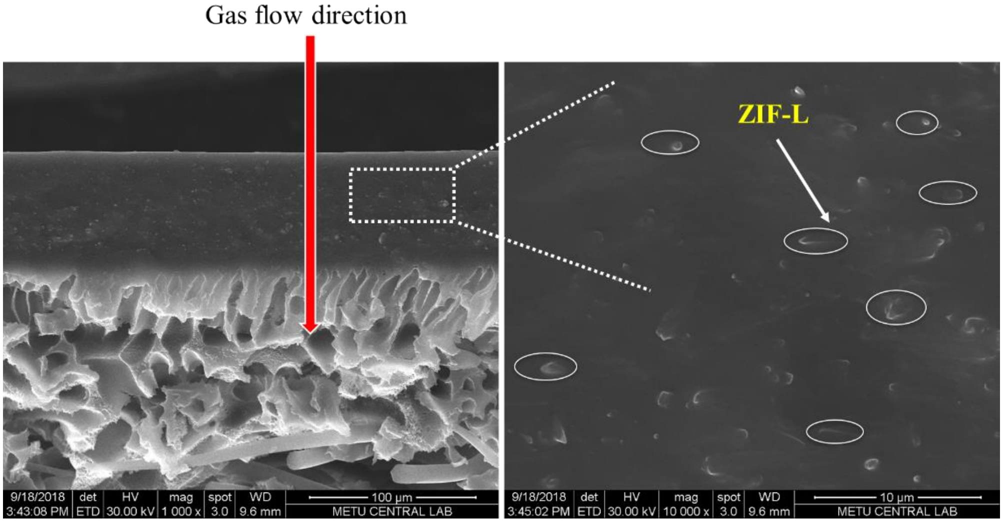

Figure 38. Gas flow direction through the 20 % ZIF-L/PDMS MMMs.

4.3.5 VOCs/N_2 Separation performance of 20 wt % ZIF loaded MMMs

A solvent recovery process usually bases on adsorption. Activated carbon is used as an adsorbent (Tsai 2002). Although carbon adsorption columns are hydrophobic, there is still some water in the mixture of N_2 and VOCs. Thus, it is essential to synthesize hydrophobic MMMs.

ZIF-8, ZIF-L, ZIF-67, ZIF-7, and ZIF-71 were chosen as a filler to synthesize PDMS based MMMs. Both ZIFs and PDMS polymer that were used in this study have hydrophobic character (Keser Demir et al. 2014; R. Chen et al. 2013; Low, Yao, et al. 2014; Li et al. 2012; Qian et al. 2012; Gücüyener et al. 2010; Ortiz et al. 2014; Park et al. 2014). These ZIFs were chosen due to their properties such as higher adsorption amount towards solvents vapors over N_2 and abundant in organic ligands that favors compatible interface morphology with PDMS without surface modification (Keser Demir et al. 2014; J.-T. Chen et al. 2013; R. Chen et al. 2013; Li et al. 2012; Qian et al. 2012; Gücüyener et al. 2010; Fang et al. 2015b). PDMS also shows selectivity to VOCs over nitrogen (Fang et al. 2015a) .

The pure PDMS membrane was used as a reference to indicate effect of ZIF addition in the polymer matrix. All MMMs contain 20 % ZIF-X by weight. Each type of membrane was synthesized at least 3 times and two part of each membrane test twice consecutively. Types of solvent and feed composition were determined with respect to conditions of a typical solvent recovery system in the industry. The membranes performance were determined by conducted the membranes a feed stream with a molar composition of EtOH:IPA:N_2=10:10:980 at 2.92 bar and 35 ^oC.

Figure 39 shows N_2 and VOCs permeability of the membranes. When we compare pure N_2 permeability value (Figure 37) with N_2 permeability in the presence of VOCs component in feed stream (Figure 39.a), it was seen that N_2 permeability increase in the presence of VOCs. In the literature, it was said that N_2 permeability value depress bellow the pure N_2 if there is a VOC in the feed stream (Lue et al. 2010; Yeom et al. 2002b). This situation was related with VOC condensability and its concentration in the feed (Leemann et al. 1996; Yeom et al. 2002b). Majumder et al. (2003) claimed that if VOCs concentration in the feed stream are too low, VOCs permeance will not be such a high that to press N_2 permeability (Majumdar et al. 2003). On the other hand, some researchers claimed that VOCs sorption in PDMS increase free volume and chain mobility of the polymer that cause the membrane swelling. Thus N_2 permeation becomes simple and its permeance value increases (Liu et al. 2009; Baker 2006). In this study, EtOH and IPA had a low molar composition in the feed, 2%, so they were not able to reduce N_2 permeability value. They might swell PDMS so N_2 permeability value increased . In addition, pure N_2 permeability value was determined at a transmembrane pressure 2 bar. However, N_2 permeability in VOCs/N_2 mixture was determined under vacuum that was applied from the permeate side which increased transmembrane pressure. This situation might also be reason of higher N_2 permeability in VOC_2/N_2 mixture than pure N_2 permeability.

EtOH vapor uptake values of ZIF-8, ZIF-67, ZIF-7 and ZIF-71 are approximately same, 6 mmol/g [7,24,25,43–46] . Therefore, it was expected that 20 wt. % ZIF-X loaded MMMs' VOCs permeability values should be closed to each other. However, VOCs permeability decreased with addition of ZIF-8 and ZIF-67 while it increased in the loading of ZIF-7 and ZIF-71 (Figure 39). This may be the result of a pore blockage. The soft PDMS chain segment might plug the pores of ZIF-8 and ZIF-67 (Fang et al. 2015a). In this case, the VOCs transition through the pores become either slow down or stops completely. The pore blockage should not occur in the pores of ZIF-71 and ZIF-7 due to having the highest and smallest pore diameter among the other ZIFs, respectively.

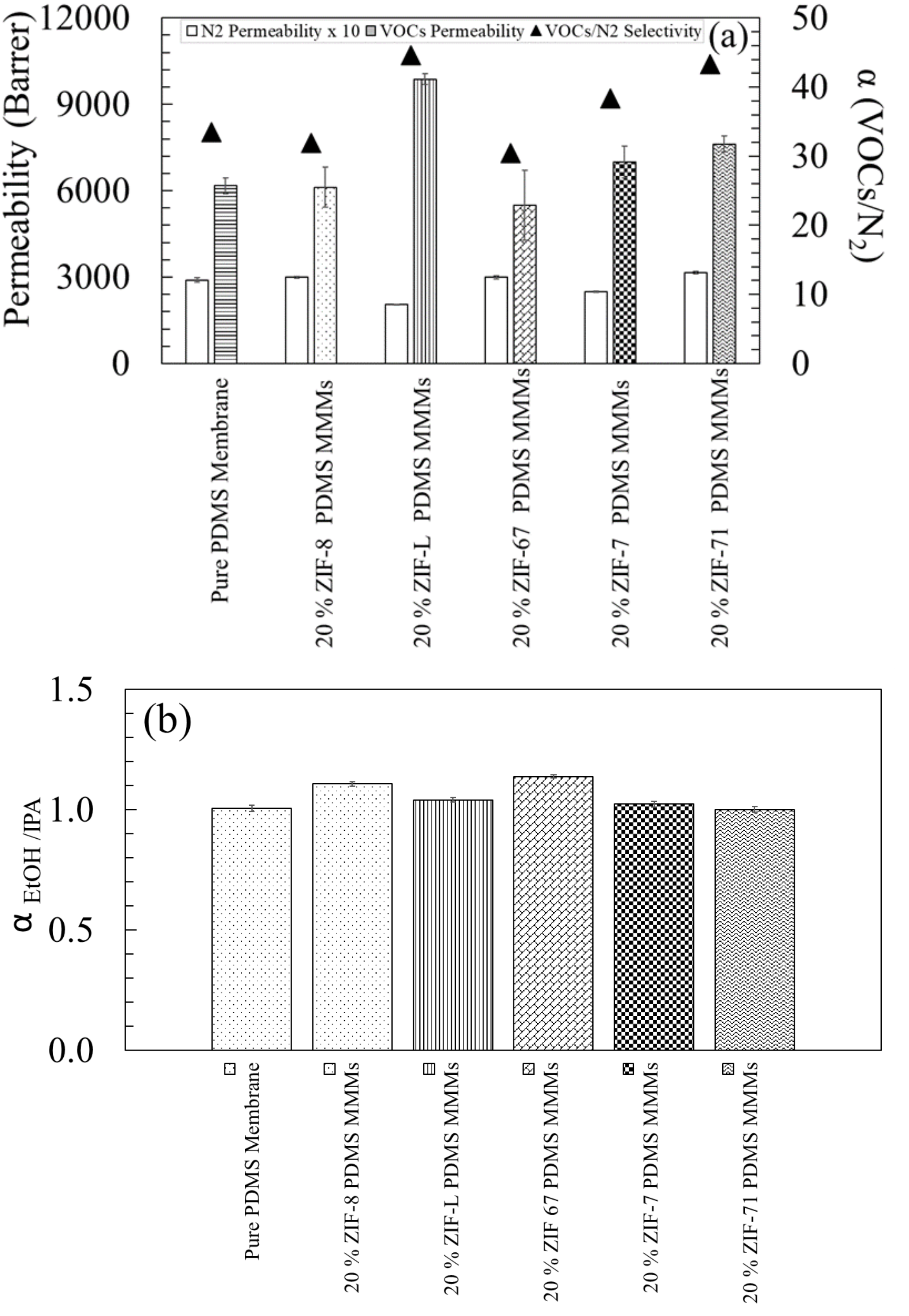

Figure 39. 20 % ZIF-X/PDMS MMMs performance (a) N_2 permeability, VOCs permeability and VOCs/N_2 selectivity (b) EtOH/IPA selectivity

(Feed molar composition EtOH:IPA:N_2= 10:10: 980 ; P_{feed} = 2.92 bar and 35 °C)

ZIF-L loading enhanced VOCs permeability, 60 %, with respect to pure PDMS membrane. To having, the highest VOCs permeability may be the reason of a leaf shape morphology of ZIF-L crystals. ZIF-L has not a channel system like the other ZIFs, so VOCs sorption cannot take place by a gate opening mechanism (R. Chen et al. 2013). However, ZIF-L has more flexible pore than the other ZIFs that have the tetrahedral structure. The pores of ZIF-L are located between two weakly connected layers that VOCs can more easily diffuse through them.

Selectivity value of pure PDMS membrane and % 20 ZIF-X/PDMS MMMs are given in Figure 39.a. There is a logical conformity between selectivity and permeability values of the same membrane. 20 % ZIF-L/PDMS MMMs display the best VOCs/N_2 selectivity value. If 20 % ZIF-L/PDMS MMMs' selectivity value is compared with pure PDMS membrane's one, it is seen that ZIF-L loading enhanced selectivity approximately 33 %.

Figure 39.b shows selectivity of EtOH/IPA, which is nearly same for all types of the membrane. However, selectivity of VOCs between themselves is not an important case in this study. Because the starting point of this study was to an enhancement of VOCs' dew point in the feed stream before condensation units of the solvent recovery process. VOCs selective membrane can increase partial pressure at the permeate side; therefore, the recovery process will be more efficient and economic.

The effect of different fillers on PDMS based membrane separation performance was determined. 20% wt ZIF-L PDMS MMMs gave the best membrane performance, so that rest of the study was carried out with it.

4.3.6 Separation of single VOC from N_2 through 20 % ZIF-L PDMS MMMs

Several studies have been carried out to specify solvent diffusion in the polymer matrix. All of these studies aimed to describe the physical properties of PDMS networks in the presence of any solvents (Masaro & Zhu 1999). Nevertheless, it is still unpredictable. It is not easy to find an appropriate membrane for a given solvent, therefore, six common solvents that are mostly preferred in the industrial application were chosen. These were methanol (MeOH), ethanol (EtOH), 1-propanol

, ethyl acetate (EtAc), 2-propanol (IPA) and butanol (ButOH). Molecular weight and vapor pressure of the solvents are given in Table 19. The solvent compatibility with PDMS polymer is determined by calculating Hansen Solubility parameter (HSP); the results are tabulated in Table 19.

20 % ZIF-L/PDMS MMMs performance was tested with single solvent vapor and N_2. For example, the feed stream molar composition was MeOH:N_2=20:980. Both permeability and selectivity value of membranes were determined at a constant temperature (35°C) and feed pressure (2.92 bar). N_2 permeability decreased (Figure 40.a) in the presence of either MeOH or EtOH or IPA or 1-propanol as demonstrated in the literature (Cen & Lichtenthaler 1995). However, N_2 permeability increased in the presence of either EtAc or ButOH. These solvents might cause the most swelling ratio of PDMS polymer matrix so that N_2 permeation became simple (Baker 2006). PDMS solubility parameter equal to 180 MPa $^{0.5}$. The closest value to PDMS belongs to EtAc, 165 MPa $^{0.5}$, which means that PDMS more likely to swell in the presence of EtAc. If a solvent and a polymer has a close δ value to each other, they are alike and compatible (Hansen 2004). When we approaches another point of view, the smallest Ra value means the highest compatibility of a solvent and a polymer (Belmares et al. 2004). According to Table 19, EtAc is once again the most compatible solvent with PDMS polymer to swell it. ButOH is the second most compatible solvent after EtAc that may cause swelling. Hence, N_2 permeability increased in the presence of EtAc and ButOH.

Table 19. Molecular weight, vapor pressure and HSP of solvents

			HSP *			Theoretical value		
Solvents	Mol.weight (g/mol)	P^{vap} (bar) (35 ^oC)	δ_D ($MPa^{0.5}$)	δ_P ($MPa^{0.5}$)	δ_H ($MPa^{0.5}$)	δ^2 (MPa)	δ ($MPa^{0.5}$)	Ra
Methanol	32.0	0.279	14.70	12.30	22.30	865	432	355
Ethanol	42.0	0.137	15.80	8.80	19.40	703	352	197
1- Propanol	60.0	0.051	16.00	6.80	17.40	605	303	125
2- Propanol	60.0	0.105	15.80	6.10	16.40	556	278	101
Butanol	74.1	0.018	16	5.70	15.80	538	269	86
Ethyl Acetate	98.6	0.205	15.8	5.30	7.20	330	165	34
PDMS			16.89	0.12	8.60	359	180	

HSP * (Charles 2000)

VOCs' permeability values versus kinetic diameter of the VOCs are given in Figure 40.b. VOCs permeation values depend on solution affinity of VOCs on the MMMs and their diffusion through it (Li et al. 2009). Diffusion depends on kinetic diameter of the permeate molecules. As it was seen from Figure 40.b, VOCs permeability value has inverse proportion with kinetic diameter (expect for EtAc). EtAc has the highest PDMS swelling ratio that may be the reason of having the highest VOCs permeability value. On the other hand, ButOH should have the second highest VOCs permeability value with respect to PDMS swelling ratio. Rumens et al., had worked on swelling ratio of PDMS with 15 different solvents (Rumens et al. 2015). They found that PDMS swelling level directly depended on how closed a solvent solubility parameter (δ) to PDMS. However, they observed that even the solvents with the same values of solubility parameter had the different swelling level. They explained that vapor pressure and molecular size of a solvent had also affected the swelling level. PDMS swell up much in case of a high vapor pressure of solvent. They added that it took longer to reach the maximum state of swelling providing that there was a large molecule. If diffusion of a large molecule is slower than the chain mobility of PDMS polymer matrix, VOCs permeance decreases. Either VOCs solubility value or kinetic diameter of them are not able to explain VOCs permeation through the membrane.

20 % ZIF-L/PDMS MMMs showed selectivity for MeOH, EtOH, IPA, EtAc, ButOH, and 1-propanol (Figure 40.c). Selectivity of EtOH/N_2 ; IPA/N_2 ; 1-propanol/N_2 ; and EtAc/N_2 are approximately same while MeOH/N_2 and ButOH/N_2 are smaller than these are. This means that 20 % ZIF-L/PDMS MMMs' separation performance depends on the solvent type.

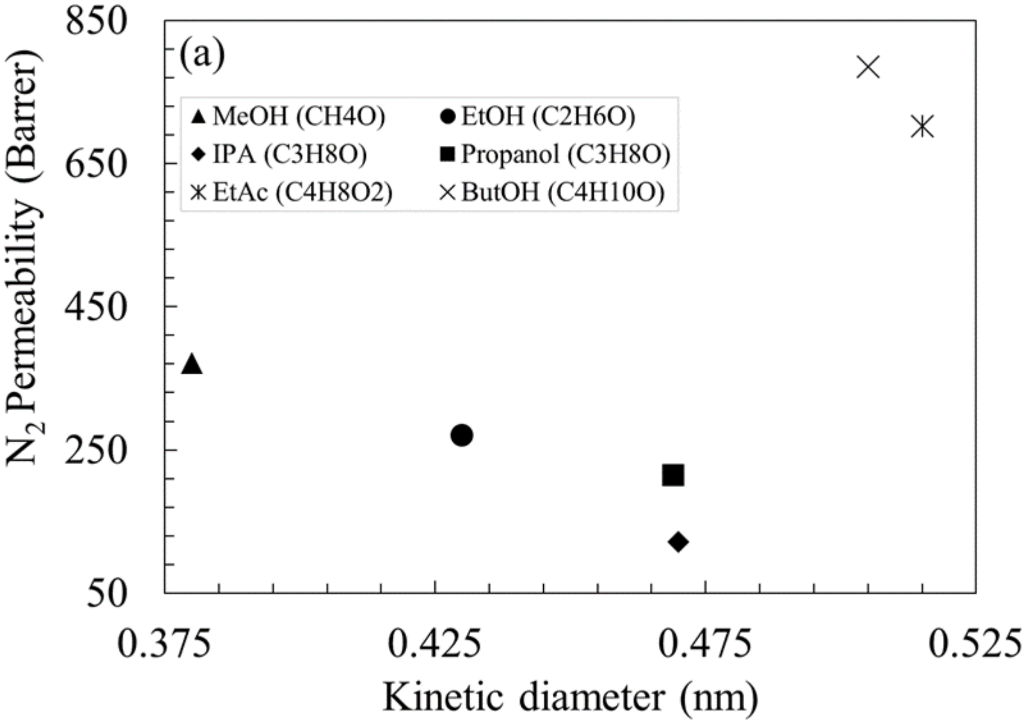
(a)
▲ MeOH (CH4O)
● EtOH (C2H6O)
◆ IPA (C3H8O)
■ Propanol (C3H8O)
✳ EtAc (C4H8O2)
× ButOH (C4H10O)
N_2 Permeability (Barrer)
850
650
450
250
50
0.375
0.425
0.475
0.525
Kinetic diameter (nm)

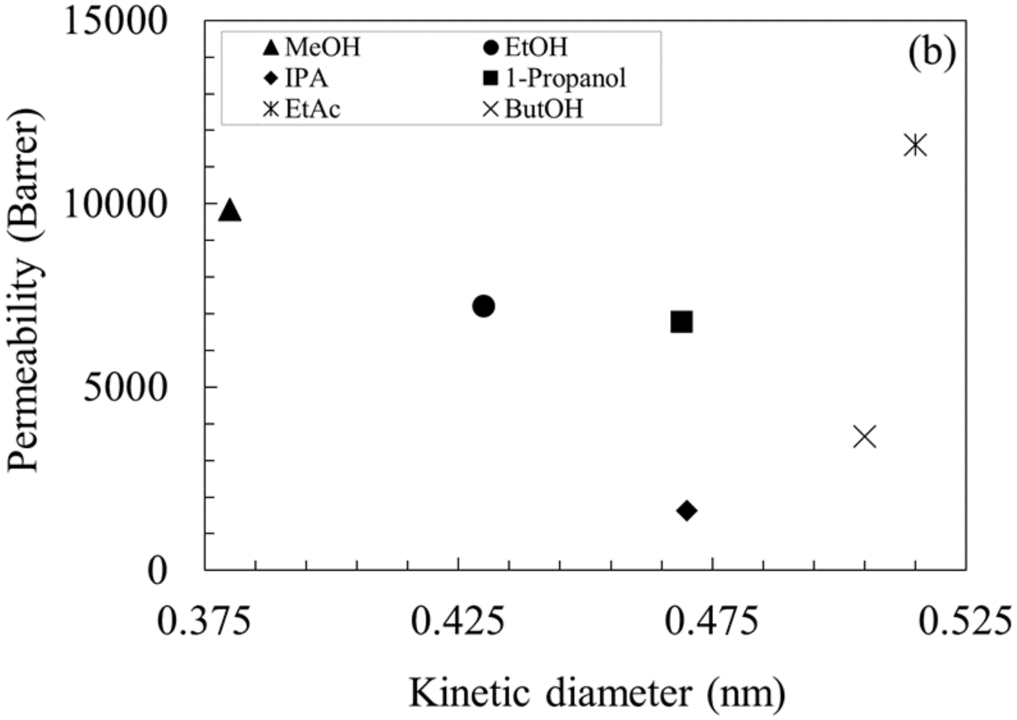
▲ MeOH
● EtOH
◆ IPA
■ 1-Propanol
✳ EtAc
× ButOH
(b)
Permeability (Barrer)
15000
10000
5000
0
0.375
0.425
0.475
0.525
Kinetic diameter (nm)

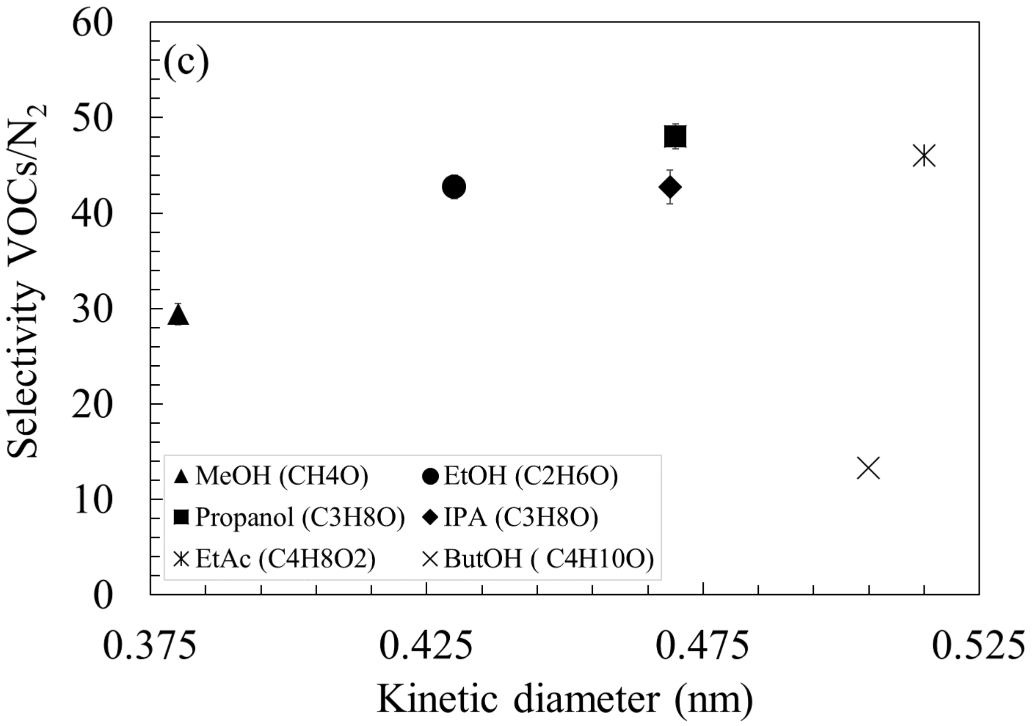

Figure 40. 20 % ZIF L/PDMS MMMs membrane performance (a) N_2 permeability value (b) VOCs permeability value (c) VOCs/N_2 selectivity

(Feed molar composition VOCs:N_2 = 20:980; P_{feed} = 2.92 bar and T_{feed} = 35 °C)

4.3.7 Effect of VOCs concentration on 20 % ZIF-L/PDMS MMMs performance

20 % ZIF-L/PDMS MMMs was tested with two different feed streams that had a molar composition of EtOH:IPA:N_2=5:5:990 and EtOH:IPA:N_2 =10:10:980 at constant feed pressure (2.92 bar) and temperature (35°C). It is known that a rise in VOCs concentration in feed stream increase chain mobility of PDMS, which affects selectivity and permeability.

As it seen in Table 20, only 1% decrease of VOCs concentration in the feed stream has a considerable change on both permeability and selectivity value. N_2 permeability value increased by % 82, at this time VOCs' permeability and $\alpha_{VOCs/N2}$ decrease 27 % and 39.5 %, respectively. VOCs and N_2 exhibit inverse effect with an increment of VOCs amount in the feed stream. Some researchers have focused on the effect of VOCs concentration on the PDMS based-membrane performance. It was pointed out that the permeation and selectivity towards VOCs represented a direct dependency with VOCs content in feed stream (Yeom et al. 2002b; Gales et al. 2002; Majumdar et al. 2003). PDMS chain mobility increased in the event of increasing VOCs concentration in the feed, thus diffusivity and permeability of VOCs would be high (Pinnau & He 2004). Gales et al. demonstrated that increasing the VOCs concentration in the feed resulted in swelling layer of the PDMS membrane so that its permeability towards VOCs increased (Gales et al. 2002). Even a slight change of VOCs concentration in the feed stream caused a very serious change in permeabilities and selectivity of $\alpha_{\text{VOCs/N2}}$ in this study too. This means that the membrane performance depends on the VOCs concentration in the feed. In view of this situation, very dilute VOCs/ N_2 mixture were handled to prove as-synthesized membrane separation performance in this study. Thus, the needs of the industry can be met in all circumstances.

Table 20. Effect of VOCs concentration on membrane performance of 20 % ZIF-L/PDMS MMMs (P_{feed} = 2.92 bar and 35 °C)

Feed stream molar composition	Permeaability (Barrer)		Selectivity
EtOH:IPA:N_2	VOCs	N_2	VOCs/N_2
10:10:980	9874	204	48
5:5:990	7178	371	19

4.3.8 Separation of multicomponent VOCs mixture from N_2 through 20 % ZIF-L/PDMS MMMs

In this study, the effect of a multicomponent mixture on separation performance of 20 % ZIF-L/PDMS MMMs was determined. The mixtures were prepared with EtOH, IPA, H_2O, and EtAc. Firstly, the mixture of EtOH and IPA (50 % and 50 % by mass) was tested. There will be water in the feed stream that is an inevitable event in an industrial process. In addition, EtAc is one of the most preferred solvent in the industrial process. Thus, N_2 /VOCs/H_2O composition of the feed was prepared by taking into consideration those situations.

20 % ZIF-L/PDMS MMMs was tested with 3 different feed stream at constant feed pressure, 2.92 bar. VOCs permeability and VOCs/N_2 selectivity increased when EtAc mass fraction was increased. Although, single vapor/N_2 selectivity value of EtOH/N_2, IPA/N_2 and EtAc/N_2 were found nearly same (Figure 40.c), it was reported that VOCs sorption onto membrane affected by presence of others. It is not easy to predict an effect of multicomponent on the membrane performance until their sorption, diffusion, and permeation behavior is well defined (Gales et al. 2002; C. K. Yeom et al. 2000).

An operating temperature of any industrial process may be high; hence, 20 % ZIF-L/PDMS MMMs' performance was determined at the temperature range from 35 ^oC to 70 ^oC. An increase in the temperature leads to an inverse effect on permeability of VOCs and N_2 (Figure 41.a). VOCs permeability diminished while there was an increment with N_2's one. It was known that permeability coefficient of a gas depends on two things: diffusion coefficient and solubility coefficient (Stern et al. 1987) . A diffusion coefficient of the gas is directly proportional to temperature; however, solubility coefficient usually shows inverse effect with the temperature increment. The N_2 permeability enhancement with respect to the temperature points out that the rise in diffusion coefficient should be higher than the reduction of the solubility coefficient. In addition, PDMS chain mobility increase with temperature, therefore, larger free volumes take shape in polymer matrix (C. K. Yeom et al. 2000). Thus, N_2 can cavalierly diffuse through them. In the literature, it was affirmed that solvents vapor and non-condensable gases exhibit contrary temperature dependence because of distinct enthalpies of sorption and diffusion (Leemann et al. 1996; Pinnau & He 2004). Leeman et al., observed that ideal selectivity of toluene-nitrogen decline from 800 to 50 when temperature increase from 30 ^oC to 140 ^oC. VOCs permeability and $\alpha_{VOCs/N2}$ decrease by increasing temperature.

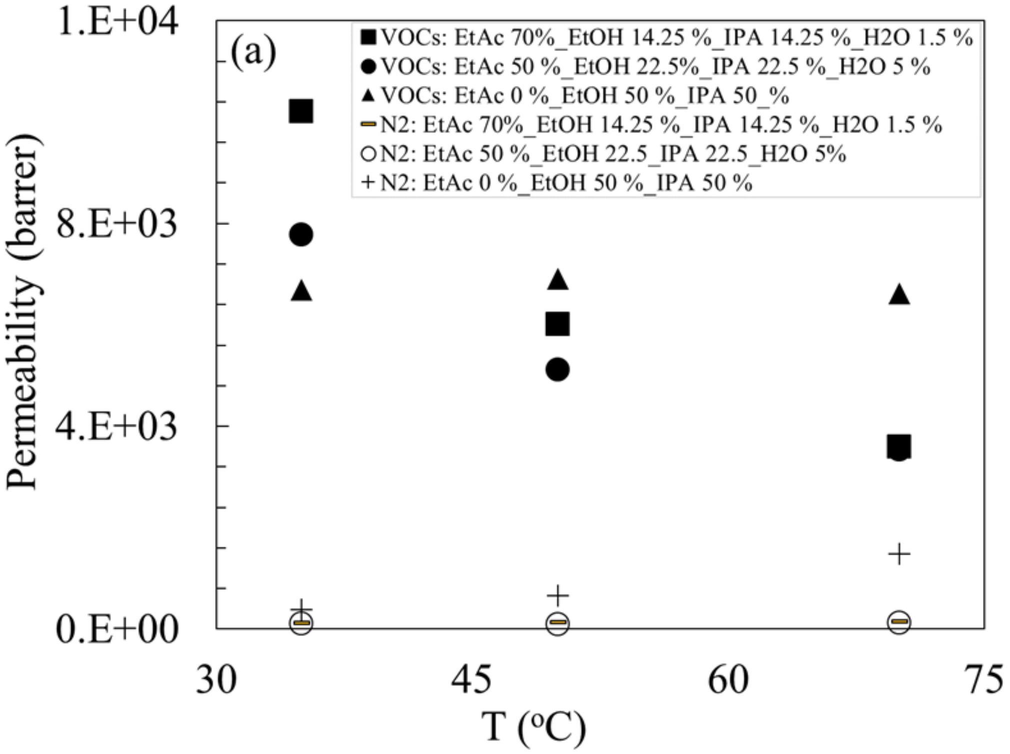
(a)
■ VOCs: EtAc 70%_EtOH 14.25 %_IPA 14.25 %_H2O 1.5 %
● VOCs: EtAc 50 %_EtOH 22.5%_IPA 22.5 %_H2O 5 %
▲ VOCs: EtAc 0 %_EtOH 50 %_IPA 50_%
− N2: EtAc 70%_EtOH 14.25 %_IPA 14.25 %_H2O 1.5 %
○ N2: EtAc 50 %_EtOH 22.5_IPA 22.5_H2O 5%
+ N2: EtAc 0 %_EtOH 50 %_IPA 50 %
Permeability (barrer)
1.E+04
8.E+03
4.E+03
0.E+00
30
45
60
75
T (°C)

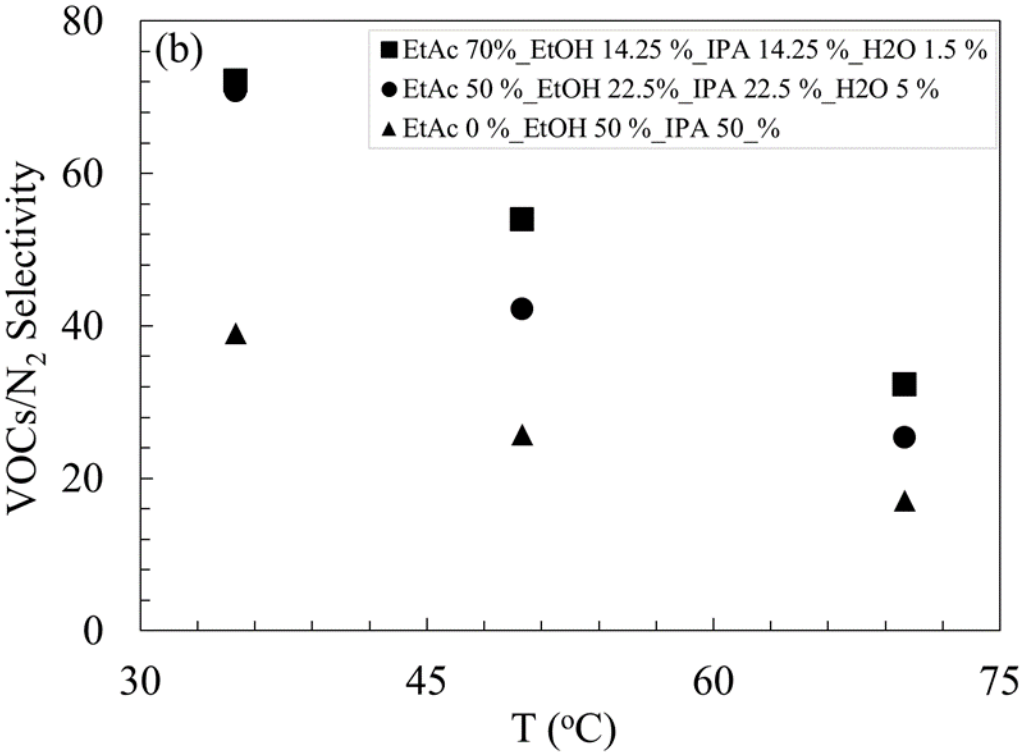
(b)
■ EtAc 70%_EtOH 14.25 %_IPA 14.25 %_H2O 1.5 %
● EtAc 50 %_EtOH 22.5%_IPA 22.5 %_H2O 5 %
▲ EtAc 0 %_EtOH 50 %_IPA 50_%
VOCs/N2 Selectivity
80
60
40
20
0
30
45
60
75
T (°C)

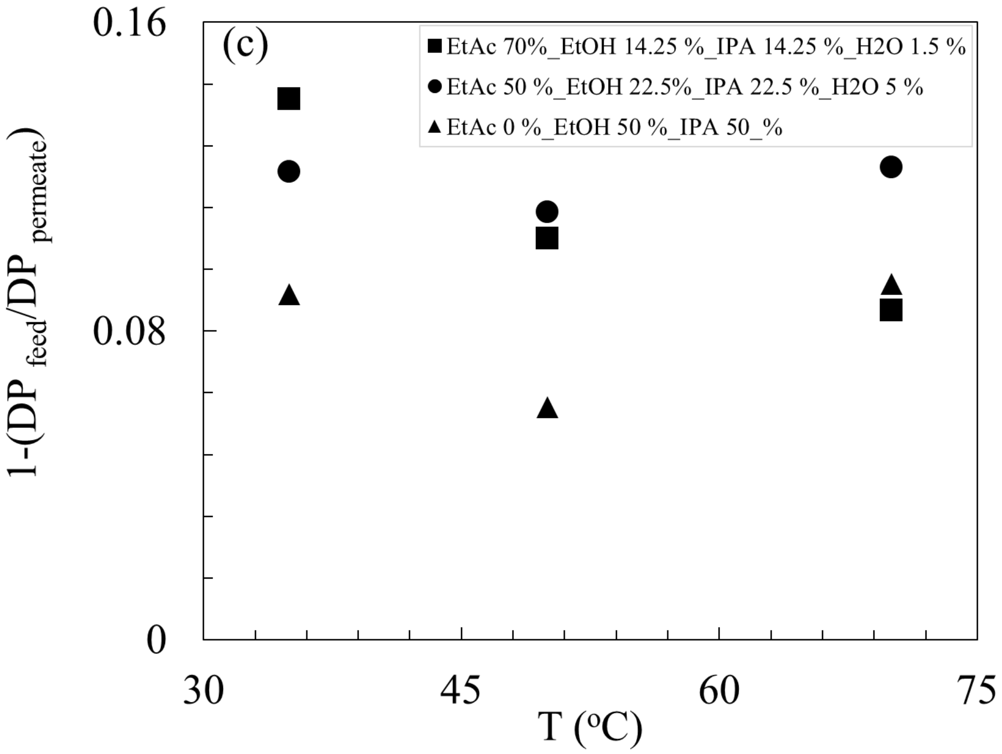

Figure 41. Performance of 20 % ZIF L/PDMS MMMs at different mass fraction and temperature (a) Permeability (b) VOCs/N_2 selectivity (c) Dew point relationship between feed and permeate

(P_{feed} = 2.92 bar and N_2 flow rate= 22 ml/min).

The dew points of feed side and permeate side were calculated by Thermosolver version 1. The higher membrane separation performance means the higher $DP_{permeate}$ value. For the sake of clarity, 1-(DP_{feed}/$DP_{permeate}$) was calculated and shown with a graph (Figure 41.c). DP_{feed} remains constant while $DP_{permeate}$ changes with respect to membrane performance. If this value approaches one, this means that DP_{feed}/$DP_{permeate}$ will approximate to zero. This is only possible with high $DP_{permeate}$ value, this is exactly what we aimed. Figure 41.c indicates that dew point is a function of both composition of VOCs in the feed stream and operating temperature.

4.4 Conclusion

The enhancement of VOCs permeability and $\alpha_{VOCs/N2}$ make the membrane a more efficient and cost-effective choice for the industrial application. The motivation of this chapter is to develop VOCs selective membrane with a high VOCs permeability value. 20 % ZIF-L/PDMS MMMs' had a VOCs permeability value of 9874 barrer and $\alpha_{VOCs/N2}$ value of 45. If those values are compared with pure PDMS membrane's ones, the results corresponds to 60 % increment in permeability and 33 % increment in selectivity.

The effect of operating temperature and VOCs concentration on 20 % ZIF-L /PDMS MMMs performance were determined. Either increasing temperature or decreasing VOCs concentration in the feed stream had negative affect on the membrane performance. Nevertheless, 20 % ZIF-L/PDMS had separation performance at the any situation.

Those results indicate that 20% ZIF-L/PDMS MMMs is a good candidate for increasing efficiency of a solvent recovery system in the industry.

REFERENCES

Abdelhamid, H.N. & Zou, X., 2018. Template-free and room temperature synthesis of hierarchical porous zeolitic imidazolate framework nanoparticles and their dye and CO $_2$ sorption. *Green Chemistry*, 20, pp.1074–1084.

Bai, Y. et al., 2013. ZIF-8 Filled Polydimethylsiloxane Membranes for Pervaporative Separation of n-Butanol from Aqueous Solution. *Separation Science and Technology (Philadelphia)*, 48(17), pp.2531–2539.

Baker, R.W., 2006. Membranes for vapor/gas separation. *Membrane Technology and research Inc*.

Banerjee, R. et al., 2008. High-throughput synthesis of zeolitic imidazolate frameworks and application to CO2 capture. *Science (New York, N.Y.)*, 319(5865), pp.939–943.

Barrer, R., Barrie, J. & Rogers, M., 1963. Heterogeneous membranes: Diffusion in filled rubber. *Journal of Polymer Science A General Papers*, 1, pp.2565–2586.

Basu, S. et al., 2010. Membrane-based technologies for biogas separations. *Chemical Society Reviews*, 39(2), pp.750–768.

Belmares, M. et al., 2004. Hildebrand and hansen solubility parameters from molecular dynamics with applications to electronic nose polymer sensors. *Journal of Computational Chemistry*, 25(15), pp.1814–1826.

Berenjian, A., Chan, N. & Malmiri, H.J., 2012. Volatile Organic Compounds removal methods: A review. *American Journal of Biochemistry and Biotechnology*, 8(4), pp.220–229.

Bergh, Johan; Gücüyener, Canan;Pidko, Evgeny;Hensen, Emiel;Gascon, Jorge;Kapteijn, F., 2011. Understanding the Anomalous Alkane Selectivity of ZIF-7 in the Separation. *Chemistry A European Journal*, 17, pp.8832–8840.

Bhattacharjee, S. et al., 2014. Zeolitic Imidazolate Frameworks: Synthesis, Functionalization, and Catalytic/Adsorption Applications. *Catalysis Surveys from Asia*, pp.101–127.

Birgül Tantekin-Ersolmaz, Ş. et al., 2001. n-Pentane/i-pentane separation by using zeolite-PDMS mixed matrix membranes. *Journal of Membrane Science*, 189(1), pp.59–68.

Brown, K.S. and C., 2002. *Air Pollution Control Technology Handbook* 1st ed., Boca Raton: CRC Press.

Cacho-Bailo, F. et al., 2016. On the molecular mechanisms for the H2/CO2separation performance of zeolite imidazolate framework two-layered membranes. *Chemical Science*, 8(1), pp.325–333.

Cen, Y. & Lichtenthaler, R.N., 1995. Chapter 3 Vapor permeation. *Membrane Science and Technology*, 2(C), pp.85–112.

Chandak, M. V. et al., 1998. Sorption and diffusion of volatile organic compounds in polydimethylsiloxane membranes. *Journal of Applied Polymer Science*, 67(1), pp.165–175.

Charles, M., 2000. *Hansen Solubility Parameters: A User's Handbook*, America: CRC Press LLC.

Chen, J.-T. et al., 2013. Surface modification of poly(dimethylsiloxane) by atmospheric pressure high temperature plasma torch to prepare high-performance gas separation membranes. *Journal of Membrane Science*, 440, pp.1–8.

Chen, R. et al., 2013. A two-dimensional zeolitic imidazolate framework with a cushion-shaped cavity for CO2 adsorption. *Chemical communications (Cambridge, England)*, 49(82), pp.9500–2.

Choi, S.H., Kim, J.H. & Lee, S.B., 2007. Sorption and permeation behaviors of a series of olefins and nitrogen through PDMS membranes. *Journal of Membrane Science*, 299(1–2), pp.54–62.

Chung, T.S. et al., 2007. Mixed matrix membranes (MMMs) comprising organic polymers with dispersed inorganic fillers for gas separation. *Progress in Polymer*

Science (Oxford), 32(4), pp.483–507.

Cravillon, J. et al., 2012. Formate modulated solvothermal synthesis of ZIF-8 investigated using time-resolved in situ X-ray diffraction and scanning electron microscopy. *CrystEngComm*, 14(2), p.492.

Dam, M., 2006. Solvent resistant microfluidics. In *Solvent-resistant elastomeric microfluidic devices and applications*. California: California Institute of Technology, pp. 24–66.

Daojun Zhang , Huaizhong Shi , Renchun Zhang , Zirui Zhang , Nan Wang , Junwei Li , Baiqing Yuan, HelongBaib, Jingchao Zhang, A. & Novel, 2013. Quick synthesis of zeoliticimidazolate framework microflowers with enhanced surpercapacitor and electrocatalytic performances. *The Royal Society of Chemistry*, 00(1–3).

Ding, B. et al., 2018. Hydrothermal preparation of hierarchical ZIF-L nanostructures for enhanced CO_2capture. *Journal of Colloid and Interface Science*, 519, pp.38–43.

Ding, L. & Yazaydin, A.O., 2013. The effect of SO_2 on CO_2 capture in zeolitic imidazolate frameworks. *Physical Chemistry Chemical Physics*, 15(28), p.11856.

Du, Y. et al., 2017. Insights into the Flexibility of ZIF-7 and Its Structural Impact in Alcohol Adsorption. *Journal of Physical Chemistry C*, 121(50), pp.28090–28095.

Fang, M. et al., 2015a. ZIF-8/PDMS mixed matrix membranes for propane/nitrogen mixture separation: Experimental result and permeation model validation. *Journal of Membrane Science*, 474, pp.103–113.

Fang, M. et al., 2015b. ZIF-8/PDMS mixed matrix membranes for propane/nitrogen mixture separation: Experimental result and permeation model validation. *Journal of Membrane Science*, 474, pp.103–113.

Freeman, Y.Y. and B., 2010. *Membrane Gas Separation* 1st ed., Hoboken: Wiley.

Gales, L., Mendes, a. & Costa, C., 2002. Removal of acetone, ethyl acetate and ethanol vapors from air using a hollow fiber PDMS membrane module. *Journal of Membrane Science*, 197(1–2), pp.211–222.

Gross, A.F., Sherman, E. & Vajo, J.J., 2012. Aqueous room temperature synthesis of cobalt and zinc sodalite zeolitic imidizolate frameworks. *Dalton Transactions*, 41(18), p.5458.

Gücüyener, C. et al., 2010. Ethane/ethene separation turned on its head: Selective ethane adsorption on the metal-organic framework ZIF-7 through a gate-opening mechanism. *Journal of the American Chemical Society*, 132(50), pp.17704–17706.

Hansen, C.M., 2004. 50 Years with solubility parameters - Past and future. *Progress in Organic Coatings*, 51(1), pp.77–84.

Hunger, K. et al., 2012. Investigation of cross-linked and additive containing polymer materials for membranes with improved performance in pervaporation and gas separation. *Membranes*, 2(4), pp.727–763.

Keser Demir, N. et al., 2014. Synthesis of ZIF-8 from recycled mother liquors. *Microporous and Mesoporous Materials*, 198, pp.291–300.

Khan, A. et al., 2018. ZIF-67 filled PDMS mixed matrix membranes for recovery of ethanol via pervaporation. *Separation and Purification Technology*, 206(May), pp.50–58.

Khan, F.I. & Kr. Ghoshal, A., 2000. Removal of Volatile Organic Compounds from polluted air. *Journal of Loss Prevention in the Process Industries*, 13(6), pp.527–545.

Kida, K. et al., 2013. Formation of high crystalline ZIF-8 in an aqueous solution. *CrystEngComm*, 15(9), p.1794.

Kim, H. et al., 2009. PDMS-silica composite membranes with silane coupling for propylene separation. *Journal of Membrane Science*, 344(1–2), pp.211–218.

Kim, S. et al., 2018. The enhanced hydrogen separation performance of mixed matrix membranes by incorporation of two-dimensional ZIF-L into polyimide containing hydroxyl group. *Journal of Membrane Science*, 549(December 2017), pp.260–266.

Koros, W.J. & Mahajan, R., 2001. Pushing the limits on possibilities for large scale gas separation: Which strategies? *Journal of Membrane Science*, 181(1), p.141.

Lape, N.K., Nuxoll, E.E. & Cussler, E.L., 2004. Polydisperse flakes in barrier films. *Journal of Membrane Science*, 236(1–2), pp.29–37.

Lee, Y.-R. et al., 2015. ZIF-8: A comparison of synthesis methods. *Chemical Engineering Journal*, 271, pp.276–280.

Leemann, M., Eigenberger, G. & Strathmann, H., 1996. Vapour permeation for the recovery of organic solvents from waste air streams: Separation capacities and process optimization. *Journal of Membrane Science*, 113(2), pp.313–322.

Li, H., Ma, H., Wang, X., Gao, J., et al., 2014. Efficient oxidation of ethylbenzene catalyzed by cobalt zeolitic imidazolate framework ZIF-67 and NHPI. *Journal of Energy Chemistry*, 23(6), pp.742–746.

Li, J.R., Kuppler, R.J. & Zhou, H.C., 2009. Selective gas adsorption and separation in metal-organic frameworks. *Chemical Society Reviews*, 38(5), pp.1477–1504.

Li, T. et al., 2012. Carbon dioxide selective mixed matrix composite membrane containing ZIF-7 nano-fillers. *Journal of Membrane Science*, 425–426, pp.235–242.

Li, T. et al., 2013. Carbon dioxide selective mixed matrix composite membrane containing ZIF-7 nano-fillers. *Journal of Membrane Science*, 425–426, pp.235–242.

Li, Y., Wee, L.H., Martens, J.A. & Vankelecom, I.F.J., 2014. ZIF-71 as a potential filler to prepare pervaporation membranes for bio-alcohol recovery. *J. Mater. Chem. A*, 2(26), pp.10034–10040.

Li, Y., Wee, L.H., Martens, J. a & Vankelecom, I.F.J., 2014. ZIF-71 as a potential filler to prepare pervaporation membranes for bio-alcohol recovery. *Journal of Materials Chemistry A*, 2, pp.10034–10040.

Li, Y., Wee, L.H., Martens, J.A. & Vankelecom, I.F.J., 2014. ZIF-71 as a potential filler to prepare pervaporation membranes for bio-alcohol recovery. *Journal of Materials Chemistry A*, 2(26), pp.10034–10040.

Li, Y.S. et al., 2010. Molecular sieve membrane: Supported metal-organic framework with high hydrogen selectivity. *Angewandte Chemie - International Edition*, 49(3), pp.548–551.

Lin, K.-Y.A. & Chang, H.-A., 2015a. Ultra-high adsorption capacity of zeolitic imidazole framework-67 (ZIF-67) for removal of malachite green from water. *Chemosphere*, 67, pp.1–8.

Lin, K.-Y.A. & Chang, H.-A., 2015b. Zeolitic Imidazole Framework-67 (ZIF-67) as a heterogeneous catalyst to activate peroxymonosulfate for degradation of Rhodamine B in water. *Journal of the Taiwan Institute of Chemical Engineers*, 000, pp.1–6.

Liu, G. et al., 2014. Enhanced desulfurization performance of PDMS membranes by incorporating silver decorated dopamine nanoparticles. *Journal of Materials Chemistry A*, 2(32), pp.12907–12917.

Liu, L. et al., 2009. Separation of VOCs from N2 using poly(ether block amide) membranes. *Canadian Journal of Chemical Engineering*, 87(3), pp.456–465.

Liu, Q. et al., 2014. Direct conversion of two-dimensional ZIF-L film to porous ZnO nano-sheet film and its performance as photoanode in dye-sensitized solar cell. *Microporous and Mesoporous Materials*, 194, pp.1–7.

Liu, X.L. et al., 2011. An organophilic pervaporation membrane derived from metal-organic framework nanoparticles for efficient recovery of bio-alcohols. *Angewandte Chemie - International Edition*, 50(45), pp.10636–10639.

Lively, R.P. et al., 2011. Ethanol and water adsorption in methanol-derived ZIF-71. *Chemical Communications*, 47(30), pp.8667–8669.

Louglin, J.C.H. and S.O., 2011. *Volatile Organic Compounds* 1st ed., Newyork: Nova Science.

Low, Z.X., Yao, J., et al., 2014. Crystal transformation in zeolitic-imidazolate framework. *Crystal Growth and Design*, 14(12), pp.6589–6598.

Low, Z.X., Razmjou, A., et al., 2014. Effect of addition of two-dimensional ZIF-L nanoflakes on the properties of polyethersulfone ultrafiltration membrane. *Journal of Membrane Science*, 460, pp.9–17.

Lue, S.J., Wang, S.F., et al., 2008. Diffusion of multicomponent vapors in a poly(dimethyl siloxane) membrane. *Desalination*, 233(1–3), pp.277–285.

Lue, S.J. et al., 2010. Sorption, diffusion, and perm-selectivity of toluene vapor/nitrogen mixtures through polydimethylsiloxane membranes with two cross-linker densities. *Journal of Membrane Science*, 349(1–2), pp.321–332.

Lue, S.J., Chen, W.W., et al., 2008. Vapor permeation modeling of multi-component systems using a poly(dimethylsiloxane) membrane. *Journal of Membrane Science*, 311(1–2), pp.380–389.

Majumdar, S., Bhaumik, D. & Sirkar, K.K., 2003. Performance of commercial-size plasmapolymerized PDMS-coated hollow fiber modules in removing VOCs from N2/air. *Journal of Membrane Science*, 214(2), pp.323–330.

Masaro, L. & Zhu, X.X., 1999. *Physical models of diffusion for polymer solutions, gels and solids*,

McEwen, J., Hayman, J.D. & Ozgur Yazaydin, A., 2013. A comparative study of CO2, CH4and N2adsorption in ZIF-8, Zeolite-13X and BPL activated carbon. *Chemical Physics*, 412, pp.72–76.

Merkel, T.C. et al., 2002. Ultrapermeable, Reverse-Selective Nanocomposite Membranes. *Science*, 296(April), pp.519–522.

Nevers, N. de, 2000. *Air pollution control engineering* 2nd ed., Boston: McGraw-Hill.

Norman N Li et al., 2008. *Advanced Membrane Technology and Applications*, New Jersey: Wiley.

Obuskovic, G., Majumdar, S. & Sirkar, K.K., 2003. Highly VOC-selective hollow fiber membranes for separation by vapor permeation. *Journal of Membrane Science*, 217(1–2), pp.99–116.

Ortiz, G. et al., 2014. Energetic performances of ‘ZIF-71-aqueous solution’ systems: A perfect shock-absorber with water. *Journal of Physical Chemistry C*, 118(37), pp.21316–21322.

Pan, Y. et al., 2011. Rapid synthesis of zeolitic imidazolate framework-8 (ZIF-8) nanocrystals in an aqueous system. *Chemical communications (Cambridge, England)*, 47(7), pp.2071–2073.

Park, E.J. et al., 2014. Hydrophobic polydimethylsiloxane (PDMS) coating of mesoporous silica and its use as a preconcentrating agent of gas analytes. *Langmuir*, 30(34), pp.10256–10262.

Park, K.S. et al., 2006. Exceptional chemical and thermal stability of zeolitic imidazolate frameworks. *Proceedings of the National Academy of Sciences of the United States of America*, 103(27), pp.10186–10191.

Peinemann, S.P.N. and K.-V., 2006. *Membrane Tecnology in the Chemical Industry* Secod., Weinheim, Germany: Wiley-VCH.

Pera-Titus, M. & Farrusseng, D., 2012. Guest-induced gate opening and breathing phenomena in soft porous crystals: Building thermodynamically consistent isotherms. *Journal of Physical Chemistry C*, 116(2), pp.1638–1649.

Phan, A. et al., 2010. Synthesis, structure, and carbon dioxide capture properties of zeolitic imidazolate frameworks. *Accounts of Chemical Research*, 43(1), pp.58–67.

Pinnau, I. & He, Z., 2004. Pure- and mixed-gas permeation properties of polydimethylsiloxane for hydrocarbon/methane and hydrocarbon/hydrogen separation. *Journal of Membrane Science*, 244(1–2), pp.227–233.

Polyzoidis, A. et al., 2016. Continuous microreactor synthesis of ZIF-8 with high space-time-yield and tunable particle size. *Chemical Engineering Journal*, 283, pp.971–977.

Qian, J., Sun, F. & Qin, L., 2012. Hydrothermal synthesis of zeolitic imidazolate framework-67 (ZIF-67) nanocrystals. *Materials Letters*, 82, pp.220–223.

Rao, H., Liu, F. & Zhang, Z., 2007. Preparation and oxygen / nitrogen permeability of PDMS crosslinked membrane and PDMS / tetraethoxysilicone hybrid membrane. *Membrane Science*, 303, pp.132–139.

Rumens, C. V. et al., 2015. Swelling of PDMS networks in solvent vapours; applications for passive RFID wireless sensors. *Journal of Materials Chemistry C*, 3(39), pp.10091–10098.

S.A.Stern, R.D.N. and, 1995. *Membrane Separations Technology* 1st ed., Amsterdam, Netherlands: Elsevier Science.

Şahin, F.; Topuz, B.;Kalıpçılar, H., 2018. Microporous and Mesoporous Materials Synthesis of ZIF-7 , ZIF-8 , ZIF-67 and ZIF-L from recycled mother liquors. *Microporous and Mesoporous Materials*, 261(November 2017), pp.259–267.

Scott, K., 1998. Separation of organic vapour/air mixtures. *Handbook of Industrial Membranes*, pp.355–372.

Shi, Y., Burns, C.M. & Feng, X., 2006. Poly (dimethyl siloxane) thin film composite membranes for propylene separation from nitrogen. *Membrane Science*, 282, pp.115–123.

Smallwood, I.M., 2002. *Solvent Recovery Handbook,* 2nd ed., Victoria, Australia: Blackwell Science Ltd.

Sridhar, S., Bee, S. & Bhargava, S.K., 2014. Membrane-based Gas Separation: Principle, Applications and Future Potential. *Chemical Engineering Digest*, pp.1–25.

Stern, S.A., Shah, V.M. & Hardy, B.J., 1987. Structure-permeability relationships in silicone polymers. *Journal of Polymer Science Part B: Polymer Physics*, 25(6), pp.1263–1298.

Thompson, J.A. et al., 2012. Hybrid Zeolitic Imidazolate Frameworks: Controlling Framework Porosity and Functionality by Mixed-Linker Synthesis. *Chemistry of*

Materials, 24, pp.1930–1936.

Tsai, W.T., 2002. A review of environmental hazards and adsorption recovery of cleaning solvent hydrochlorofluorocarbons (HCFCs). *Journal of Loss Prevention in the Process Industries*, 15(2), pp.147–157.

Venna, S.R., Jasinski, J.B. & Carreon, M. a., 2010. Structural evolution of zeolitic imidazolate framework-8. *Journal of the American Chemical Society*, 132(51), pp.18030–18033.

Venna, S.R., Jasinski, J.B. & Carreon, M. a, 2010. Supporting Information structural evolution of zeolitic imidazolate framework-8. *Journal of the American Chemical Society*, 132(51), pp.1–6.

Wang, X. et al., 2014. Rapid and Cost-Effective Synthesis of Nanosized Zeolitic Imidazolate Framework-7 with N , N ’ -Dimethylformamide as Solvent and Metal Acetate Salt as Metal Source. *ChemPlusChem*, 0000(00), pp.1–7.

Wang, X. et al., 2016. ZIF-7/PDMS mixed matrix membranes for pervaporation recovery of butanol from aqueous solution. *Separation and Purification Technology*, 163, pp.39–47.

Wu, F. et al., 2006. Operational Model for Evaluating the Permeation of Mixed Gas Through Poly(dimethylsiloxane) Membrane. *Chinese Journal of Chemical Engineering*, 14(5), pp.700–707.

Yao, J., He, M. & Wang, H., 2015. Strategies for controlling crystal structure and reducing usage of organic ligand and solvents in the synthesis of zeolitic imidazolate frameworks. *CrystEngComm*, 17(27), pp.4970–4976.

Yeom, C.K. et al., 2000. Analysis of permeation transients of pure gases through dense polymeric membranes measured by a new permeation apparatus. *Journal of Membrane Science*, 166(1), pp.71–83.

Yeom, C.K. et al., 2002a. Vapor permeations of a series of VOCs/N2 mixtures through PDMS membrane. *Journal of Membrane Science*, 198(1), pp.129–143.

Yeom, C.K. et al., 2002b. Vapor permeations of a series of VOCs/N2 mixtures through

PDMS membrane. *Journal of Membrane Science*, 198(1), pp.129–143.

Yeom, C.K., Lee, S.H. & Lee, J.M., 2000. Study of Transport of Pure and Mixed CO 2 / N 2 Gases through Polymeric Membranes. *Journal of Applied Physics*, 78, pp.179–189.

Yin, H. et al., 2017. Free-standing ZIF-71/PDMS nanocomposite membranes for the recovery of ethanol and 1-butanol from water through pervaporation. *Journal of Membrane Science*, 529(September 2016), pp.286–292.

Yunpan Ying, Yuanlong Xiao, Jing Ma, Xiangyu Guo, Hongliang Huang, Qingyuan Yang, D.L., Zhong, C. & Metal-organic, 2013. Recovery of Acetone from Aqueous Solution by ZIF-7/PDMS Mixed Matrix Membranes. *The Royal Society of Chemistry*, 00(1–3).

Zhang, K. et al., 2013. Exploring the framework hydrophobicity and flexibility of zif-8: From biofuel recovery to hydrocarbon separations. *Journal of Physical Chemistry Letters*, 4(21), pp.3618–3622.

Zhong, Z. et al., 2015. Oriented two-dimensional zeolitic imidazolate framework-L membranes and their gas permeation properties. *J. Mater. Chem. A*, 3(30), pp.15715–15722.

APPENDICES

A. Reproducibility of ZIFs

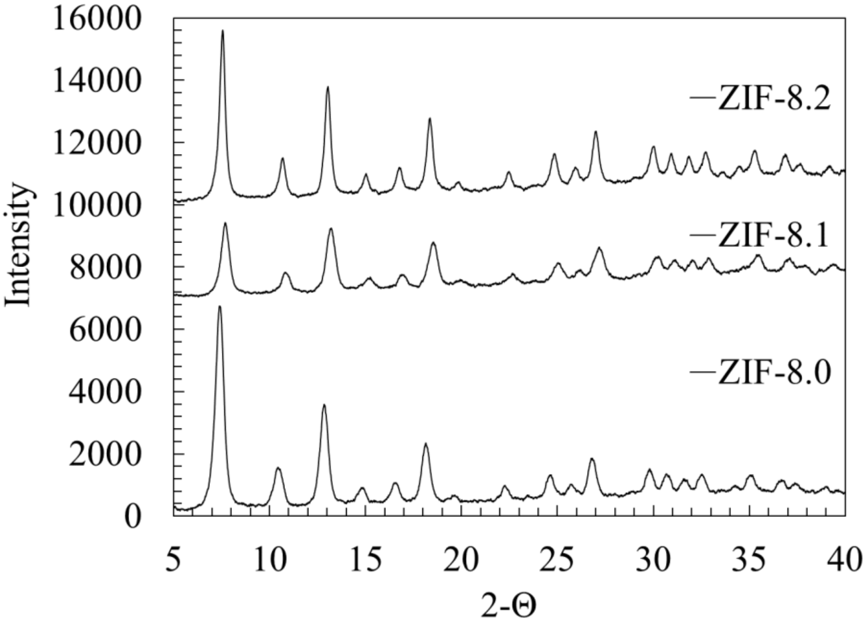

Trial 1

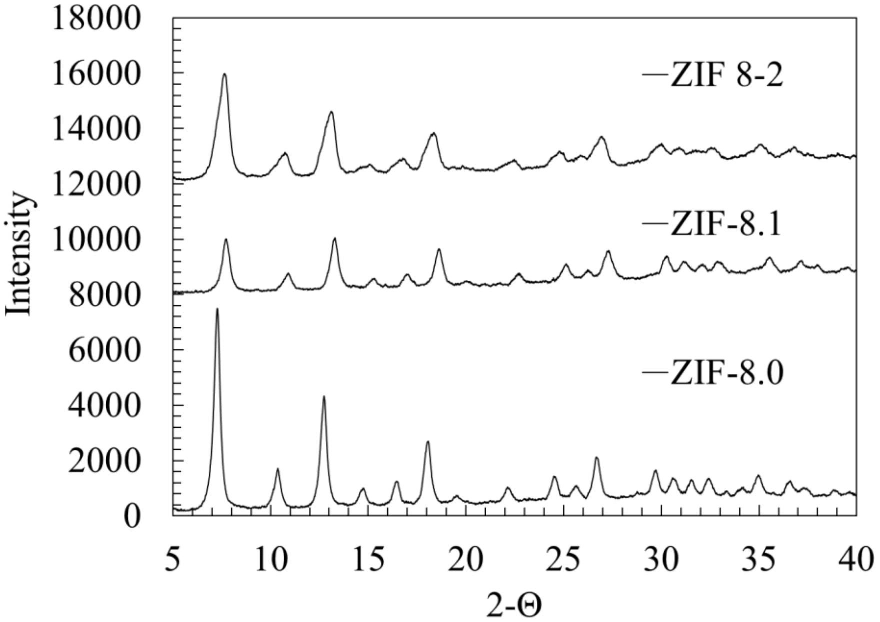

Trial 2

Figure A. 1. XRD Patterns of ZIF-8 crystals with different batches

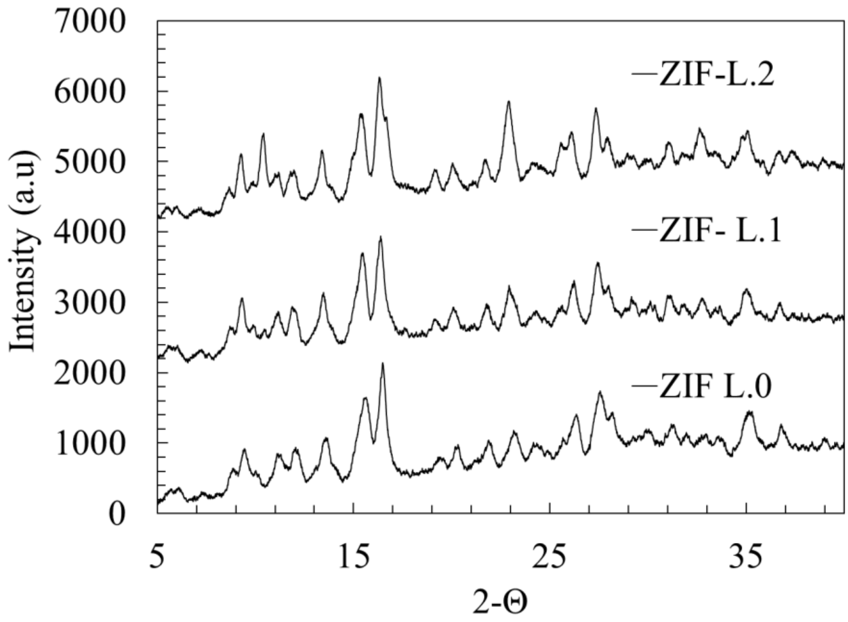

Trial 1

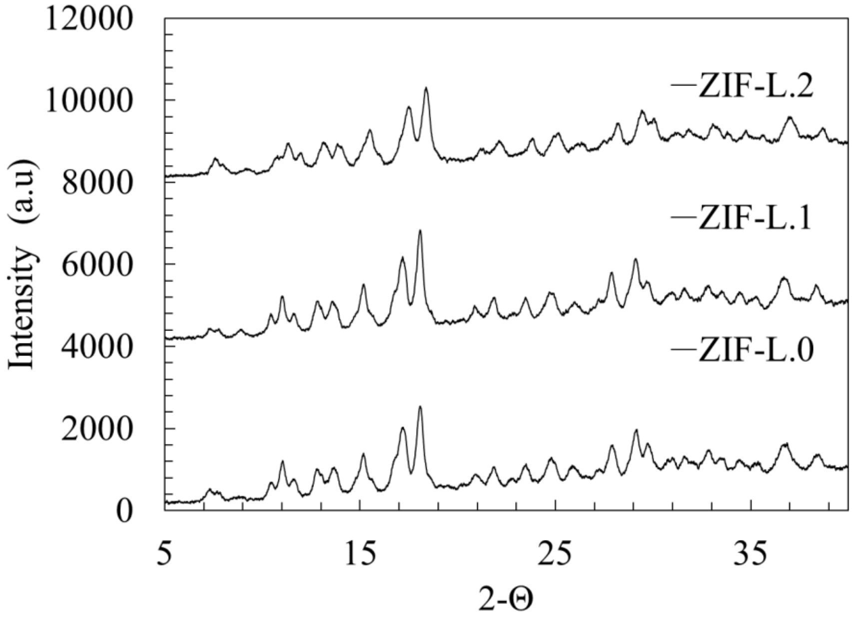

Trial 2

Figure A. 2. XRD Patterns of ZIF-L crystals with different batches

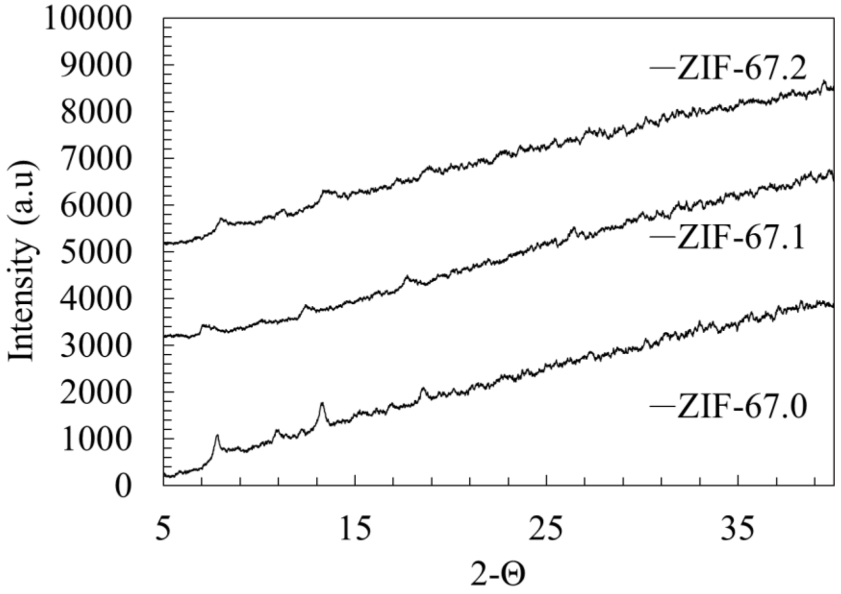

Trial 1

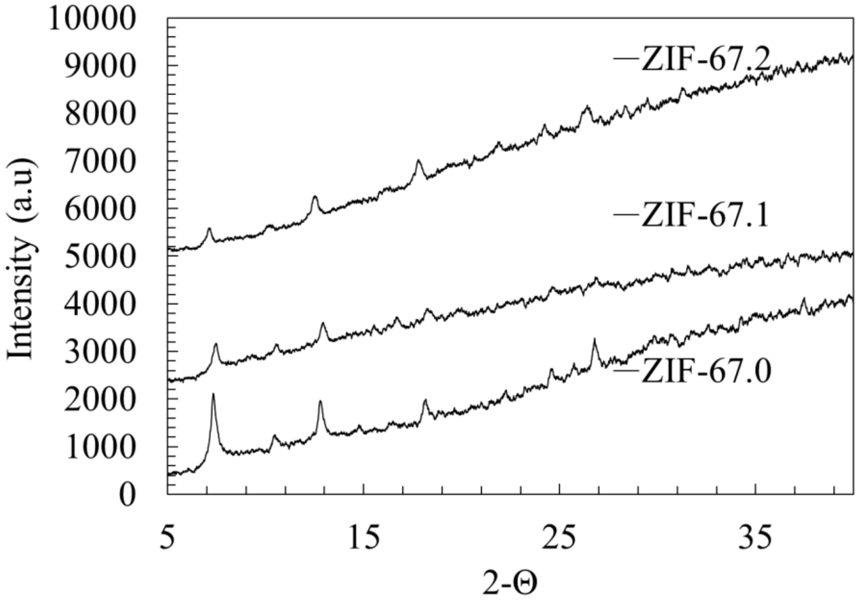

Trial 2

Figure A. 3. XRD Patterns of ZIF-67 crystals with different batches

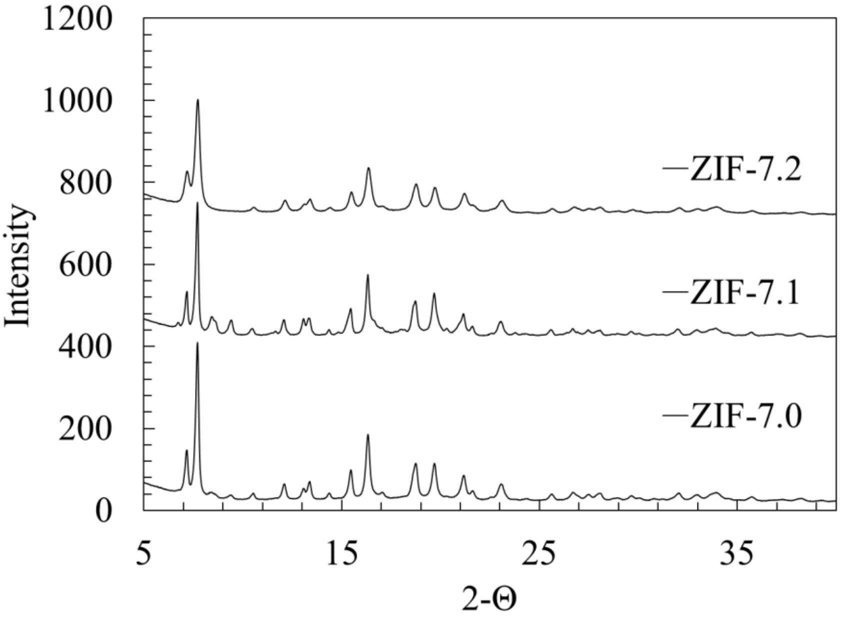

Trial 1

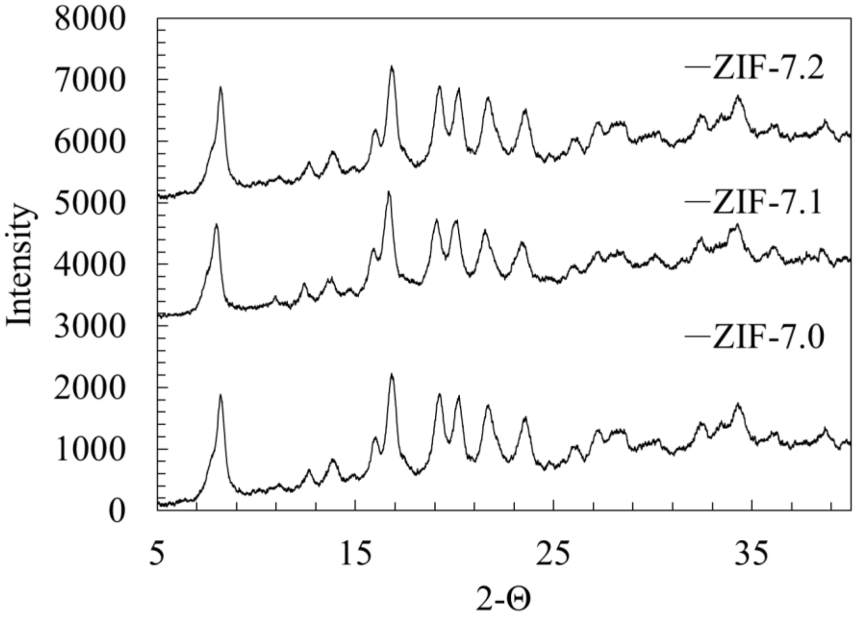

Trial 2

Figure A. 4. XRD Patterns of ZIF-7 crystals with different batches

B. Relative Crystallinity of ZIFs

Relative crystallinity of ZIF-X.1 and ZIF-X.2 were determined relating to ZIF-X.0. ZIF-X.0 was assumed 100 % then ZIF-X.1 and ZIF-X.2 were calculated with respect to this.

Table B. 1. Relative crystallinity of ZIF-8 crystals

ZIF-8					
ZIF-8.0		ZIF-8.1		ZIF-8.2	
2-Θ (degree)	Intensity (a.u)	2-Θ (degree)	Intensity (a.u)	2-Θ (degree)	Intensity (a.u)
7.24	1418	7.28	1081	7.28	1806
10.30	244	10.34	199	10.34	286
12.63	487	12.68	418	12.68	608
14.64	88	14.64	73	14.66	104
16.37	105	16.43	87	16.41	120
17.96	213	17.98	185	17.98	264
22.06	59	22.10	47	22.08	67
24.44	79	24.46	62	24.48	91
Total	2693		2152		3345
Crystallinity %	100		80		155

Table B. 2. Relative crystallinity calculation results of ZIF-L crystals

ZIF-L					
ZIF-L.0		ZIF-L.1		ZIF-L.2	
2-Θ (degree)	Intensity (a.u)	2-Θ (degree)	Intensity (a.u)	2-Θ (degree)	Intensity (a.u)
7.30	103	7.24	120	7.24	97
7.76	61	7.69	71	7.69	73
8.97	47	8.88	50	8.88	51
10.40	92	10.32	97	10.32	107
10.99	161	10.91	163	10.91	175
11.59	100	11.51	94	11.49	97
12.74	101	12.63	102	12.65	109
12.98	87	12.88	76	12.90	76
13.52	95	13.41	88	13.43	96
13.76	83	13.66	80	13.66	91
14.70	62	14.60	55	14.60	53
15.14	154	15.05	140	15.05	147
15.61	61	15.50	55	15.50	60
16.69	83	16.59	71	16.61	84
17.08	137	17.14	133	17.14	137
17.25	156	17.23	74	17.23	84
18.05	250	17.94	217	17.94	230
18.60	49	18.50	44	18.50	49
20.18	30	20.12	27	20.10	29
20.83	51	20.75	46	20.75	52
21.78	70	21.69	63	21.72	70
22.78	33	22.70	29	22.70	34
23.46	62	23.42	47	23.42	56
24.67	53	24.67	38	24.67	42
24.93	50	24.91	33	24.91	38
Total	2231		2014		2137
Crystallinity %	100		90		96

Table B. 3. Relative crystallinity calculation results of ZIF-67 crystals

ZIF-67					
ZIF-67.0		ZIF-67.1		ZIF-67.2	
2-Θ (degree)	Intensity (a.u)	2-Θ (degree)	Intensity (a.u)	2-Θ (degree)	Intensity (a.u)
7.36	562	7.36	301	7.28	394
9.96	16	9.96	19	9.95	18
13.26	16	13.26	19	13.27	17
15.86	13	15.82	15	15.81	13
17.69	13	17.71	16	17.68	13
19.98	12	19.94	14	19.97	11
21.73	12	21.77	15	21.72	11
23.33	13	23.33	15	23.23	11
toplam	656		412		488
Crystallinity %	100		63		74

Table B. 4. Relative crystallinity calculation results of ZIF-7 crystals

ZIF-7					
ZIF-7.0		ZIF-7.1		ZIF-7.2	
2-Θ	Intensity (a.u)	2-Θ	Intensity (a.u)	2-Θ	Intensity (a.u)
7.19	128	7.19	147	7.19	134
7.75	301	7.73	409	7.73	351
12.17	57	12.11	64	12.09	65
13.43	60	13.40	70	13.36	69
15.50	77	15.47	99	15.47	92
16.38	136	16.34	185	16.34	175
18.75	96	18.75	115	18.75	110
19.70	87	19.70	115	19.70	129
21.19	73	21.19	85	21.17	79
21.54	45	21.54	43	21.54	43
23.12	57	23.10	63	23.06	61
toplam	1115		1394		1307
Crystallinity %	100		125		117

C. Yield of Crystallization Reactions

The yield was calculated via dividing the obtained amount of ZIF crystals from 100 g of synthesis solution by the maximum possible amount of ZIF, which can be obtained from 100 g of synthesized mixture if all limiting reactant is consumed. Sample calculation:

	Fresh Soln	1st ML	2nd ML	Total
Obtained amount of ZIF-L from synthesized solution (g)	0.590	0.337	0.463	1.390
Obtained amount of ZIF-L from synthesized solution (mol)	0.005			
If all Zn cosumed ZIF-L that should be obtained (mol)	0.005			
If all Zn cosumed ZIF-L that should be obtained (g)	1.381			
ZIF-L that obtained by experiment (g)	1.163			
ZIF-L that obtained by experiment (mol)	0.004			
Total yield	84			

Table C. 1. Product yields of ZIF-8 crystals

	ZIF-8.0	ZIF-8.1	ZIF-8.2
#	Yield	Yield	Yield
1	69	35	65
2	67	36	63
3	69	32	59
4	69	46	63
5	66	26	59
Avg	68	35	62
Std	2	7	3

Table C. 2. Product yields of ZIF-L crystals

	ZIF-L.0	ZIF-L.1	ZIF-L.2
#	Yield	Yield	Yield
1	83	70	20
2	84	70	22
3	83	70	22
4	84	73	35
5	84	73	40
6	83	70	20
7	84	70	20
Avg	84	71	26
Std	0	2	8

Table C. 3. Product yields of ZIF-67 crystals

	ZIF-67.0	ZIF-67.1	ZIF-67.2
#	Yield	Yield	Yield
1	65	15	30
2	66	15	24
3	66	22	30
4	66	16	22
Avg	66	17	27
Std	0	3	4

Table C. 4. Product yields of ZIF-7 crystals

	ZIF-7.0	ZIF-7.1	ZIF-7.2
#	Yield	Yield	Yield
1	51	41	19
2	50	44	18
3	51	35	19
Avg	51	40	18
Std	0	5	0

D. Mass Flow Controller (Mfc) Calibration Curve

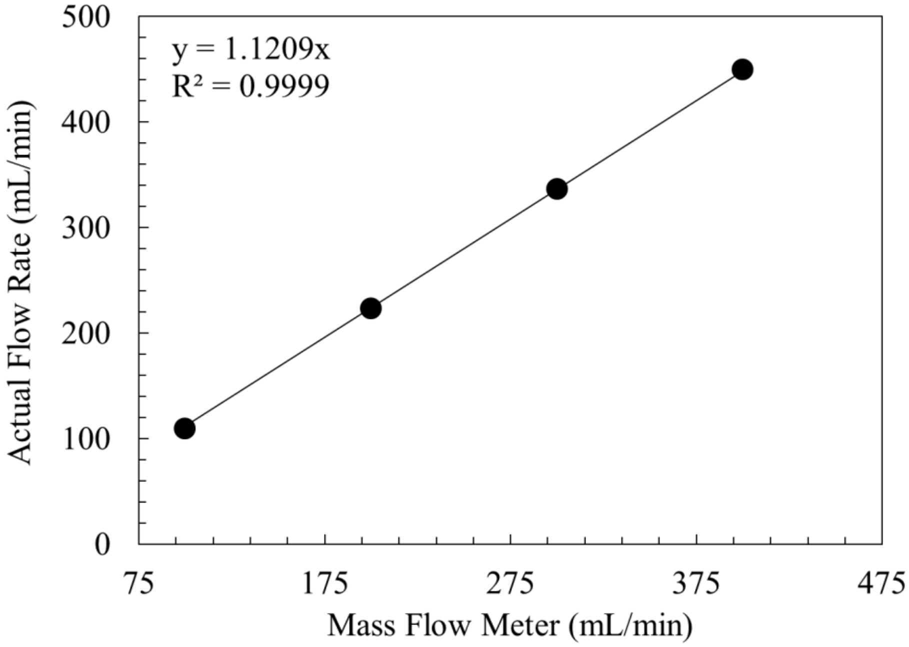

Figure D. 1. MFC-1 calibration curve

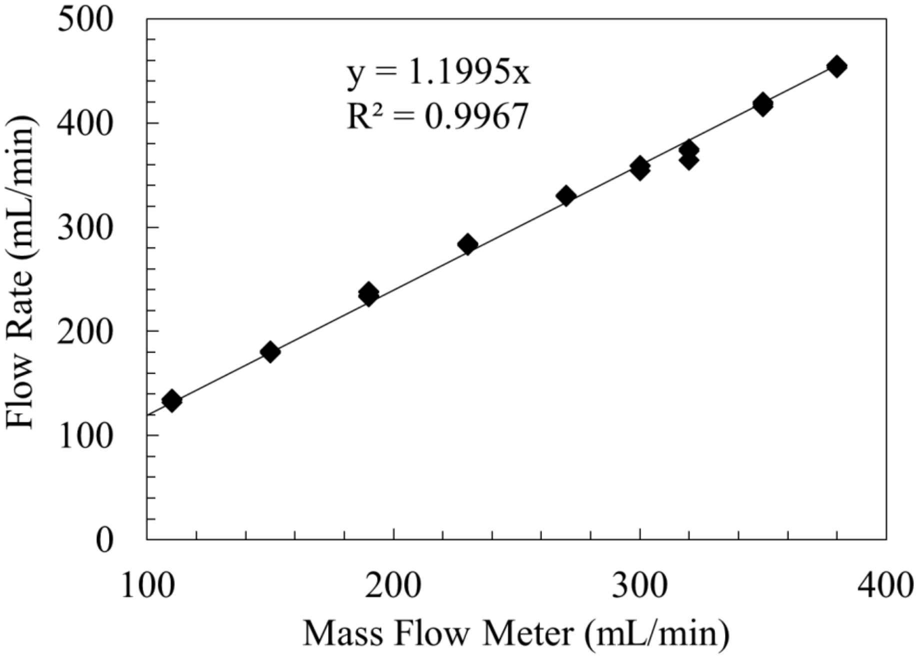

Figure D. 2. MFC-2 calibration curve

E. Gas Chromatography Calibration Curve

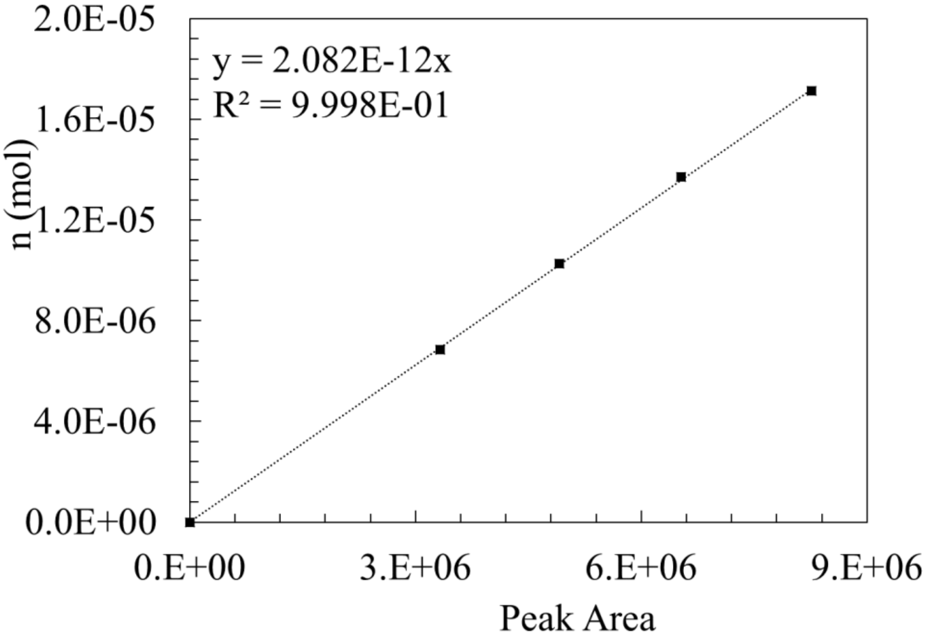

Figure E. 1. GC calibration curve of ethanol

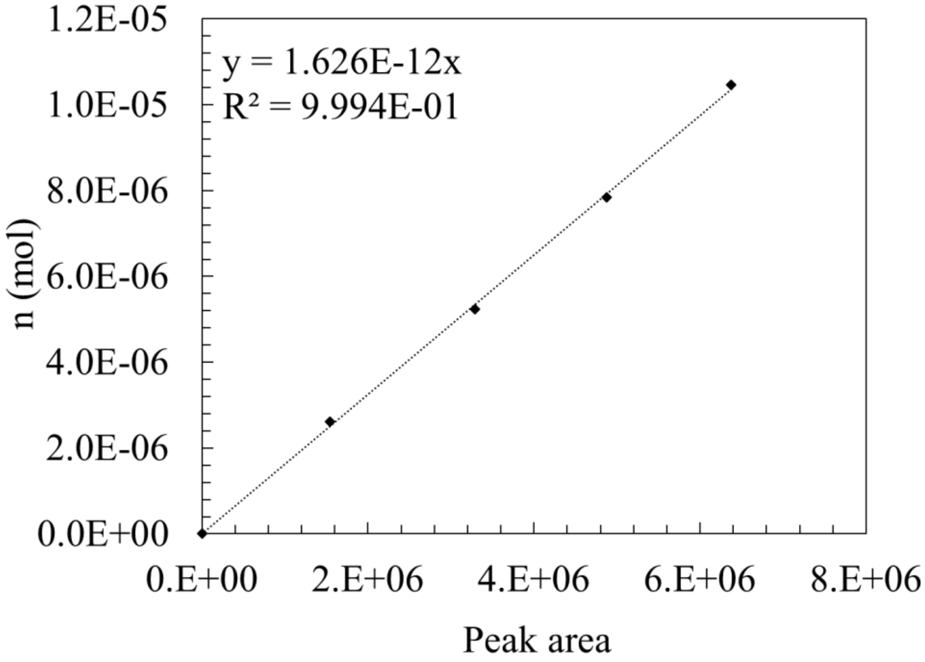

Figure E. 2. GC calibration curve of IPA

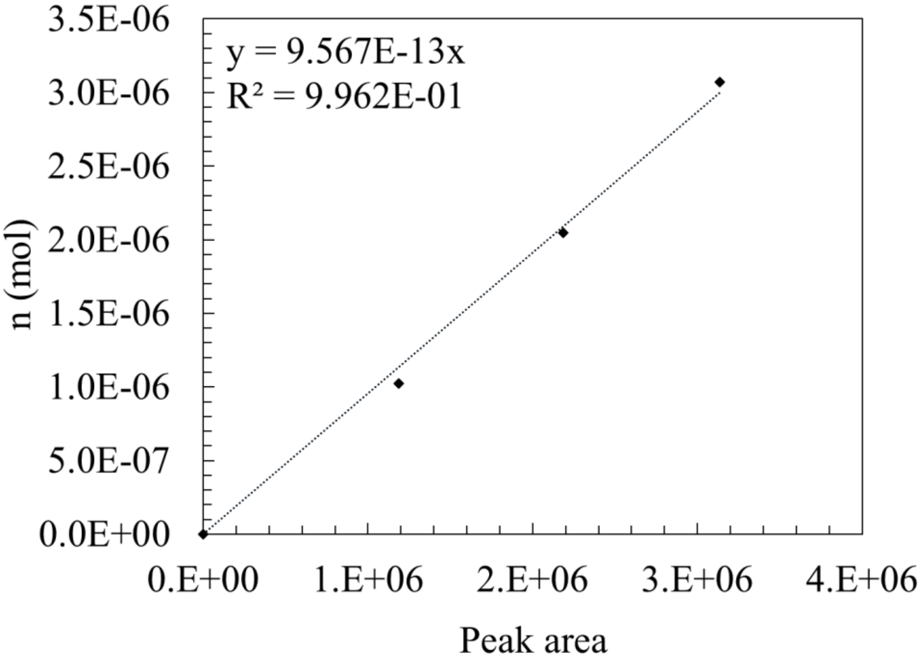

Figure E. 3. GC calibration curve of ethyl acetate

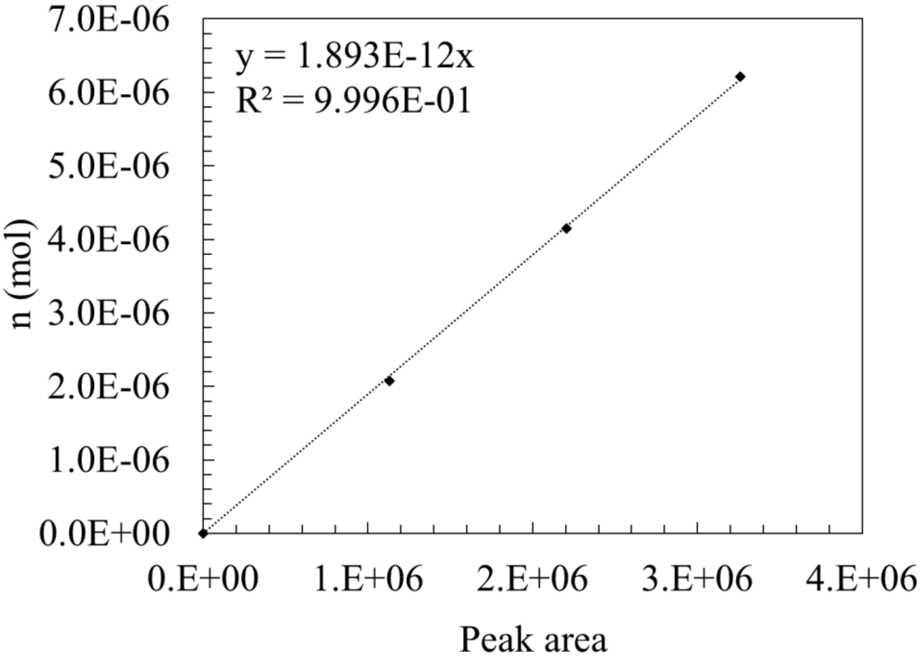

Figure E. 4. GC calibration curve of propanol

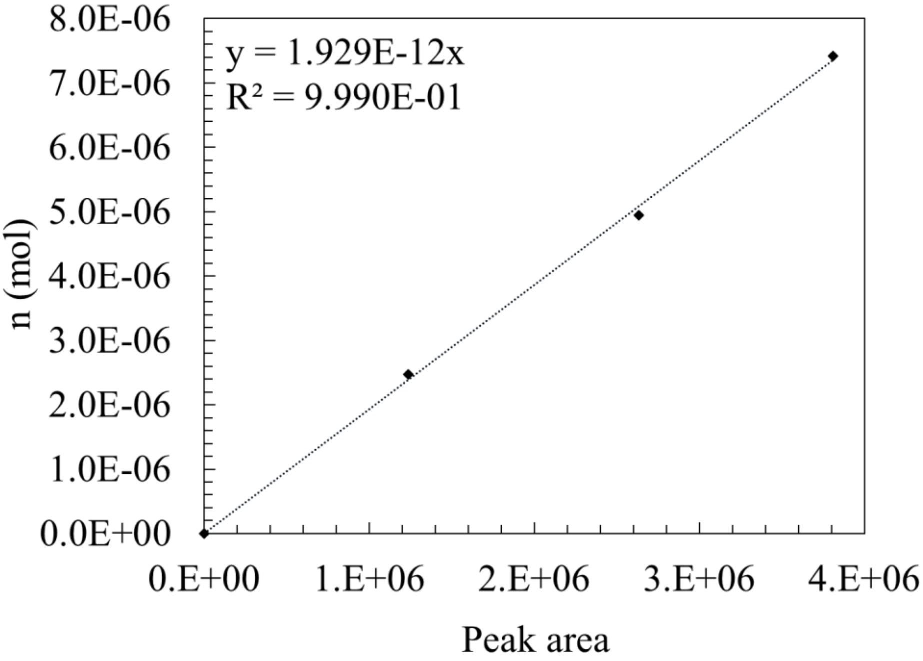

Figure E. 5. GC calibration curve of methanol

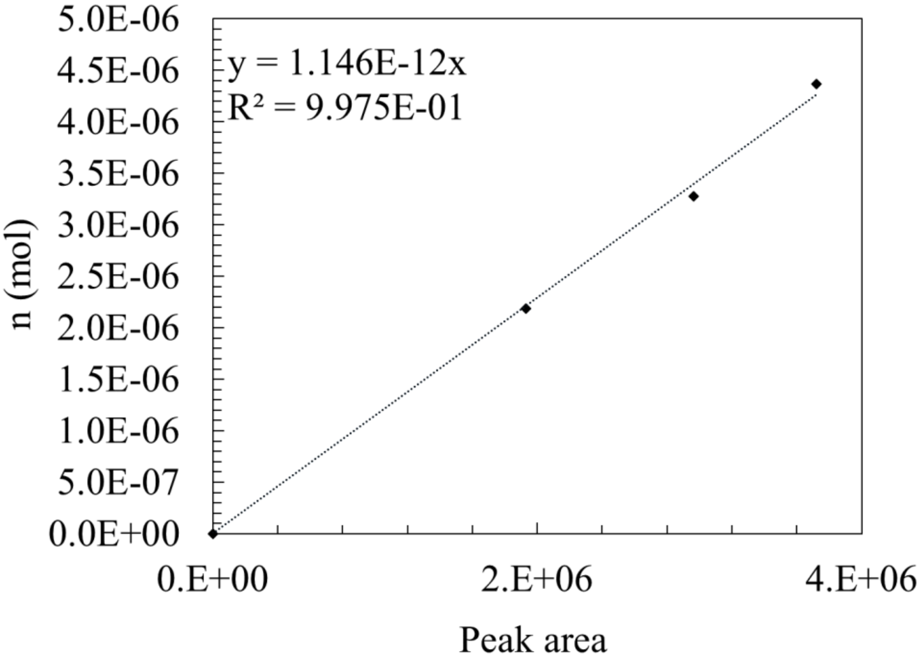

Figure E. 6. GC calibration curve of butanol

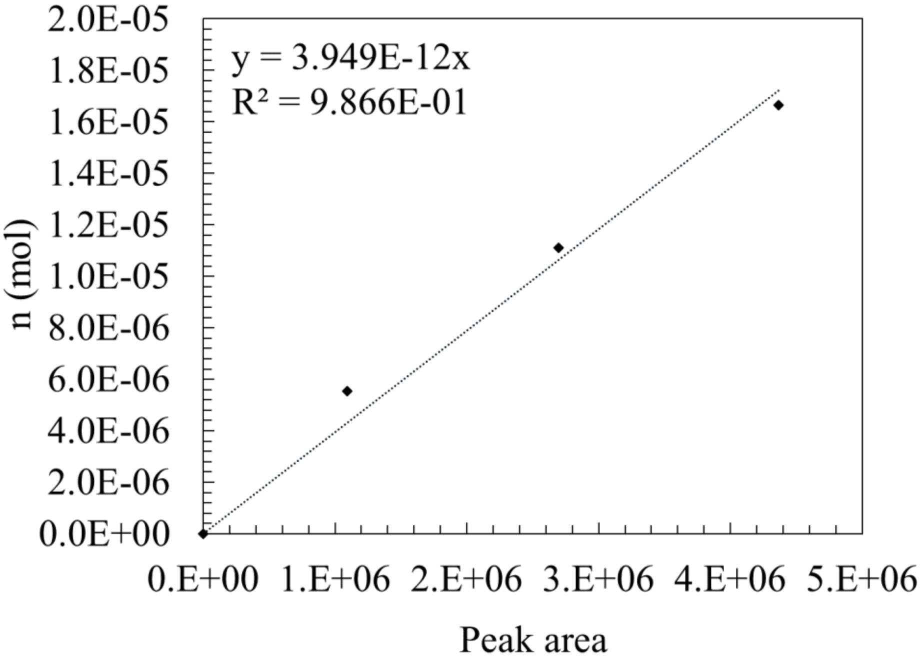

Figure E. 7. GC calibration curve of water

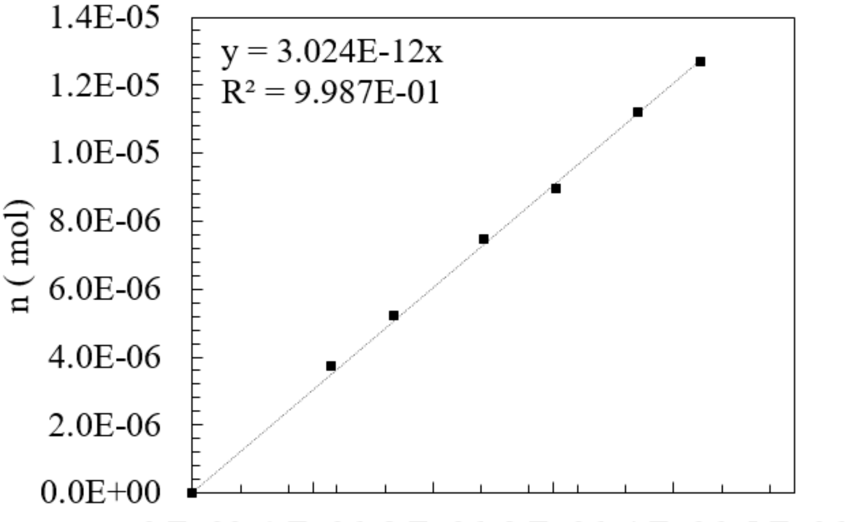

Figure E. 8. GC calibration curve of nitrogen

F. TGA Curves of 20 % ZIF-X PDMS MMMs' Pieces

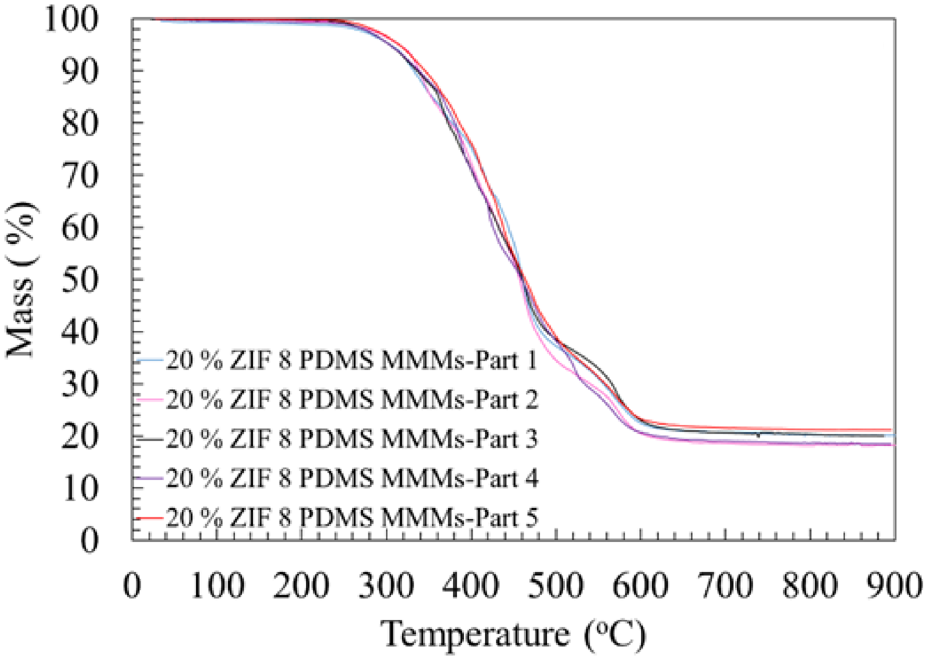

Figure F. 1. TGA curves of 20 % ZIF-8 PDMS MMMs

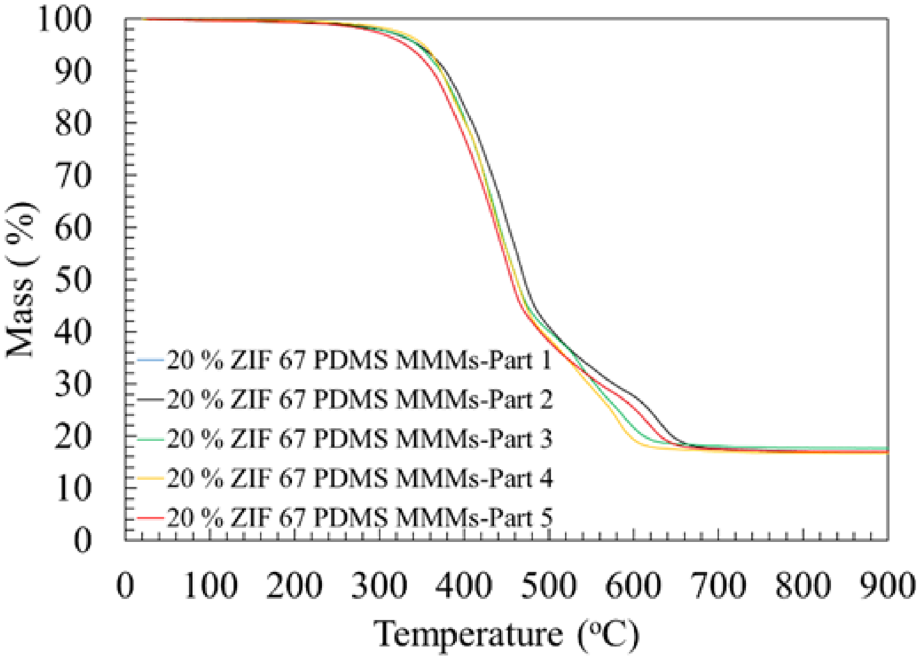

Figure F. 2. TGA curves of 20 % ZIF-67 PDMS MMMs

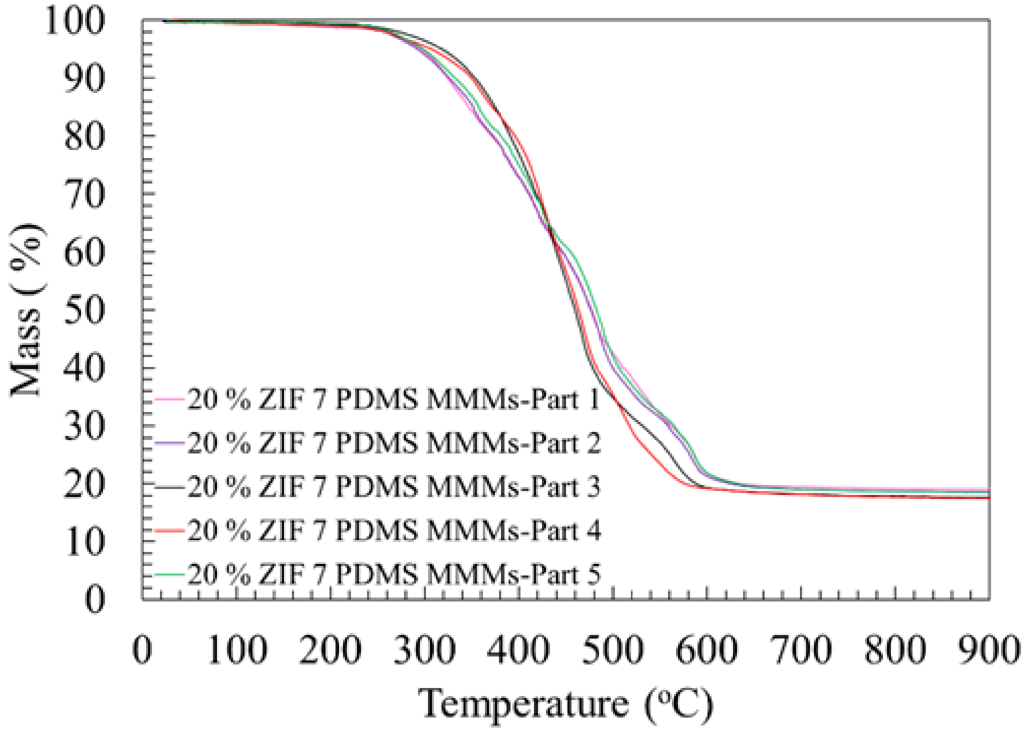

Figure F. 3. TGA curves of 20 % ZIF-7 PDMS MMMs

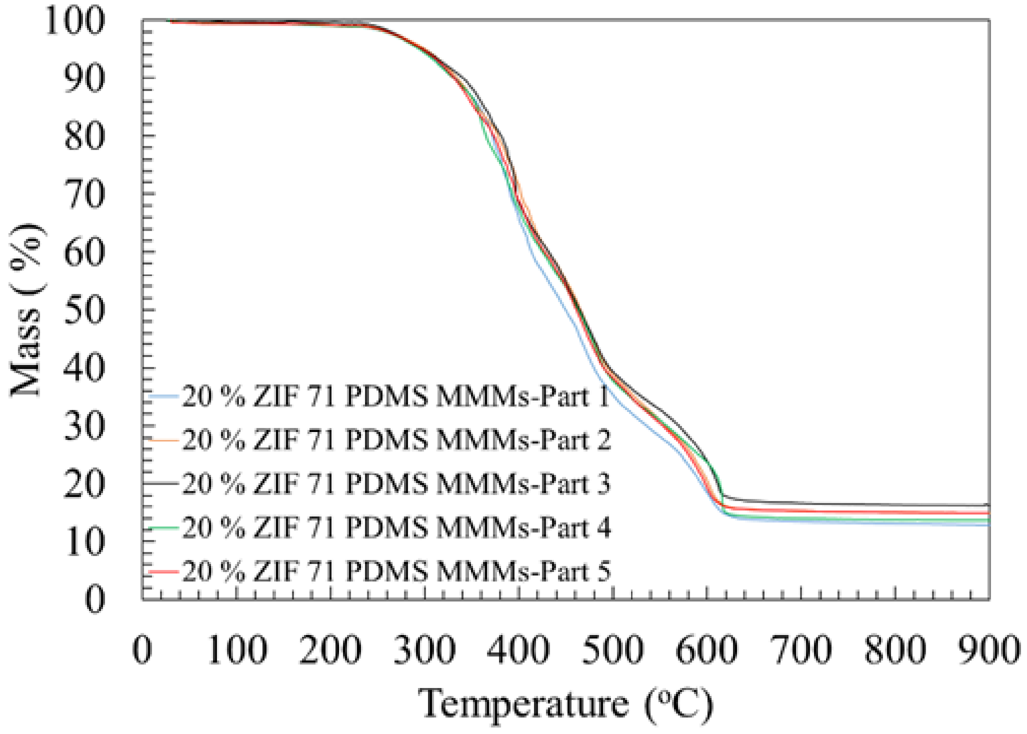

Figure F. 4. TGA curves of 20 % ZIF-71 PDMS MMMs

CURRICULUM VITAE

PERSONAL INFORMATION

Surname, Name: Şahin, Fatma
Nationality: Turkish (TC)
Date and Place of Birth: 23 March 1984, Ankara
Marital Status: Single
Phone: +90 505 600 26 49
email: fatmasahin.metu@gmail.com

EDUCATION

Degree	**Institution**	**Year of Graduation**
BS	Izmir Institute of Technology Chemical Engineering	2008
High School	Atatürk Anatolian High School, Ankara	2003

WORK EXPERIENCE

Year	**Place**	**Enrollment**
2018-Present	Hitit University department of Chemical Engineering	Research Assistant
2014-2017	METU department of Chemical Engineering	Research Assistant
2009-2014	Hitit University department of Chemical Engineering	Research Assistant
2006 July	Drogsan	Intern Engineering Student
2007 July	MKEK- Mechanical and Chemical Industry Company	Intern Engineering Student

FOREIGN LANGUAGES

Advanced English

PUBLICATIONS

Şahin, F.; Topuz, B.;Kalıpçılar, H. 2018. ‘Microporous and Mesoporous Materials Synthesis of ZIF-7 , ZIF-8 , ZIF-67 and ZIF-L from Recycled Mother Liquors’. Microporous and Mesoporous Materials 261(November 2017):259–267.

Proceedings of International Conferences

Şahin, F.; Topuz, B.;Kalıpçılar, H.; “ZIF Based PDMS MMMs for Separation Ethanol and IPA from Nitrogen”, Euromembrane 2018, Valencia, Spain, 2018- Oral Presentation

Şahin, F.; Topuz, B.;Kalıpçılar, H.; “Oriented-ZIF L/PEBAX MMMs for CO_2/N_2 Separation”, Euromembrane 2018, Valencia, Spain, 2018- Poster Presentation

Şahin, F.; Topuz, B.;Kalıpçılar, H.; “ZIF-L/ PDMS Mixed Matrix Membranes for Separation of Ethyl Alcohol and Isopropyl Alcohol from Nitrogen”, 11th International Congress on Membranes and Membrane Processes, San Francisco, ABD, 2017- Poster Presentation

Şahin, F.; Topuz, B.;Kalıpçılar, H., “Solvent Recovery by PDMS/ZIFs Mixed Matrix Membranes”, Euro membrane, Aachen, Germany, 2015- Poster Presentation

Şahin,F.; “ Preparation and properties of biodegradable food packing films from corn starch blending with hemicelluloses particles”, 20th International Congress of Chemical and Process Engineering, Prague, Czech Republic, 2014- Oral Presentation

Şahin,F.; Basan S., “Investigation of Thermal Properties Sulphonated Maleic Anhydride-Styrene Copolymer Membrane”, International Science and Technology Conference Rome, Italy, 2013- Oral Presentation

Şahin,F.; Basan S., “Examination of Sulphonated Maleic Anhydride-Styrene Copolymer Membrane’s Properties by Proton Exchange Membrane Fuel Cell “, 20th International Congress of Chemical and Process Engineering Prague, Czech Republic, 2012- Oral Presentation

Proceedings of National Conferences

Şahin, F.; Topuz, B.;Kalıpçılar, H.; “Separation of Ethanol and IPA from Nitrogen by PDMS Membrane”, National Research Center on Membrane Technologies Symposium, İstanbul, Turkey, 2017.

Şahin, F.; Topuz, B.;Kalıpçılar, H.; “Separation of VOCs / Nitrogen Mixtures with Polymeric Membranes”, 10th National Chemical Engineering Congress, İzmir, 2016.

Şahin,F.; “Evaluation of the Current Legislation for the Usage of Dry Heat Stylized Dry Medical Wastes as Industrial Fuel”, 10th National Chemical Engineering Congress, İstanbul, Turkey, 2012.

Şahin,F.; Basan S.,”Investigation of the Effect of Maleichydrite Containing Terpolymers on the Thermomechanical Properties of Triple Mixtures of PVC”, 9th National Chemical Engineering Congress, Ankara, Turkey, 2010.

Şahin,F.; Basan S.,” The Effect of Composition on the Mechanical Properties of Polymer-Concrete Composites”, 2010 3rd National Polymer Congress, Kocaeli, Turkey.

Şahin,F.; Basan S., “ Utilization of Waste Polymers as Hydrogen Source by TVA-SATVA Method”, 4th National Hydrogen Conferences, Kocaeli, Turkey, 2009.

HOBBIES

Basketball, Badminton, Zumba, Flute, Cross-stitch